RITA DA SILVA FERREIRA

BARREIRAS METABÓLICAS NA TRANSDIFERENCIAÇÃO DE FIBROBLASTOS EM MIÓCITOS INDUZIDOS DO TIPO CARDÍACO

METABOLIC BARRIERS IN THE TRANSDIFFERENTIATION OF FIBROBLASTS INTO INDUCED CARDIAC-LIKE MYOCYTES

Universidade de Aveiro
Ano 2022

RITA DA SILVA FERREIRA

BARREIRAS METABÓLICAS NA TRANSDIFERENCIAÇÃO DE FIBROBLASTOS EM MIÓCITOS INDUZIDOS DO TIPO CARDÍACO

METABOLIC BARRIERS IN THE TRANSDIFFERENTIATION OF FIBROBLASTS INTO INDUCED CARDIAC-LIKE MYOCYTES

Dissertação apresentada à Universidade de Aveiro para cumprimento dos requisitos necessários à obtenção do grau de Mestre em Biomedicina Molecular, realizada sob a orientação científica da Doutora Sandrina Nóbrega Pereira, Equiparada a Investigadora Auxiliar do Departamento de Ciências Médicas da Universidade de Aveiro

Dedico este trabalho ao meu Avô Fernando, que sempre me ensinou a "Saber ser pessoa".

o júri

presidente

Professor Doutor Rui Gonçalo Viegas Russo da Conceição Martinho
Professor Auxiliar em Regime Laboral da Universidade de Aveiro

vogais

Professora Doutora Rita Maria Pinho Ferreira
Professora Auxiliar da Universidade de Aveiro

Doutora Sandrina Nóbrega Pereira
Equiparada a Investigadora Auxiliar da Universidade de Aveiro

agradecimentos

À professora Sandrina Nóbrega Pereira, orientadora desta dissertação, pela disponibilidade, ajuda, compreensão e acompanhamento prestados ao longo deste ano.

Ao professor Bruno Jesus, por me ter acolhido na rotação e por todas as sugestões dadas, que me permitiram melhorar o meu trabalho.

À Magda e ao Francisco, por toda a paciência, disponibilidade e ajuda no laboratório.

À Sara Pinheiro pela ajuda estatística, mas principalmente por estar sempre disponível para me ouvir, apoiar e motivar.

À Ana e à Diana por terem partilhado comigo esta etapa e me terem ajudado e motivado quando mais precisei.

À Sara e à Patrícia que, mesmo que por vezes mais longe, continuam presentes quando é necessário.

Aos restantes amigos e familiares pela motivação.

Por último, mas não menos importante, aos meus pais, ao meu irmão e ao Joel. Palavras não chegam para agradecer tudo o que têm feito por mim. Muito obrigada por tudo.

palavras-chave   Insuficiência Cardíaca; Conversão direta cardíaca; Envelhecimento; Cardiomiócitos; Metabolismo; Mitocôndria

resumo   As doenças cardiovasculares são a principal causa de morte a nível mundial. Estas patologias podem ser caracterizadas pela perda de cardiomiócitos que, devido à sua capacidade muito limitada de regeneração, podem levar à insuficiência cardíaca. Deste modo, várias estratégias regenerativas foram desenvolvidas ao longo dos últimos anos. A conversão cardíaca direta (DCC) é uma estratégia promissora, gerando miócitos induzidos do tipo cardíaco (iCLMs), através do uso de fatores cardiogénicos (MGT; Mef2c, Gata4 e Tbx5), a partir de fibroblastos, tirando partido da sua presença no coração, que cresce após a lesão. No entanto, esta estratégia ainda tem pouca eficácia, especialmente em células envelhecidas, e o impacto das manipulações metabólicas continua por caracterizar.

Utilizando fibroblastos embrionários de ratinho (MEFs) e fibroblastos da pele de orelha adultos (AEFs), realizámos uma análise de imunofluorescência da rede mitocondrial, que revelou que a DCC é acompanhada de uma remodelação significativa das mitocôndrias nos iCLMs derivados tanto de MEFs como de AEFs, progredindo mais lentamente nos últimos. A análise de vários marcadores metabólicos (gotículas lipídicas, massa mitocondrial, mitocôndrias despolarizadas e espécies reativas de oxigénio) revelou que os fibroblastos embrionários se aproximam de um metabolismo semelhante ao dos cardiomiócitos, enquanto os fibroblastos adultos parecem ter mais barreiras no processo. Além disso, também melhorámos a eficiência do DCC em MEFs através do uso de 2-DG, um inibidor glicolítico.

Em suma, o nosso estudo mostra que existem diferenças claras entre os iCLMs derivados de fibroblastos embrionários e adultos, o que pode ser um ponto de partida para melhorar a eficácia da reprogramação de fibroblastos adultos e envelhecidos.

keywords

Heart failure; Direct cardiac conversion; Aging; Cardiomyocytes; Metabolism; Mitochondria

abstract

Cardiovascular diseases are the leading cause of death worldwide. These pathologies can be characterized by the loss of cardiomyocytes which, due to their very limited ability to regenerate, can lead to heart failure. Several regenerative strategies have been developed over the last years. Direct cardiac conversion (DCC) shows great promise by generating induced cardiac-like myocytes (iCLMs), through the use of cardiogenic factors (MGT; Mef2c, Gata4, and Tbx5), from fibroblasts, taking advantage of their presence in the heart, that grows after injury. Nevertheless, this strategy still lacks efficiency, especially in aged cells, and the impact of metabolic manipulations remains elusive.

Using mouse embryonic fibroblasts (MEFs) and adult ear fibroblasts (AEFs), we performed an immunofluorescence analysis on mitochondrial network, revealing that DCC is accompanied by significant remodeling of the mitochondria in both MEFs and AEFs-derived iCLMs, progressing slower in the latter. We also analyzed several metabolic markers (lipid droplets, mitochondrial mass, depolarized mitochondria and reactive oxygen species) which revealed that embryonic fibroblasts are approaching a metabolism that resembles the cardiomyocytes', while adult fibroblasts seem to have more barriers to the process. Moreover, we also improved DCC efficiency in MEFs through the use of 2-DG, a glycolytic inhibitor.

Overall, our study shows that there are clear differences between embryonic and adult-derived iCLMs, which can be a starting point in improving the efficiency of the reprogramming for adult and old fibroblasts.

Contents

List of figures

List of Tables

Abbreviations

2-DG	2-Deoxi-d-glucose
α-KG	α-Ketoglutarate
αMHC	α Muscle Heavy Chain
AEFs	Adult Ear Fibroblasts
AR	Aspect Ratio
Au	Arbitrary units
BSA	Bovine Serum Albumin
CF	Cardiac fibroblasts
CTCF	Corrected Total Cell Fluorescence
cTnT	Cardiac troponin T
CVDs	Cardiovascular diseases
D	Day
DCC	Direct Cardiac Conversion
DMEM	Dulbecco′s Modified Eagle′s Medium
DMSO	Dimethyl sulfoxide
Dox	Doxycycline
Drp1	Dynamin-related protein 1
FAO	Fatty acid oxidation
FBS	Fetal Bovine Serum
FF	Form Factor
Fis1	Fission protein 1
GFP	Green Fluorescent Protein
H3K27me3	histone3-lysine27-trimethylation
H3K4me3	histone3-lysine4-trimethylation
HSP-60	Heat shock protein-60
HEK 293 T	Human Embryonic Kidney 293 T
iCLMs	induced Cardiac-like Myocytes
iCM	induced Cardiac Myocyte
IDH3α	Isocitrate dehydrogenase3α
IMM	Inner mitochondrial membrane
IMS	Intermembrane mitochondrial space
iPSCs	induced Pluripotent Stem Cells
iPSC-CMs	induced Pluripotent Stem Cell-derived Cardiomyocytes
MEFs	Mouse Embryonic Fibroblasts
MFI	Median Fluorescence Intensity
Mfn1	Mitofusin 1
MGT	Mef2c, Gata4 and Tbx5
miRs	micro-RNAs
mtDNA	mitochondrial DNA
Nrf1	Nuclear respiratory factor 1
OMM	Outer mitochondrial membrane
OPA1	Optic atrophy protein 1

OXPHOS	Oxidative phosphorylation
PBS	Phosphate Buffer Saline
PGC1-α	Peroxisome proliferator-activated receptor gamma coactivator 1-α
Pink1	PTEN-induced putative kinase 1
qPCR	Quantitative Polymerase Chain Reaction
ROS	Reactive Oxygen Species
rpm	revolutions per minute
RT	Room Temperature
SAM	S-adenosylmethionine
SD	Standard deviation
TCA	Tricarboxylic acid cycle
TOM	Translocase of the Outer Membrane
TTFs	Tail-tip fibroblasts

Introduction

1. Cardiovascular diseases and heart failure

Cardiovascular diseases (CVD) are the leading cause of death worldwide, accounting for about 32% of the total, according to the World Health Organization (*Cardiovascular Diseases*, n.d.). Several CVDs, including myocardial infarction, hypertension, heart valve disease, and myocarditis, can lead to heart failure, which is associated with a poor prognosis (Bacmeister et al., 2019).

Following the extensive death or injury with subsequent loss of cardiomyocytes, a fibrotic response is initiated. Myofibroblasts start proliferating and secrete collagen fibers, which accumulate in the injured area giving rise to a fibrotic scar (**Figure 1**). This leads to reduction of perfusion, as well as loss of contractile function of the myocardium which, in turn, can originate heart failure (González et al., 2018).
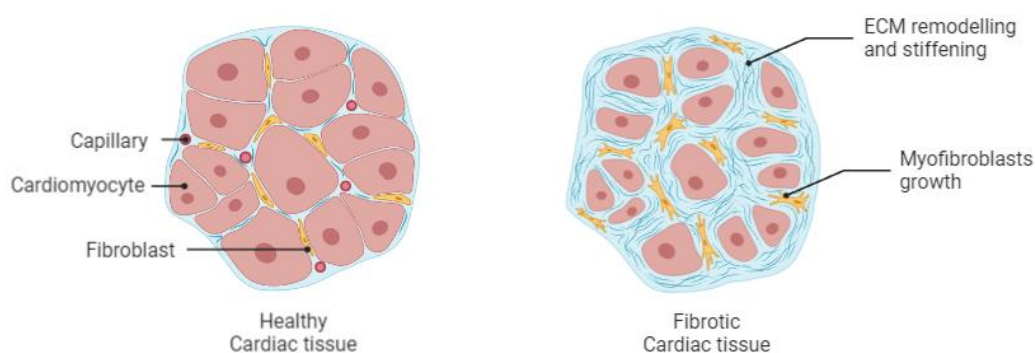
Figure 1. Healthy (left) and fibrotic (right) cardiac tissue. Image made with Biorender.

Neonatal hearts are capable of regenerating for a short period of time after birth through proliferation of pre-existing cardiomyocytes. However, with the post-natal loss of proliferation there is also a loss of regenerative capacity (Cardoso et al., 2020). Interestingly, this is accompanied by a switch from glycolysis to oxidative phosphorylation (OXPHOS), named the fetal metabolic switch. Although there has been reported an increase of division of pre-existing cardiomyocytes in the areas adjacent to the injury, this is very limited and not enough to restore contractile function (Cardoso et al., 2020; Senyo et al., 2013).

Several pharmacological therapies, like Angiotensin-converting enzyme inhibitors and beta-blockers, are currently available and have been successfully employed in patients with heart failure (Mann, 1999). However, in more severe cases the only viable solution is heart transplantation which, due to the low number of organs available, as well as age affecting the eligibility, is an insufficient solution (Kojima & Ieda, 2017). Therefore, understanding the molecular mechanisms, including metabolic reprogramming, that govern regeneration and repair of lost myocardium is warranted for improving heart function upon damage.

2. The fetal metabolic switch and metabolism of the healthy heart

In the fetus, cardiomyocytes are highly reliant on glycolysis as their energy supplier, while presenting low of levels fatty acid oxidation (FAO) (less than 15%) due to the low oxygen and fatty acid levels in the environment (Lopaschuk & Jaswal, 2010). Despite being less efficient energy-wise, glycolysis accommodates the needs of the developing heart, as its reactions happen rapidly and provide intermediate metabolites required for the synthesis of macromolecules during the growth and proliferation of the cells (Ng & Ng, 2017).

Shortly after birth, cardiomyocytes transition from glycolysis to OXPHOS, during the fetal metabolic switch. This accommodates the higher energetic needs of the adult heart and leads to an increase in Reactive Oxygen Species (ROS) which, in turn, contributes to cardiomyocytes exiting the cell cycle, due to oxidative damage and activation of the DNA damage response (Cardoso et al., 2020). From this point, these cells seem to lose most of their ability to proliferate, with adult cardiomyocytes presenting a turnover rate of about 0,76% per year, which reduces with age (Senyo et al., 2013). Their growth starts happening mostly through an increase in size (hypertrophy) (Lopaschuk & Jaswal, 2010).

Adult cardiomyocytes use mostly fatty acid oxidation for ATP production. Fatty acyl-CoA, generated through lipolysis or free fatty acids uptake, is converted in the mitochondria through FAO generating acetyl-CoA, which enters the tricarboxylic acid cycle (TCA). FAO and TCA generate $FADH_2$ and NADH, that are utilized as electron donors during OXPHOS to generate ATP (Correia et al., 2022). The adult heart requires around 6 Kg of ATP per day for myocardial contraction. Mitochondria are the main supplier of energy to cardiomyocytes, providing around 90% of the cell's ATP, therefore presenting a crucial role in these cells (A. Li et al., 2020).

Glycolysis has a more secondary role as energy source in adult cardiomyocytes, being responsible for supplying ion pumps with ATP for their activity. However, the process remains crucial as it supplies the cell with intermediate metabolites for other pathways, regulating cell proliferation and transcription (Correia et al., 2022).

3. *Mitochondrial structure and function*

In the majority of eukaryotic cells, mitochondria are crucial organelles (A. Li et al., 2020). They consist of an outer membrane (OMM), which surrounds an inner membrane (IMM), with a small intermembrane space (IMS) between. The IMM contains the mitochondrial respiratory chain and delimits the mitochondrial matrix, which is where the mitochondrial DNA (mtDNA) and metabolic enzymes are located (**Figure 2**) (Giacomello et al., 2020; A. Li et al., 2020).
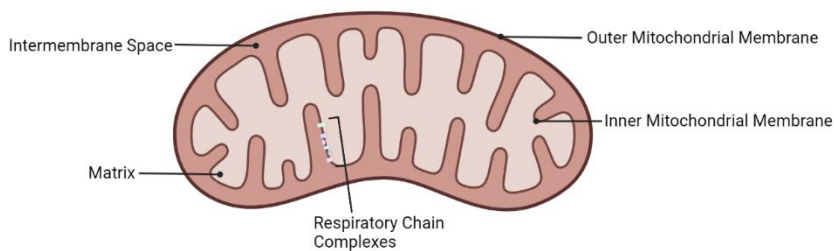
Figure 2. Mitochondria and its components. Image made with Biorender. Adapted from (Giacomello et al., 2020).

Mitochondria are considered "the powerhouses of the cell", since they efficiently generate ATP through TCA and OXPHOS (Giacomello et al., 2020; A. Li et al., 2020). During TCA, several chemical reactions occur, providing reducing equivalents (NADH and FADH2) to OXPHOS. These reducing equivalents supply electrons that are transferred to Oxygen in the mitochondrial respiratory chain, leading to the generation of ATP (Giacomello et al., 2020). During these reactions, the proton pumps generate the mitochondrial membrane potential, which is a crucial part in energy storage (Zorova et al., 2018). Moreover, Reactive Oxygen Species can also be generated during OXPHOS, with mitochondria being their main source (Orrenius et al., 2007).

Adding to their energetic function, mitochondria have also been implicated in an increasing number of cellular processes as cell signaling, calcium homeostasis, stem cell differentiation and cell death (A. Li et al., 2020) (Giacomello et al., 2020).

3.1 Mitochondrial homeostasis and dynamics

Mitochondria are regulated through several mechanisms to avoid cell dysfunction or death. Particularly, mitochondria homeostasis is maintained by biogenesis, the generation of new organelles, and mitophagy, the degradation of damaged ones (**Figure 3**). Mitochondrial biogenesis occurs through the division of pre-existing mitochondria or through their "growth" (by fusion, for example). This process allows for the increase of mitochondrial mass, and consequently the increase of the energy production, being important for adapting to metabolic changes or energy depletion. One of the key factors of biogenesis is peroxisome proliferator-activated receptor gamma coactivator 1-α (PGC1-α), which coactivates several transcription factors such as nuclear respiratory factor-1 (Nrf1). Nrf1, in turn, activates transcription factor A, mitochondrial (TFAM), promoting the replication of the mitochondrial genome, as well as the expression of some mtDNA-encoded genes (Tronstad et al., 2014). The degradation of damaged mitochondria through mitophagy is done by the lysosomal-autophagic machinery. Several proteins are involved in this process, including PTEN-induced putative kinase 1 (Pink1), and a component of E3 ubiquitin ligase complex, Parkin. When Pink1 accumulates in the OMM, following mitochondrial depolarization, Parkin is recruited (Tronstad et al., 2014). This promotes the mitophagy signaling through the generation phosphorylated ubiquitin which binds P62 and LC3, for example, in the autophagosome and the degradation process is initiated (Y. Li et al., 2021).

The location and morphology of mitochondria, as well as their distribution as separated organelles or as part of an interconnected network, are also important for their function, being regulated by fission and fusion (A. Li et al., 2020) (**Figure 3**). The division of mitochondria happens through fission, which is regulated in the OMM by dynamin-related protein 1 (Drp1). When the process is initiated, Drp1 is dephosphorylated and mobilized to the mitochondrial surface binding to its receptors, for example Fission protein 1 (Fis1). This leads to the constriction of the membrane, resulting in the division into two mitochondria (Giacomello et al., 2020). The joining of mitochondria through fusion is regulated in the OMM through mitofusin 1 (Mfn1), and through optic atrophy protein 1 (OPA1) in the IMM. The OMMs of two mitochondria tether through the Mfn1 proteins leading to the docking of the two membranes. The fusion of the two OMMs is followed by the fusion of the IMMs which is regulated by OPA1 (A. Li et al., 2020).
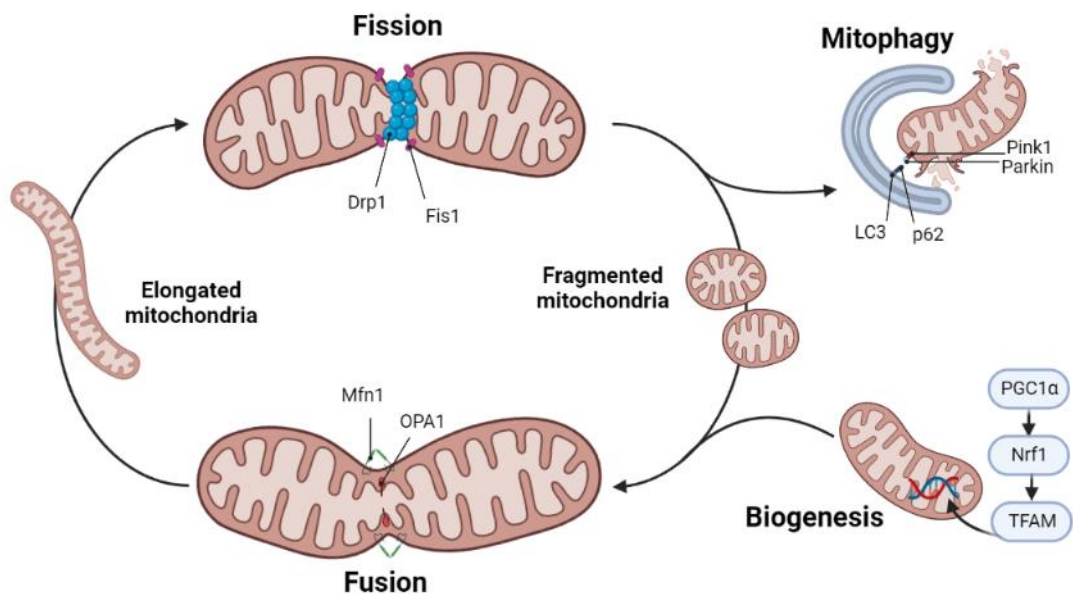
Figure 3. Mitochondria dynamics and homeostasis and proteins involved. Image made with Biorender. Adapted from (Giacomello et al., 2020; Y. Li et al., 2021)

These events of mitochondrial dynamics and homeostasis are interconnected. In order to undergo mitophagy, mitochondria need to be divided through fission for the removal of the damaged mitochondrion. The healthy mitochondria are then fused to share intramitochondrial content and lipid membranes. Moreover, biogenesis seems to be promoted by either inhibiting fission or inducing fusion and PGC-1α was also implicated in the regulation of proteins involved in mitochondrial dynamics (A. Li et al., 2020).

3.2 Metaboloepigenetics

Apart from their role in the metabolism, intermediate metabolites derived from the mitochondria have been increasingly implied as substrates or cofactors for epigenetic modifications, specifically acetylation and methylation marks (Chi, 2020), nowadays referred as mitochondrial metaboloepigenetics.

Histone acetylation, which leads to the opening of the chromatin and activation of gene transcription, is catalyzed by histone acetyltransferases through the transfer of acetyl groups from acetyl-CoA in the cytosol. However, this metabolite, which is converted from pyruvate in the mitochondria, is only able to leave the organelle after being converted to citrate. When in the cytosol, citrate can then be cleaved back to acetyl-CoA, being an important source for acetylation reactions. These reactions can have variable roles in stem-cell differentiation and can be regulated through metabolic changes (Intlekofer & Finley, 2019). In pluripotent stem cells undergoing differentiation, it was found that low levels of acetyl-CoA, due to decreased glycolysis, led to a decrease of histone acetylation (Moussaieff et al., 2015). Moreover, by replenishing this metabolites levels, the differentiation was impaired. However, for progenitor cells, increased histone acetylation promotes the expression of the lineage-specific genes, with low levels of acetyl-CoA debilitating the differentiation (Intlekofer & Finley, 2019).

Histone methylation can either repress or activate transcription, while DNA methylation leads to repression of transcription. These are regulated by methyl marks which are transferred by methyltransferase enzymes from S-adenosylmethionine (SAM) to histones in lysine and arginine residues and DNA in mostly cytosine nucleotides. SAM can be obtained from the methionine cycle or through import by amino acid importers. The loss of methyl marks can occur passively, due to cell division, or through the action of demethylase enzymes. Some of these enzymes are dependent on α-Ketoglutarate (α-KG), an intermediate metabolite of the TCA (Intlekofer & Finley, 2019). Like acetyl-CoA, α-KG can also have a role in stem cell differentiation. Indeed, intracellular levels of α-KG were shown to promote the pluripotency of mouse embryonic stem cells. Conversely, downregulation of α-KG, through knockdown of its regulator Psat1, was found to increase histone methylation, promoting differentiation of embryonic stem cells (Hwang et al., 2016). Therefore, the mitochondrial metabolism can have an important role in reprogramming.

3.3 Mitochondria in the heart

At embryonic day 9.5, mitochondria in cardiomyocytes were found to be fragmented and immature, as well as low in number. As these cells develop, mitochondria mature and fuse, creating an interconnected and filamentous network that spreads through the cell (**Figure 4, left**). Concomitantly to this evolution of the mitochondrial network, the fetal metabolic switch occurs (Chi, 2020) (A. Li et al., 2020).

As the heart continues to mature, mitochondria appear to fragment, as adult cardiomyocytes have spheroid mitochondria aligned longitudinally (**Figure 4, right**). This was shown to allow for a quick and efficient energy flow and lead the organelle to occupy around 40% of the cells' volume (A. Li et al., 2020). However, it was found that with aging, this longitudinal conformation is lost as mitochondria start grouping irregularly, with most organelles being swollen and damaged (di Fonso et al., 2021).
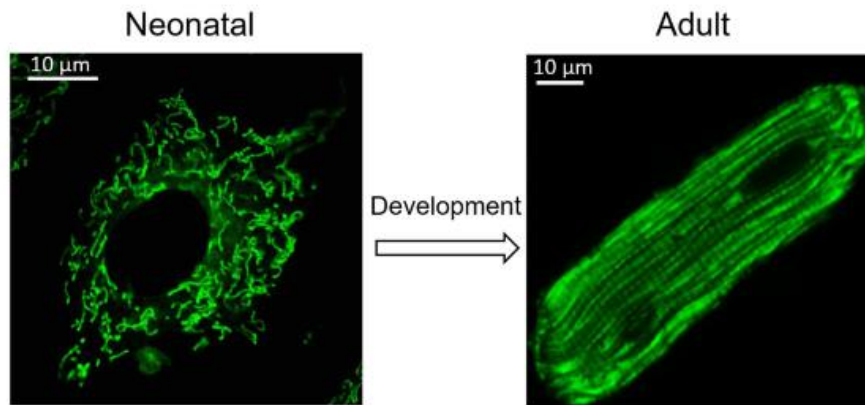
Figure 4. Mitochondria in neonatal (left) and adult (right) cardiomyocytes. Adapted from (A. Li et al., 2020)

In addition to fusion, it was also reported that, in cardiomyocytes, mitochondria exchange their metabolic components with each other through a process in which two adjacent mitochondria touch and, without fusing, rapidly separate (A. Li et al., 2020).

4   Cardiac regenerative strategies

Several regenerative strategies have gained a more prominent role in heart disease therapy in the recent years. These include activation of cardiomyocyte proliferation, activation of cardiac progenitor cells, differentiation of induced pluripotent stem cells and direct cardiac conversion (Correia et al., 2022).

A promising therapeutic strategy consists in activating cardiomyocyte proliferation by either forcing their re-entry in the cell cycle or by manipulating their metabolism to switch to glycolysis ("reverting" the fetal metabolic switch that happens concomitantly to the loss of regenerative ability). However, with only a limited increase in proliferation and improvement in cardiac function achieved and in multiple studies, this strategy still needs further research (Johnson et al., 2021).

In the healthy heart, the replenishment of the cardiomyocyte population is mostly made through the proliferation of existing cardiomyocytes. However, after injury, the recruitment and differentiation of endogenous progenitor cells gains a more prominent role (Malliaras et al., 2013). Cardiac progenitor cells can differentiate into cardiomyocytes and non-myocytes (Brade et al., 2013), with hypoxia and supplementation with the metabolic substrates glucose and glutamine shown to either increase the migration or the proliferation of these progenitor cells (André et al., 2019; Tang et al., 2009).

Induced pluripotent stem cells (iPSCs) are stem cells that can be generated from somatic cells through the use of reprogramming factors. iPSCs can then be differentiated into cardiomyocytes (iPSC-CMs) and, since they can be generated from the patient's own cells, present reduced risk of an immune response (Pushp et al., 2021). Despite presenting several properties characteristic of primary human cardiomyocytes, including molecular, mechanical and metabolic, iPSC-CMs still present an immature phenotype (Karakikes et al., 2015). Furthermore, this technique presents a potential risk of tumorigenesis, as well as poor survival rate when transplanted (Kojima & Ieda, 2017).

Direct cardiac conversion (DCC) is the reprogramming of fibroblasts into cardiomyocytes *in situ*, without passing through a pluripotent state, thus overcoming some of iPSCs disadvantages. Moreover, it takes advantage of the resident population of fibroblasts in the heart that grow and replace lost cardiomyocytes after injury (Kojima & Ieda, 2017). This strategy will be addressed in this work.

4.1 Direct Cardiac Conversion

DCC was first described by Ieda and colleagues, in 2010. They screened fourteen transcription factors involved in heart development and concluded that Mef2c, Gata4 and Tbx5 were capable, through transduction, of generating induced Cardiac Like Myocytes (iCLMs) from mouse postnatal cardiac fibroblasts (CF) as well as tail-tip fibroblasts (TTFs). These iCLMs expressed several cardiac genes including cardiac Troponin, Actc1, and Myh6 and showed spontaneous ability to contract (Ieda et al., 2010). These experiments, performed *in vitro*, were later done *in vivo* also leading successful transdifferentiation (Qian et al., 2012).

Since then, several other transcription factors, microRNAs and small molecules have been described to successfully induce DCC both *in vitro* and *in vivo*. For example, adding transcription factor Hand2 to the MGT cocktail (GHMT) was shown to increase the efficiency of the process in almost five-fold over only MGT transduction (Song et al., 2012). As for micro-RNAs (miRs), the combination of miR-1, miR-133, miR-208, and miR-499, which are involved in cardiomyocyte differentiation and development, was also able to successfully induce DCC both *in vitro* and *in vivo* (Jayawardena et al., 2015). To overcome the risks associated with genetic modification of the previous viral-based methods, Fu and colleagues developed a chemical cocktail (CRFVPT with CHIR99021, RepSox, Forskolin, VPA, Parnate and TTNPB) that led to the generation of chemical-iCLMs from mouse embryonic fibroblasts (MEFs) and TTFs (Fu et al., 2015).

Human fibroblasts have also been subjected to DCC experiments. However, MGT transduction was proven to be insufficient to generate iCLMs, highlighting the need for other transcription factors (Wada et al., 2013). Indeed, by adding Mesp1 and Myocd to GMT (GMTMM), both human CFs and dermal fibroblasts were able to generate iCLMs that expressed cardiac proteins and were able to contract synchronously in coculture with murine cardiomyocytes (Wada et al., 2013). Moreover, the combination of micro-RNAS (miR-1 and miR-133) and transcription factors (Gata4, Hand2, Myocd and Tbx5-GHMT) also led to successful reprogramming, with some iCLMs displaying sarcomere-like structures and spontaneous contractility (Nam et al., 2013).

Despite all these progresses made, DCC still presents low efficiency, which could be due to several factors. For instance, the cell type influences the outcome, as MEFs have been shown to be more easily converted to iCLMs than CFs, with TTFs presenting lower efficiency. Other factors like the stoichiometry of the reprogramming factors, epigenetics and metabolism have also been shown to influence the process (Kojima & Ieda, 2017).

4.1.1 MGT Reprogramming factors

The forced expression of the transcription factors Mef2c, Gata4, and Tbx5 was found to be enough to reprogram fibroblasts into iCLMs. These factors are crucial for the development of the heart, by coactivating the expression of cardiac genes and inducing the differentiation of cardiomyocytes, while regulating each other's expression (Ieda et al., 2010) (Olson, 2006). More specifically, Mef2c is important in the formation of cardiac structures, and, along with Gata4, regulating contractile protein genes (Olson, 2006). In addition to cardiac development, both Mef2c and Gata4 have been shown to have a role in the injured heart by regulating contractility and cardiac function (Olson, 2006). Tbx5 has been shown involved in the establishment of the cardiac conduction system (Olson, 2006). Moreover, Gata4 is thought to open the chromatin, being called a "pioneer" factor, which allows the binding of the other two factors to their target sites and activation of the cardiac program (Ieda et al., 2010).

Wang and colleagues generated 6 different polycistronic constructs, by switching the order of the M,G,T factors, and concluded that the stoichiometry affected the efficiency of DCC. Although all the combinations lead to deactivation of fibroblast markers, some (TMG, TGM; GMT and GTM) weren't able to induce a significant activation of cardiac markers. Ultimately, the MGT polycistronic construct that led to higher levels of Mef2c expression relative to Gata4 and Tbx5 presented the best outcome (L. Wang et al., 2015).

4.1.2   Epigenetic Barriers

For a successful conversion into iCLMs, fibroblasts must be able to activate cardiac genes, while repressing fibroblast genes (Kojima & Ieda, 2017). For this, they need to overcome epigenetic barriers, which regulate the expression of the genome through modifications of histones and DNA that either increase or decrease chromatin accessibility (Liu et al., 2016).

Liu and colleagues have studied the expression of histone3-lysine27-trimethylation (H3K27me3), associated with inactive transcription, and histone3-lysine4-trimethylation (H3K4me3), associated with active transcription during DCC. They found decreased H3K27me3 and increased H3K4me3, at day 3 post-transduction, at cardiac promoter sites, while at fibroblast promoter sites there was still increased H3K27me3 and decreased H3K4me3 at day 10. They concluded that, during DCC, while cardiac genes were rapidly activated, the repression of the fibroblast genes were a lengthier process (Liu et al., 2016). Moreover, it was reported that through inhibition of Ezh2, a component of the complex responsible for catalyzing H3K27me2/3, lead to increased efficiency of the DCC process (Hirai & Kikyo, 2014). On the other hand, through knockdown of Bmi1, a component of the polycomb repressive complex 1, there was an increase of H3K4me3 at cardiogenic genes including Gata4, which led to a successful reprogramming with only exogenous Mef2c and Tbx5 (Zhou et al., 2016).

4.1.3   Metabolic switch in direct reprogramming

Fibroblasts are metabolically different from cardiomyocytes, relying mostly on glycolysis as their energy supplier, while the latter, with larger energetic demands, rely on OXPHOS (**Figure 5**). Therefore, a metabolic switch has been reported to accompany the reprogramming process, similar to what happens during the fetal metabolic switch in the developing heart, being a crucial part of the process (H. Wang et al., 2021).
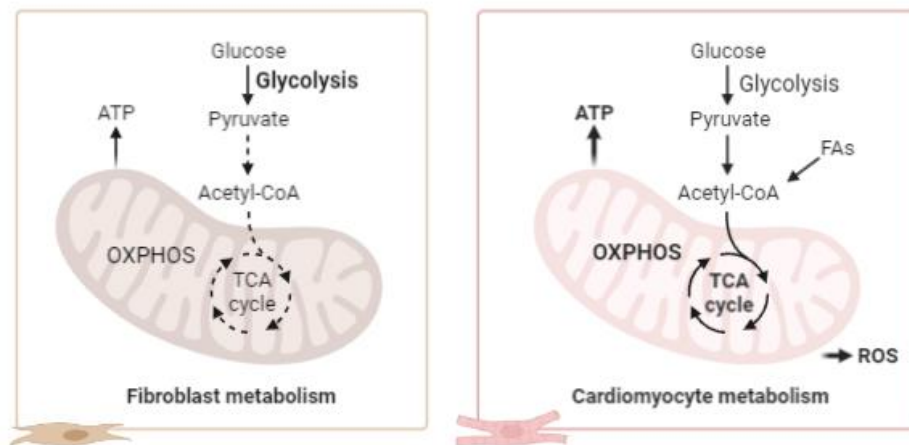
Figure 5. Fibroblast and Cardiomyocyte Metabolism. Image made with Biorender.

Therefore, manipulating fibroblast metabolism to resemble that of cardiomyocytes seems to be a good strategy to improve direct cardiac reprogramming efficiency. Fibroblasts with downregulation of HIF-1α, an important regulator of glycolysis, are more successfully reprogrammed (Stone et al., 2019). Conversely, the use of rotenone, an inhibitor of mitochondria respiration, and knockdown of the TCA cycle enzyme isocitrate dehydrogenase3α (IDH3 α) decreases reprograming efficiency, while IDH3 α upregulation led to increased reprogramming (Ishida et al., 2021). High ROS levels can also affect the efficiency of the process, and the use of antioxidants could boost this process. Selenium and ascorbic acid (vitamin C) supplementation have been

shown to enhance reprogramming efficiency, in vitro, by increasing cardiac gene expression (Talkhabi et al., 2015; X. Wang et al., 2016), and vitamin E nicotinate promotes heart damage repair through reprogramming in vivo (Suzuki & Shults, 2019). Despite these advances in the modulation of the metabolism to improve the reprograming of fibroblasts into iCLMs, the mechanisms underlying the metabolic switch and its impact in DCC remains elusive.

Objectives

Direct Cardiac Conversion (DCC) has gained a great deal of interest over the last years as a regenerative strategy for cardiac diseases. However, it is still an inefficient process, particularly in adult fibroblasts. Moreover, despite being an important component of the process, there is still little knowledge of the metabolic switch that occurs during the process and how it affects the cells, particularly the mitochondria.

Therefore, the main objectives of this work are:

- Characterize the mitochondrial metabolic reprogramming taking place during DCC of mouse embryonic fibroblasts and adult skin ear fibroblasts into iCLMs.
- Evaluate the impact of metabolic modulation in the reprogramming of fibroblasts into iCLMs.

Methods

Cell Culture

During the experiments, the following cell lines were used: the primary cells Mouse Embryonic Fibroblasts (MEFs) and Adult Ear Fibroblasts (AEFs) and the immortalized cell lines icMEFs (Vaseghi et al., 2016), Human Embryonic Kidney 293T (HEK 293T) and HL-1 (Claycomb et al., 1998).

AEFs were prepared from adult (4-6 months) mouse skin from the ears (Rodrigues & Roelen, 2020), while MEFs were prepared from mouse embryos (13.5 days) (Rodrigues & Roelen, 2020). MEFs and AEFs were cultured in Dulbecco′s Modified Eagle′s Medium (DMEM) (Gibco) high glucose (4.5g/L glucose) or low glucose (1g/L glucose), supplemented with 10% Fetal Bovine Serum (FBS) (SIGMA) and 1% Penicillin/Streptomycin (100 U/ml:100 μg/ml). For Retroviral Infection, 28.000 and 170.000 cells were counted and seeded in 24-well plates (with glass coverslips for Immunocytochemistry protocol) and 6-well plates, respectively, coated with 0.1% gelatin. Cells were incubated at 37ºC with 5% CO_2.

HL-1, which is a cardiac muscle cell line from mice, was cultured in Claycomb medium (SIGMA) with 10% FBS, 1% Penicillin/Streptomycin (100 U/ml:100 μg/ml), 0.1 mM Norepinephrine (SIGMA) and 2 mM L-Glutamine (Gibco). For experiments, 2.000/3.000 cells were counted and seeded in 24-well plates with glass coverslips.

icMEFs is a cell line from immortalized MEFs from embryonic α muscle heavy chain-green fluorescent protein (αMHC-GFP) cardiac reporter strain mice (13.5 days), kindly provided to our lab (Vaseghi et al., 2016). This cell line contains a TeTOn system encoding MGT, which is induced by doxycycline (Dox). For experiments, icMEFs were seeded at a density of 10.000/15.000 cells per well in 24 well plates (with glass coverslips for Immunocytochemistry protocol) coated with 0.01% gelatin. The following day, media was changed to induced Cardiac Myocyte (iCM) growth medium consisting of 4:1 DMEM:M199 (Zenbio) with 10% FBS and 1% Penicillin/Streptomycin (100 U/ml:100 μg/ml) with 1/2 μg/mL doxycycline (SIGMA).

2-Deoxi-d-glucose (2-DG, SIGMA) was added to MEFs and icMEFs at 1/2 mM.

For trypsinization, medium was removed, cells were washed with Phosphate Buffered Saline (PBS) (Fisher Bioreagents) and 0.05% Trypsin-EDTA 1x (Gibco) was added. After incubation at 37ºC with 5% CO_2, trypsin was inactivated with 10%FBS containing DMEM medium.

For cell passaging, cells were trypsinized, counted and seeded in the new plate. To count cells, Trypan Blue (AMRESCO) was added to a microtube with an aliquot of cells. The mix was then added to the hemocytometer and cells were counted, using the formula Total cells/ml = (Total cells counted x Dilution factor x 10,000 cells/ml)/ Number of squares counted.

To freeze cells, following trypsinization, cells were centrifuged for 3 minutes at 1000 revolutions per minute (rpm) and resuspended in FBS + 10% Dimethyl sulfoxide (DMSO) (Sigma-Aldrich), placed in a gradual freezing container and stored at -80ºC.

Retroviral Infection for Direct Cardiac Conversion

MEFs and AEFs were retroviral infected according to the following procedure. On day 1, for each transfection, $5x10^6$ HEK 293T cells were seeded onto a 10 cm dish in growth media containing DMEM plus 10% FBS. 4 μg of plasmid DNA (pMXsMGT, a polycistronic vector containing the reprogramming factors Mef2c, Gata4 and Tbx5 (MGT) (L. Wang et al., 2015), or pMXsEmpty) was mixed with 4 μg pCL-Ampho (packaging plasmid). Separately, 576 μl Opti-MEM (Gibco) media containing 24 μl of X-tremeGENE 9 DNA (Roche) incubated for 5 minutes at room temperature (RT), being then joined with the plasmid mixtures, and incubated at RT for 45 min before adding to HEK cells. Medium was changed the next day (day 2) and virus containing-supernatant was collected 48 hours after transfection (day 3), followed by filtration through a 0.45

μm cellulose acetate filter and supplementation of 1 μg/ml polybrene (Milipore), and added to target cells immediately. This step was performed twice a day for 2 days.

On day 5, the virus containing medium was replaced with growth media and changed every 3-4 days until the day of analysis. For positive selection, puromycin (SIGMA) at 2 μg/ml was added to target cells three days after viral infection and maintained in growth medium at the concentration of 1 μg/ml. For some experiments, iCM maturation medium consisting of 4:1 DMEM:M199 with 10% FBS and 1% Penicillin/Streptomycin (100 U/ml:100 μg/ml) was used.

Flow cytometry

For live staining, cells were incubated with the following reagents and conditions (**Table 1**). After incubation, cells were washed with PBS and trypsinized. Cells were then centrifuged (5 minutes, 1000 rpm, RT), washed with PBS and resuspended in 0.05% Bovine Serum Albumin (BSA) (SIGMA) + PBS 1x.

Table 1. Reagents used in Flow Cytometry with respective concentration, incubation time and temperature.

	Mitotracker Deep Red (Life technologies)	**Bodipy** (Invitrogen)	**TMRE** (Abcam)	**Mitosox** (Invitrogen)	**CellROX** (Invitrogen)
Concentration	2nM	0.15 μg/mL	100 nM	5 μM	2 μM
Incubation	15 min RT dark	10 min RT dark	20 min 37ºC	15 min 37ºC	20 min 37ºC

For intracellular staining, cells were incubated with Mitotracker Deep Red (200 nM) in the dark, at RT for 15 minutes. Cells were trypsinized and centrifuged as before. The pellet was resuspended in PBS, fixed with 4% formaldehyde (Thermo Scientific) and incubated on ice for 15 min. Cells were washed with PBS, followed by centrifugation at 1200 rpm for 5 minutes at 4ºC. After permeabilization with 0.5% tween (MARCA) 20 + 0.5% DMSO for 10 minutes in rotation and a spin (1200 rpm, 5 min), cells were treated with Stain Buffer (0.5% BSA + PBS 1x) for 10 min at RT followed by incubation with anti-cTnT (cardiac troponin T) mouse primary antibody (1:200) (Abcam) for 1 hour in rotation at RT. Cells were washed with Stain Buffer, centrifuged (1200 rpm, 5 min) and incubated with anti-mouse Alexa 488 secondary antibody (1:800) (Invitrogen) for 45 min in rotation in the dark. Cells were washed with Stain Buffer and centrifuged as before and resuspended in Stain Buffer.

Prior to analysis, cells were filtered through a 40 μm cell strainer and acquisition was made in an Accuri™ C6 Flow Cytometer (BD Biosciences). Analysis was conducted in FlowJo software, where a gating for alive and singlets events was performed before analysis of populations of interest with fluorescent marker.

Immunocytochemistry and Fluorescence Microscopy

Cells were washed with PBS three times, fixed with 4% formaldehyde at RT for 15 minutes, washed again and stored at 4ºC in PBS between 1 – 7 days.

After permeabilization with 0.1% Triton/PBS for 10 minutes (with three subsequent PBS washes) and blocking in 1% BSA for 30 minutes, cells were treated with primary antibody at 4ºC overnight and secondary antibody for 1h30 at RT. The cells were then mounted with Vectashield with DAPI (Vector Laboratories). The following antibodies and reagents were used: anti-HSP60 mouse (1:200) (BD Biosciences), anti-mouse Alexa 488 (1:500) (Invitrogen), anti-phalloidin 568 (1:200), anti-TOM20 rabbit (1:100 and 1:150) (Proteintech), anti-rabbit Alexa 488 (1:500) (Invitrogen), anti-cTnT mouse (1:150) (Abcam), anti-mouse Alexa 594 (1:500) (Invitrogen) and α-GFP Alexa 488 (Invitrogen).

Images were acquired using a 63x oil objective of the Zeiss LSM 880 confocal fluorescence microscope. The mitochondrial network and morphology were evaluated by ImageJ/Fiji plug-in Mitochondrial

Analyzer (Chaudhry et al., 2020) (**Figure 6**). The corrected total cell fluorescence (CTCF) was also analyzed in ImageJ/Fiji and was calculated using the formula: CTCF = Integrated Density – (Area of selected cell x Mean fluorescence of background readings) (Hammond, 2014).
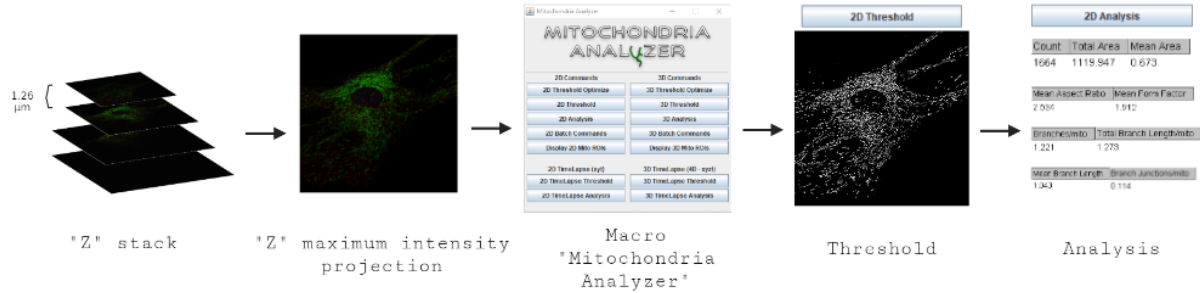
Figure 6. Overview of the quantification of mitochondrial network. Briefly, a z-stack of images (with an interval of 1,26 µm) was acquired using a Zeiss LSM 880 confocal fluorescence microscope. Using ImageJ/Fiji, maximum intensity projections were obtained from each z-stack. Images were thresholded and analyzed trough macro "Mitochondrial Analyzer" (Chaudhry et al., 2020). Figure made using BioRender.

Reverse Transcriptase Reaction

RNA samples from MEFs and AEFs cells in their respective conditions (Empty and MGT), previously extracted and isolated in the lab, were retrotranscribed to cDNA using the "NZY First-Strand cDNA Synthesis Flexible pack" and following the manufacturer instructions. Briefly, 1 µg of RNA was mixed with 1.5 µl of Oligo(dT)$_{12-18}$, 1.5 µl of Random hexamer mix, 1 µl of dNTP Mix and DEPC-treated H_2O to make up 16 µl. This mixture was incubated at 65 °C for 5 min and chilled on ice. To the mixture were then added 2 µl of Reaction Buffer, 1 µl of NZY Ribonuclease Inhibitor and 1 µl of NZY Reverse Transcriptase, making up a volume of 20 µl of reaction. It proceeded to incubation at 25 °C for 10 min, followed by 50 °C for 50 min and then, to inactivate the reaction, 85 °C for 5 min. The reaction chilled on ice, before 1 µl of NZY RNase H was added, with subsequent incubation of 37 °C for 20 min. The generated cDNA was diluted at 1:5 and stored at -20ºC.

Quantitative Polymerase Chain Reaction (qPCR)

For each reaction, 5 µl of cDNA (at 1:5) was mixed with 7.5 µl of SYBR Green (Thermo Fisher Scientific), 0.4 µl of each forward and reverse primers (see **Table 2**) and 1.7 µl of H_2O, making up a final volume of 15 µl. qPCR was performed using Applied Biosystems 7500 Real-Time PCR System and 18S rRNA was used as housekeeping gene. Values were given by $2^{-\Delta\Delta Ct}$, through the ΔΔCt method ($\Delta C_{T(test)} - \Delta C_{T(calibrator)}$).

Table 2. Amplified genes and primer sequences used for qPCR.

Amplified Genes	Sequence (F: forward primer, R: reverse primer)
18S	F: AGGATGTGAAGGATGGGAAGT
	R: CAGGTCCTCACGCAGCTTG
TFAM	F: AACACCCAGATGCAAAACTTTCA
	R: GACTTGGAGTTAGCTGCTCTTT
NRF1	F: AGCACGGAGTGACCCAAAC
	R: AGGATGTCCGAGTCATCATAAGA
PINK1	F: TTCTTCCGCCAGTCGGTAG
	R: CTGCTTCTCCTCGATCAGCC
OPA-1	F: TGGAAAATGGTTCGAGAGTCAG
	R: CATTCCGTCTCTAGGTTAAAGCG

Mfn1	F: ATGGCAGAAACGGTATCTCCA
	R: GCCCTCAGTAACAAACTCCAGT
Parkin	F: GAGGTCGATTCTGACACCAGC
	R: CCGGCAAAAATCACACGCAG
LC3	F: TTATAGAGCGATACAAGGGGGAG
	R: CGCCGTCTGATTATCTTGATGAG
Mef2c	F: GAGCCGGACAAACTCAGACA
	R: TCAAAGCTGGGAGGTGGAAC
Gata4	F: TGTGCCAACTGCCAGACTAC
	R: TGGGCTTCCGTTTTCTGGTT
Tbx5	F: CTTCTATCGCTCGGGCTACC
	R: GCTATAGGAGGGCATGCTGG
Myl7	F: TCGGGAGGGTAAGTGTTCC
	R: GTCCGTCCCATTGAGCTTCTC
Tnnt2	F: GAGCTACAGACTCTGATCGAGG
	R: CCGCTCATTGCGAATACGC
ACTC1	F: TGCCCCCGGCTGCTC
	R: GTTCTGTAGGCGTGCTAGGG
Col3a1	F: CTGTAACATGGAAACTGGGGAAA
	R: CCATAGCTGAACTGAAAACCACC
Eln	F: TGTCCCACTGGGTTATCCCAT
	R: CAGCTACTCCATAGGGCAATTTC
PGC1-α	F: TATGGAGTGACATAGAGTGTGCT
	R: CCACTTCAATCCACCCAGAAAG
Fis1	F: AGAGCACGCAATTTGAATATGCC
	R: ATAGTCCCGCTGTTCCTCTTT
Mtfp1	F: GCTACGCCAATGAGGTGGG
	R: AGACTGCCACACAAAGGTGTC
Col1a1	F: GCTCCTCTTAGGGGCCACT
	R: CCACGTCTCACCATTGGGG
P62	F: AGGATGGGGACTTGGTTGC
	R: TCACAGATCACATTGGGGTGC

Statistical Analysis

The results are presented as mean values and standard deviations (mean ± SD) or standard error of the mean (mean ± SEM) for each experimental group.

Differences between samples comparing with the control conditions were estimated by T student test. Multiple comparisons were performed with One-way ANOVA or Kruskal Wallis with a false discovery rate correction. For normality, the Shapiro-wilk test was performed. A P value < 0.05 was regarded statistically significant. Details of the sample numbers can be found in the appropriate figure legend.

Statistical analysis was performed using GraphPad Prism.

Results

1. Direct Cardiac Conversion presents low efficiency in mouse adult fibroblasts

DCC is a very promising cardiac regenerative technique, although it still lacks efficiency (Chen et al., 2012). Indeed, at day 11 (D11) post transduction and puromycin selection of MGT-retroviral infected cells, only 4% of MGT-transduced embryonic fibroblasts (MEFs) are positive for the cardiac marker cTnT, detected by flow cytometry (**Figure 7**). Moreover, aging leads to an even further decrease of efficiency as adult fibroblast cells (from the skin or cardiac origin) appear to have more difficulty in the process, when compared to embryonic fibroblasts (Kojima & Ieda, 2017).
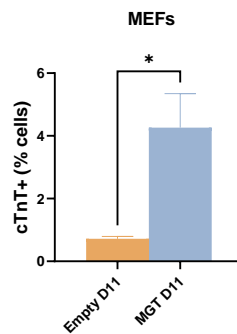
Figure 7. Reprogramming efficiency quantified by flow cytometry for the percentage of cTnT+ cells at 11 days (D11) after infection of MEFs with retroviruses expressing MGT. Cells infected with empty vector viruses were used as control and cTnT intracellular staining (conjugated to anti-mouse Alexa 488 secondary antibody) detected in the FL1 channel .Cells were cultured with 4:1 DMEM low glucose:M199 + 10% FBS + 1% Penicillin/Streptomycin.
Data is presented as Mean ± SEM (n = 3 from 1 independent experiment); statistical significance was determined by Student t-test. *P < 0.05.

In order to see how DCC affects the gene expression profile in both embryonic and adult fibroblasts, we evaluated several markers by qPCR in MGT and Empty-retroviral infected cells at D12 post-transduction. Analysis of the expression of the *MGT* genes (Mef2c, Gata4 and Tbx5) (**Figure 8**) revealed that, as expected, the expression of the reprograming factors was increased in both MEFs and AEFs-transduced with MGT, when compared to their Empty counterparts.
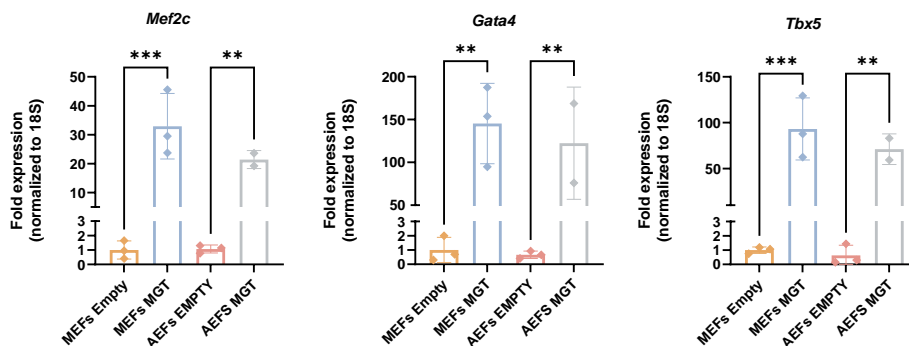
Figure 8. Reprogramming genes expression profile of MEFs and AEFs groups in their respective conditions (Empty and MGT) normalized to 18S rRNA and represented as the fold change over MEFs Empty, at D12 post transduction. Cells were cultured with 4:1 DMEM high glucose:M199 + 10% FBS + 1% Penicillin/Streptomycin.

Data is presented as Mean ± SD (n=2/3 from 1 independent experiment); statistical significance was determined by One-way ANOVA with False Discovery Rate multiple comparisons test. **P < 0.01; ***P < 0.001.

It has been reported that, during DCC, there is first an activation of cardiac genes at as early as D3 post transduction and a deactivation of fibroblast genes at around D10 post transduction (Kojima & Ieda, 2017). Analysis of the expression of cardiac (*Myl7*, *Tnnt2* and *Actc1*) and fibroblast (*Col1a1*, *Col3a1* and *Eln*) markers by qPCR (**Figure 9**) revealed that, at D12 post transduction, a significant increase of the expression of all cardiac genes is observed in MEFs transduced with MGT, when compared with MEFs Empty, as well as a significant decrease of all fibroblast markers. However, for AEFs transduced with MGT, the expression of cardiac genes only shows a slight tendency to increase (e.g., *Myl7),* while the levels of all fibroblast markers remain unchanged compared to the control. Moreover, the expression of fibroblast markers, particularly *Col1a1* and *Eln*, decreases significantly in control (Empty) adult fibroblasts compared to embryonic MEFs. These results were further validated at the protein level, with MEFs MGT presenting higher level of cTnT expression than AEFs MGT, as detected by immunofluorescence and confocal microscopy (**Figure 10**).
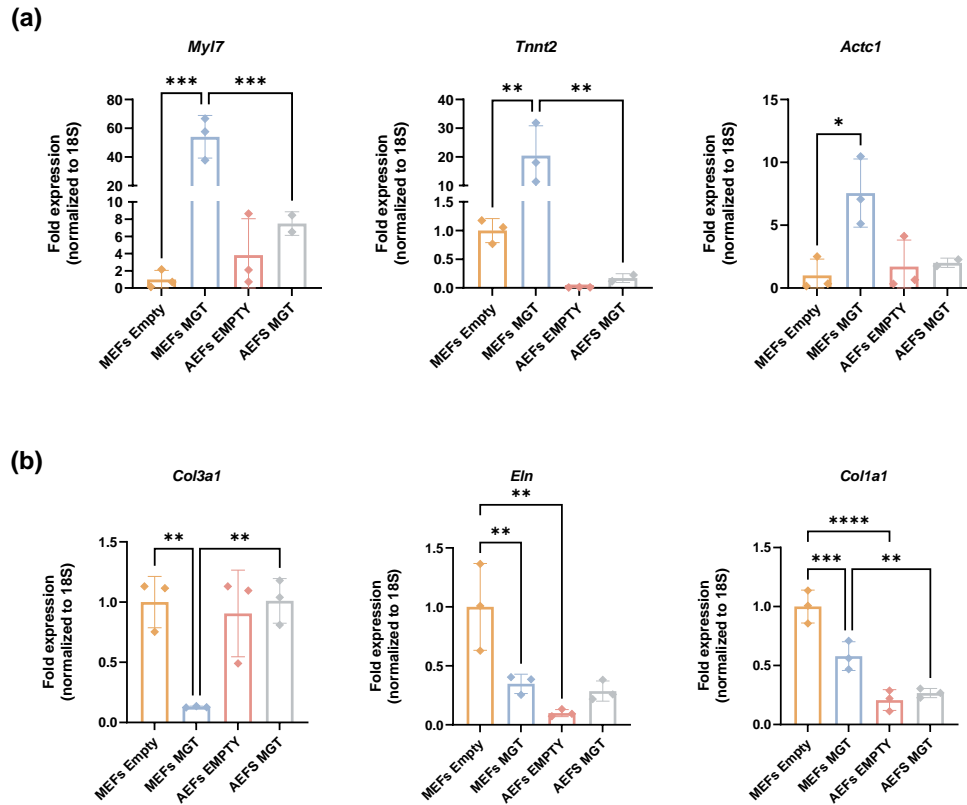
Figure 9. Cardiac (**a**) and fibroblast (**b**) genes expression profile of MEFs and AEFs groups in their respective conditions (Empty and MGT) normalized to 18S rRNA and represented as the fold change over MEFs Empty, at D12 post-transduction. Cells were cultured with 4:1 DMEM high glucose:M199 + 10% FBS + 1% Penicillin/Streptomycin.
Data is presented as Mean ± SD (n=2/3 from 1 independent experiment); statistical significance was determined by One-way ANOVA with False Discovery Rate multiple comparisons test. *P < 0.05; **P < 0.01; ***P < 0.001; ****P < 0.0001.
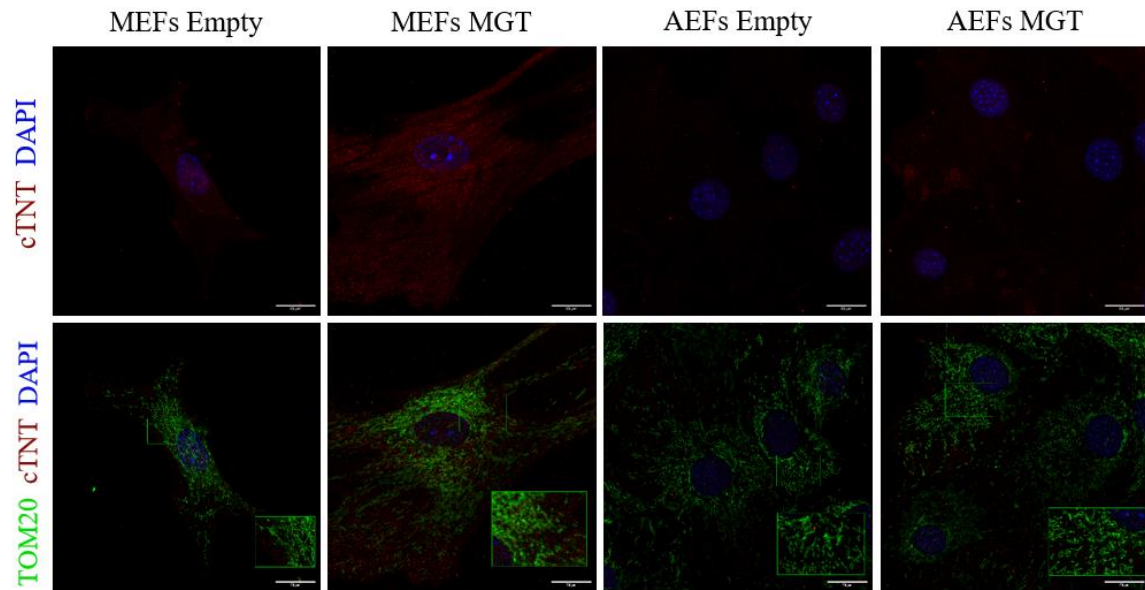
Figure 10. Representative immunocytochemistry images of MEFs and AEFs infected with Empty and MGT retroviruses at D11 post-transduction and stained with cTnT (cardiac troponin) (upper) and double labelling of cTnT and TOM20 (mitochondria) with 2.0x zoom (lower). DAPI stains for nuclei. Scale bar equals 20 μm.

Overall, these results show that both MEFs and AEFs underwent forced expression of the cardiogenic factors with activation of *MGT* expression. Moreover, at D11/12 post transduction, embryonic transdifferentiated fibroblast cells already show an activation of cardiac markers and deactivation of fibroblast markers, while, at the same timepoint, adult fibroblasts cells do not show major differences compared to empty controls especially in fibroblast genes suppression.

2. Direct Cardiac Conversion is accompanied by alterations in the mitochondria network

During DCC, the fibroblasts undergo a metabolic switch from glycolysis to OXPHOS (H. Wang et al., 2021). With this, mitochondria gain a more prominent role in supplying the cell with energy, which requires some changes in the network. Indeed, cardiomyocytes also go through a similar energetic transformation, the fetal metabolic switch, leading to a maturation of the cell, as well as a remodeling of the mitochondria (A. Li et al., 2020). However, the exact changes in the mitochondrial network that accompany DCC remain uncharacterized.

To address the remodeling of the mitochondrial network during DCC of embryonic and adult fibroblasts, MEFs and AEFs MGT-infected (D11 post-transduction) were used for immunofluorescence detection of the mitochondrial protein TOM20, a component of the mitochondrial Translocase of the Outer Membrane (TOM) complex (Giacomello et al., 2020), through confocal microscopy using a Zeiss LSM 880 confocal fluorescence microscope (**Figure 10**). Images were analyzed through Fiji's macro *"Mitochondria Analyzer"* (Chaudhry et al., 2020), with the evaluated parameters briefly summarized in **Table 3** and the quantifications expressed at **Figure 11.**

MITO COUNT	1	1	1
TOTAL AREA	↓	↑	↑↑
MEAN AREA	↓	↑	↑↑
ASPECT RATIO	= 1 (Round)	> 1 (Elongated)	> 1 (Elongated)
FORM FACTOR	= 1 (Round)	> 1 (Elongated)	> 1 (Elongated)
BRANCH	1 (I)	1 (I)	3 (I-III)
BRANCH JUNCTION	0	0	2 (1-2)
MEAN BRANCH LENGHT	↓	↑↑	↑
TOTAL BRANCH LENGHT	↓	↑	↑↑

Table 3. Summary of morphological and network parameters used to describe mitochondria on a round mitochondrion (Left), a long mitochondrion (Middle) and mitochondria with multiple branches (I-III) and junctions (1-2) (Right). Adapted from (Chaudhry et al., 2020).

The number of mitochondria is given by Mito Count (normalized to the cell area) where MEFs present the highest organelle number, followed by AEFs (**Figure 11a**), and no difference between MGT and Empty was observed. The Total Area occupied by the mitochondria (normalized to the cell area) (**Figure 11b**) displayed higher levels in MEFs MGT than AEFs MGT, both surpassing their corresponding Empty. MEFs MGT present the highest Mean Area of mitochondria particles (**Figure 11c**), while in adult fibroblasts, Empty present higher than MGT transduced. The shape is reflected in the Form Factor (FF) and Aspect Ratio (AR), where 1 is equivalent to round particles and increases with more elongated particles (**Table 3**). In **Figure 11d-e**, it is possible to evaluate that MGT-transduced MEFs present highest AR and FF than corresponding Empty, while in AEFs, MGT transduction produced a decrease or no significant differences in AR and FF, respectively. The mitochondrial network is described by the number of Branches (connected mitochondria), the Junctions between them (connecting points) and their size which is given by both Mean and Total Branch Length (**Table 3**), all normalized to the number of mitochondria. In all these parameters (**Figure 11f-i**), MGT-transduction produced increase levels in MEFs whereas no major differences were observed for AEFs transduced cells comparing to Empty. Moreover, analysis of TOM-20 staining intensity, performed using Fiji, further revealed that at D11, MGT-transduced MEFs present higher total TOM-20 fluorescence levels compared to corresponding Empty transduced cells (**Figure 12a**), whereas AEFs MGT transduced show similar values to AEFs Empty (**Figure 12b**).

With this analysis, it is visible that, at D11 post-transduction, MEFs infected with MGT acquire a more filamentous and interconnected network characteristic of higher energetic demands (as of induced cardiomyocytes), when comparing with Empty-infected MEFs. However, at the same timepoint (D11), AEFs transduced with MGT do not show differences in the majority of the parameters analyzed, especially for the network, compared to Empty-transduced AEFs.
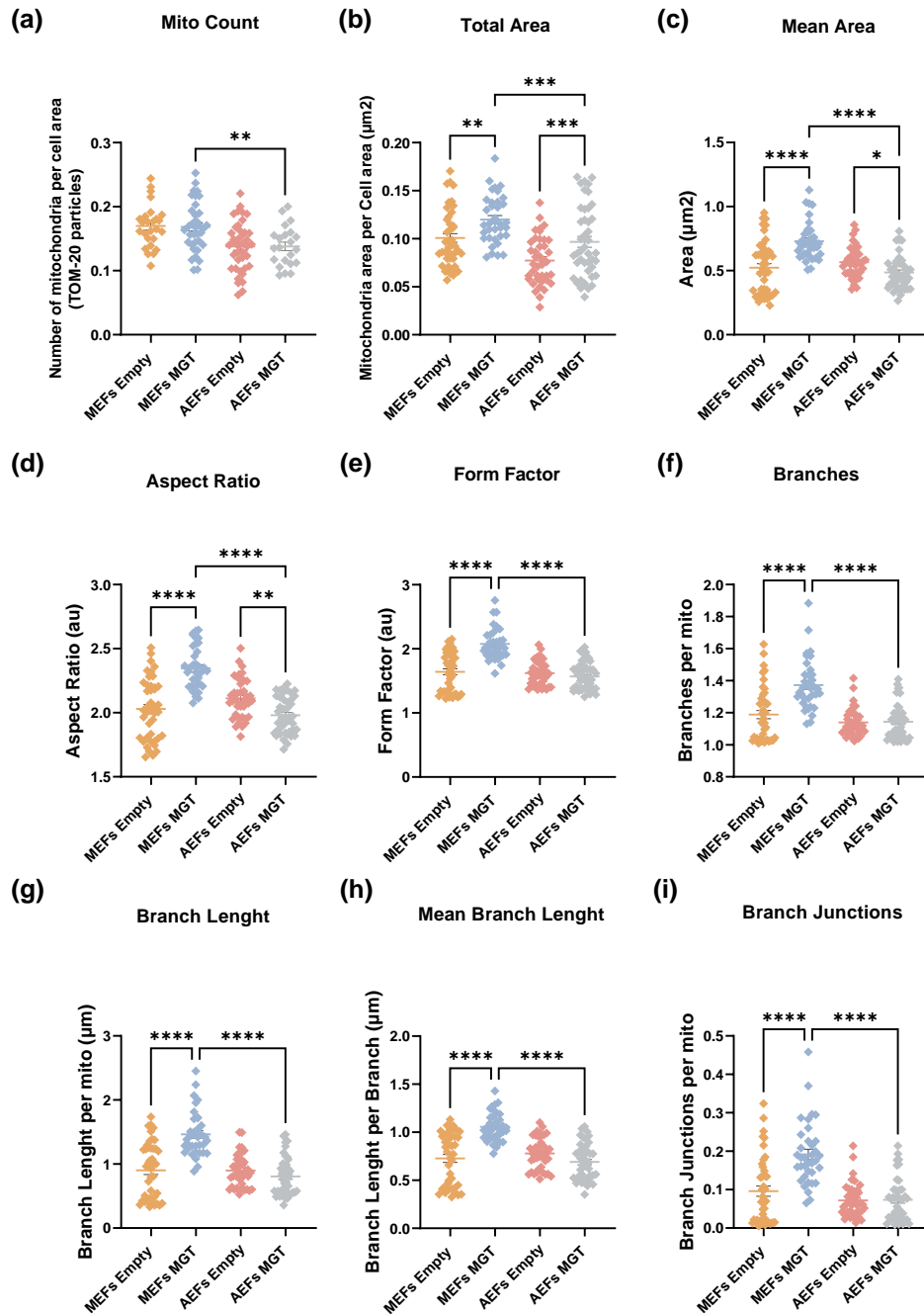
Figure 11. Quantitative analysis and comparison of TOM-20 stained mitochondria number **(a)**, area **(b-c)**, shape **(d-e)** and network **(f-i)** parameters (briefly summarized in table 3), between MEFs and AEFs in their respective conditions (Empty and MGT), at D11 post transduction. Cells were cultured with 4:1 DMEM high glucose:M199 + 10% FBS + 1% Penicillin/Streptomycin (experiment 1) and 4:1 DMEM low glucose:M199 + 10% FBS + 1% Penicillin/Streptomycin (experiment 2). Au = Arbitrary units

Data is presented as Mean ± SEM (n=22/40 from 1-2 independent experiments); statistical significance was determined by One-way ANOVA or Kruskal-Wallis with False Discovery Rate multiple comparisons test. *P < 0.05; **P < 0.01; ***P < 0.001; ****P < 0.0001.
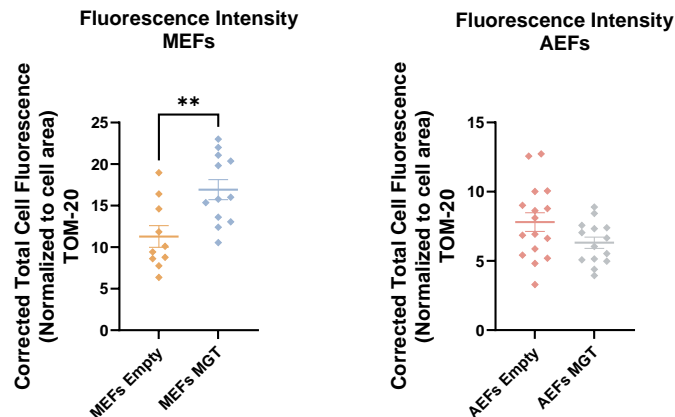
Figure 12. Quantitative analysis and comparison of TOM-20 fluorescence intensity between MEFs Empty and MGT (a) and AEFs Empty and MGT (b), at D11-days post transduction. Cells were cultured with 4:1 DMEM low glucose:M199 + 10% FBS + 1% Penicillin/Streptomycin.
Data is presented as Mean ± SEM (n = 10/16 from 1 independent experiment); statistical significance was determined by Student t-test. **P < 0.01.

A similar analysis by immunofluorescence was performed using the alternative mitochondrial marker HSP-60, a stress protein involved in the folding of proteins (Pellegrino et al., 2013) (**Supplementary Figure 1**) where, additionally, the cardiac HL-1 cell line was used as positive control for cardiomyocytes. Regarding mitochondria number (**Supplementary Figure 1a**), HL-1 presents the highest value, followed by both MEFs and AEFs with no significant differences between MGT and Empty conditions. In Total area (**Supplementary Figure 1b**), an increase is seen in MEFs MGT comparing to corresponding Empty, with no significant differences between AEFs' conditions. For Mean Area as well as all shape and network parameters (**Supplementary Figure 1c-i**), both MEFs and AEFs MGT transduced present higher values than corresponding Empty, being similar to HL-1. Analysis of HSP-60 staining intensity (**Supplementary Figure 2**) revealed no significant differences between MEFs and AEFs experimental groups with HL-1 presenting the highest HSP-60 total fluorescence levels. Overall, in this analysis, age doesn't seem to have an impact in the mitochondrial changes that accompany DCC, in contrast to TOM-20 evaluation (**Figure 11**), with both MEFs and AEFs MGT transduced presenting a more filamentous network than their Empty counterparts and approaching the cardiac cell line HL-1.

Despite the high efficiency of retroviruses used for MGT infection (with around 90% of infected cells with a similar plasmid encoding GFP, pMXsGFP, data not shown), which is further incremented by Puromycin-selection (L. Wang et al., 2015), DCC is an inefficient and unsynchronized process as not all cells undergo DCC at the same time (Liu et al., 2017). Therefore, to evaluate the mitochondrial parameters specifically in MGT-transduced cells that already express cardiac markers, we used the cardiac marker cTnT to stratify the MEFs MGT-infected cells into cTnT-positive and cTnT-negative (**Figure 10**). No significant differences were observed regarding mitochondria number, total area and mean area between Empty, cTnT-negative and cTnT-positive (**Figure 13a-c**). However, there is a marked increase in shape (AR, FF) and branch related parameters in cTnT-positive compared to cTnT-negative cells, reaching significance only in relation to MEFs Empty (**Figure 13d-i**), in agreement with **Figure 11**. This suggests that, as expected, MGT-transduced cells that already express cardiac markers have a more filamentous and interconnected mitochondria network than the remaining MGT-transduced cTnT-negative cells. Indeed, the MEFs MGT cTnT-positive are closely followed by the cTnT-negative, especially in shape parameters (**Figure 13d-e**), showing a tendency to increase in branch parameters compared to MEFs Empty (**Figure 13f-i**), suggesting that these cells are also undergoing

changes in their mitochondrial network, despite not yet expressing cardiac markers. Similar results were obtained with the same analysis performed on adult fibroblast cells, with a tendency to increased branch number, length and junctions in AEFs MGT-cTnT positive compared to Empty (**Supplementary Figure 3**), however the low number of analyzed cells did not allow to reach significance.
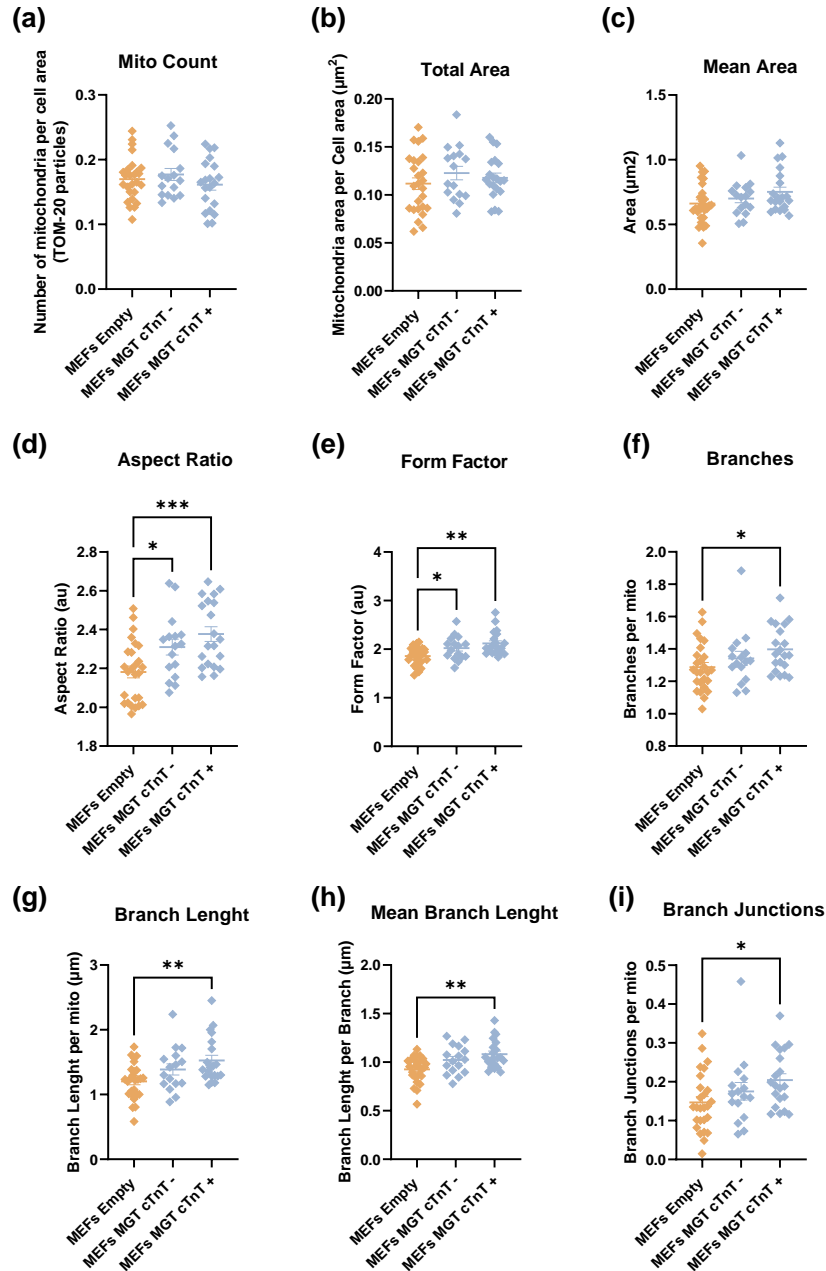
Figure 13. Quantitative analysis and comparison of TOM-20 stained mitochondria number (**a**), area (**b-c**), shape (**d-e**) and network (**f-i**) parameters (briefly summarized in table 3), between MEFs Empty and MGT, divided in cTnT-negative and cTnT-positive, at D11-days post-transduction. Cells were cultured with 4:1 DMEM low glucose:M199 + 10% FBS + 1% Penicillin/Streptomycin.

Data is presented as Mean ± SEM (n = 16/26 from 1 independent experiment); statistical significance was determined by One-way ANOVA or Kruskal-Wallis with False Discovery Rate multiple comparisons test. *P < 0.05; **P < 0.01; ***P < 0.001.

In order to assess the evolution of the mitochondria network with the progression of DCC, the same mitochondrial parameters (**Table 3**) were evaluated at late stages of DCC in AEFs at D21 post-transduction by immunofluorescence detection of TOM20, depicted as fold to corresponding Empty (**Figure 14**). Apart from Mito Count, (**Figure 14a**) where no differences were observed, all remaining parameters (**Figure 14b-i**) measured at AEFs 21 days display higher values than AEFs 11 days, with a tendency to surpass the values present in MEFs 11 days, confirming the slower progress of AEFs during DCC.
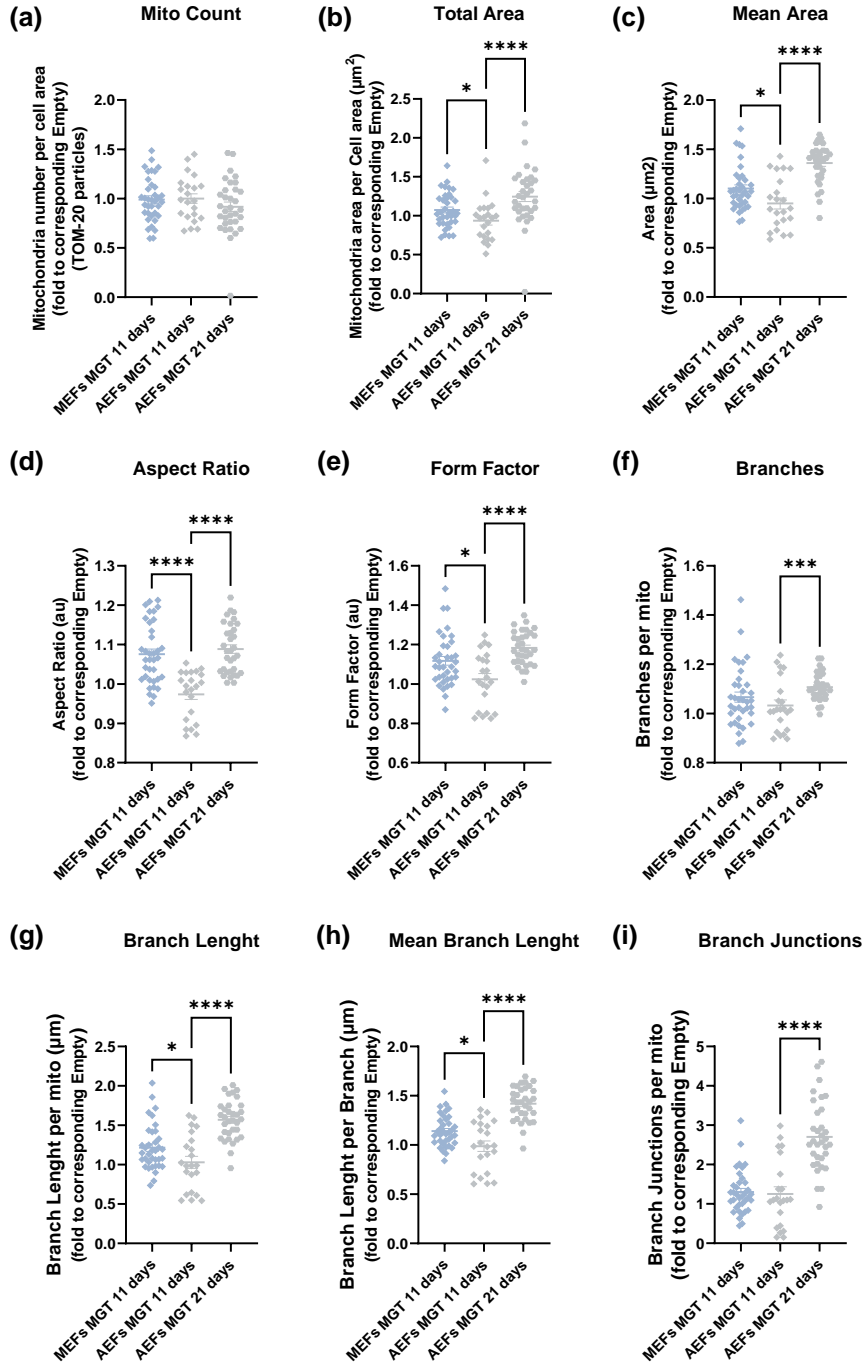
Figure 14. Quantitative analysis and comparison of TOM-20 stained mitochondria number (a), area (b-c), shape (d-e) and network (f-i) parameters (briefly summarized in table 3), between MEFs and AEFs groups MGT-infected (Fold to corresponding Empty), D11 and D21 post-transduction. Cells were cultured with 4:1 DMEM low glucose:M199 + 10% FBS + 1% Penicillin/Streptomycin.

Data is presented as Mean ± SEM (n=22/36 from 1 independent experiment); statistical significance was determined by Kruskal-Wallis with False Discovery Rate multiple comparisons test. *P < 0.05; ***P < 0.001; ****P < 0.0001.

We reasoned that modulating of signaling pathways that control cell fate conversion, including mitochondrial metabolism, may increase the efficiency of DCC and bring new opportunities for direct cardiac reprogramming. In that sense, in the lab we are using an inducible reprogrammable mouse embryonic fibroblast cell line, icMEFs, kindly provided by LiQian lab, in which MGT expression is induced by the addition of doxycycline (Dox), enabling the temporal control of reprogramming factor expression. This cell line presents a reprogramming efficiency of up to 20% (Vaseghi et al., 2016), and allows for a more accurate analysis of reprogrammed cells, since transdifferentiated fibroblasts are easily detected by the expression of the reporter Green Fluorescent Protein (GFP) protein by immunofluorescence, which is controlled by the cardiac promoter α muscle heavy chain (αMHC) (**Figure 15**). In order to evaluate if DCC of this inducible cell line is also accompanied by mitochondrial network remodeling as it is for the primary fibroblasts (**Figure 11**), we evaluated the same parameters as before (**Table 3**) by immunofluorescence detection of HSP-60 in icMEFs 3 days after Dox administration (**Figures 15 and 16**). Interestingly, a statistically increase in all parameters analyzed, except for the Mean Area, was observed in GFP-expressing icMEFs with Dox compared to icMEFs without Dox (**Figure 16a-i**), confirming that fibroblasts from the icMEFs cell line that have undergone reprogramming, marked by the expression of the cardiac reporter αMHC-GFP, gain a more filamentous network, in agreement to what was observed for primary MGT-transduced MEFs (**Figure 11** and **Supplementary Figure 1**).
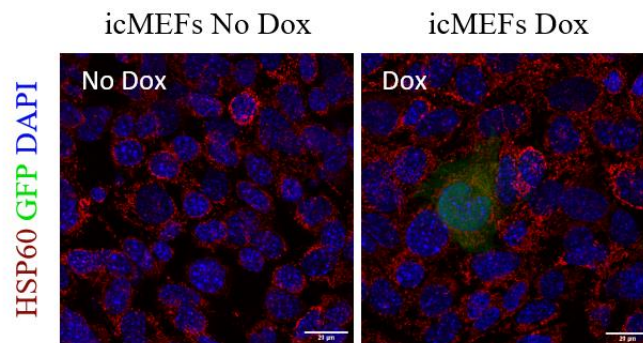
Figure 15. Representative immunocytochemistry images of icMEFs without or 3 days post-doxycycline administration and stained with HSP60 (mitochondria). DAPI stains for nuclei. Scale bar equals 20 μm.
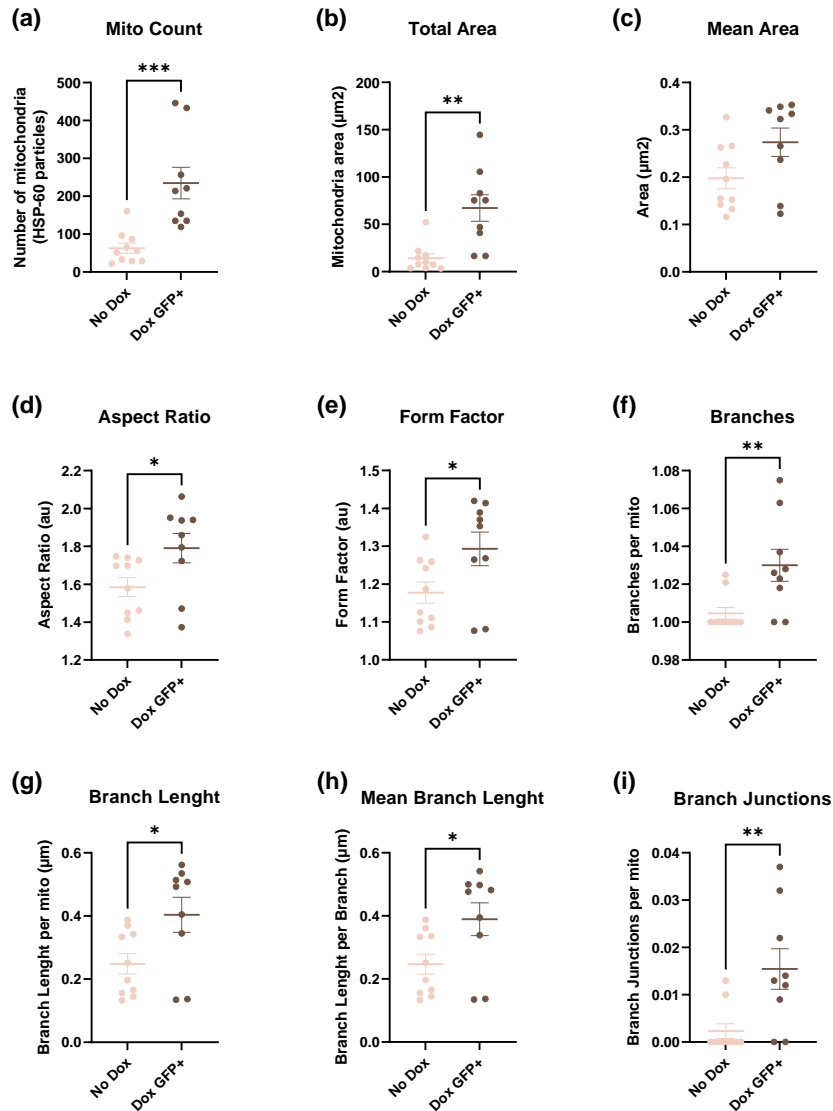
Figure 16. Quantitative analysis and comparison of HSP-60 stained mitochondria number (a), area (b-c), shape (d-e) and network (f-i) parameters (briefly summarized in Table 3), between icMEFs without or 3 days post-doxycycline administration in GFP-positive cells. Cells were cultured with 4:1 DMEM low glucose:M199 + 10% FBS + 1% Penicillin/Streptomycin.
Data is presented as Mean ± SEM (n=9/10 from 1 independent experiment); statistical significance was determined by Student t-test. *P < 0.05; **P < 0.01; ***P < 0.001.

Mitochondria network remodeling depends on processes such as mitochondrial biogenesis, mitophagy, and fusion and fission dynamics (Tronstad et al., 2014). Therefore, to start dissecting the mechanism that leads to remodeling of the mitochondrial network during DCC of embryonic and adult fibroblast cells into iCLMs, the expression of several genes involved in these processes was evaluated through qPCR (**Figure 17**). Analysis of the mitochondria biogenesis genes *PGC1- α*, *Nrf1*, and *TFAM* (**Figure 17a-c**), shows that MEFs MGT-transduced express significant less *PGC1-α* compared to AEFs MGT, whereas for the other genes, no major differences were observed, only a trend to increase expression in MGT transduced compared to corresponding Empty fibroblasts. Regarding mitochondrial dynamics, with fusion genes *Opa1* and *Mfn1* and fission genes *Mtfp1* and *Fis1* (**Figure 17d-g**), no significant differences were observed, only a tendency to increase in AEFs MGT over Empty in all four genes. Regarding mitophagy, we assessed the expression of the mitophagy-specific *Pink1* and *Parkin* genes as well as the autophagy-related *LC3* and *SQSTM1* (p62 coding gene) (**Figure 17h-k**). For *Pink1* and *Parkin*, AEF MGT-transduced cells present a trend

to increase levels than corresponding Empty, whereas the opposite occurs in MEFs. Indeed, AEFs MGT-transduced cells express significantly higher *Parkin* than MEFs-MGT (**Figure 17i**). Regarding the autophagy genes, there is a general trend to higher *LC3* expression between MGT and corresponding Empty, with AEFs-MGT expressing significantly more *LC3* than AEFs-Empty and MGT-transduced MEFs (**Figure 17j**). However, for the *SQSTM1*, the same trend to increase expression between MGT and Empty is observed only for MEFs, with MGT-transduced AEFs expressing significantly lower levels than MEFs-MGT (**Figure 17k**).
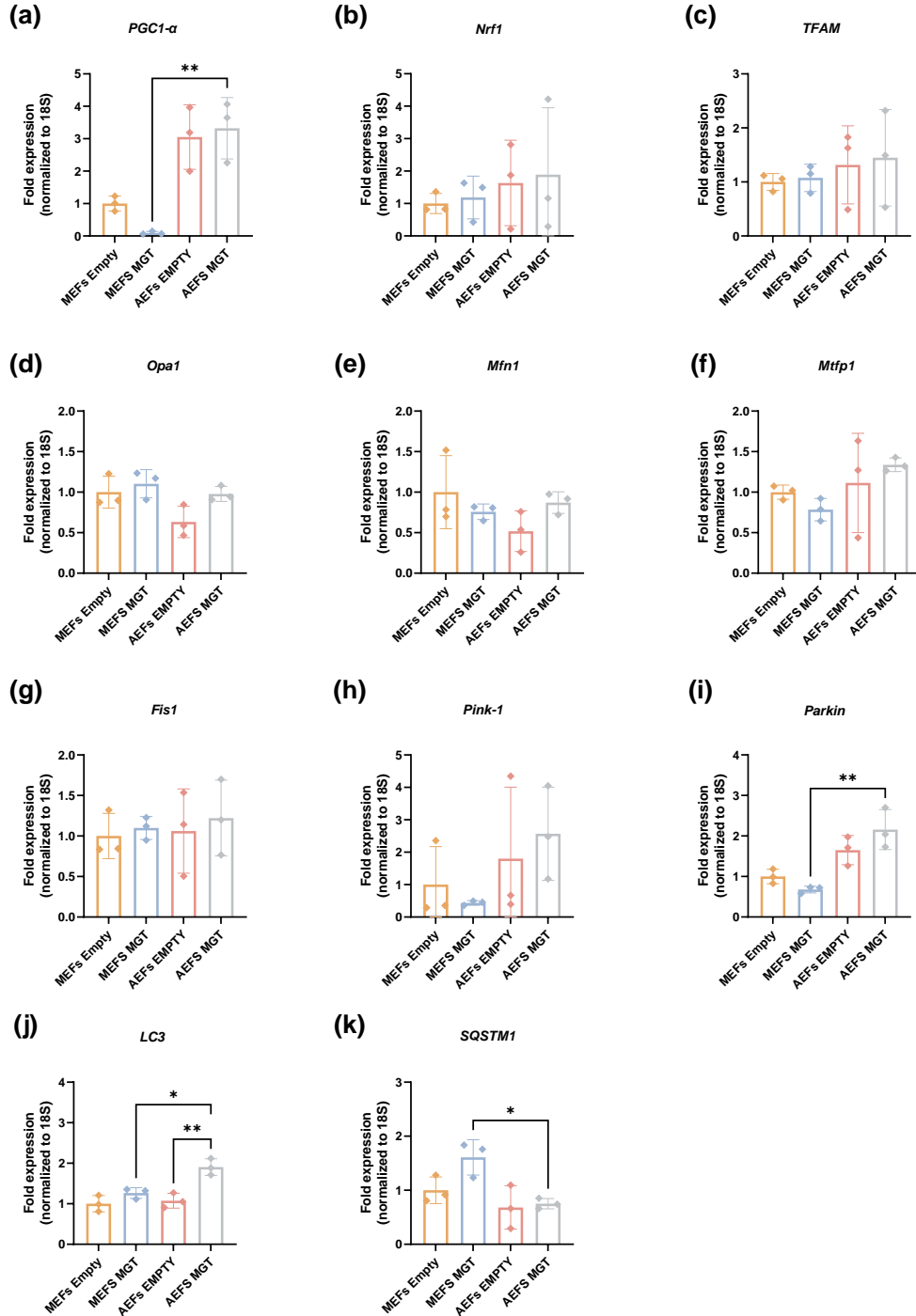
Figure 17. Gene expression profile of MEFs and AEFs transduced with Empty and MGT retroviruses at D12 post transduction, displaying mitochondrial biogenesis (a-c), dynamics (d-g) and autophagy (h-k) genes, all normalized to 18S rRNA and represented as the fold change over MEFs Empty. Cells were cultured with 4:1 DMEM high glucose:M199 + 10% FBS + 1% Penicillin/Streptomycin.

These results show that, despite the remodeling in the mitochondrial network during DCC taking more time in AEFs and being more evident in MEFs; the expression of key biogenesis, fusion and fission genes overall appear unaltered, suggesting a very dynamic balance between these processes or other regulatory mechanisms. As for mitophagy, the increase in expression in Parkin and LC3 in adult MGT transduced cells, while decreasing the expression of *SQSTM1*, could suggest a potential deregulation of the mitophagy process in adult transduced fibroblasts.

3. *The metabolism of adult and embryonic fibroblasts differs during Direct Cardiac Conversion*

As mentioned previously, a metabolic switch is expected to occur during DCC (H. Wang et al., 2021), highlighting the potential of metabolic interventions to increase DCC efficiency specially in adult fibroblasts. To better understand the metabolic changes occurring through the DCC process in embryonic and adult fibroblasts, a flow cytometry assessment of metabolic markers was conducted at different days post-transduction (D6, D11/13 and D21/28).

Cardiomyocytes depend heavily on mitochondrial OXPHOS for their large energy demands (Vásquez-Trincado et al., 2016). In order to complement the results obtained with the evaluation of mitochondrial proteins by immunocytochemistry (**Figures 11-16**), the mitochondrial mass was preliminarily measured in several time-points during DCC using Mitotracker (**Figure 18**). Indeed, MEFs MGT present a non-significant tendency to increase Mitotracker staining compared to corresponding Empty and over-time. AEFs-MGT-transduced cells, despite presenting lower levels of Mitotracker staining than corresponding AEFs Empty at initial time points (D6 and D11), present increasing levels of Mitotracker over-time during the DCC process (from D6 to D28), compatible with a slower acquisition of mitochondrial mass in adult compared to embryonic iCLMs. Mitotracker staining was additionally performed in icMEFs (**Supplementary Figure 4**), with icMEFs Dox GFP-positive (3 days) presenting higher levels of Mitotracker staining than DOX GFP-negative and cells with no Dox, similarly to what was seen in MEFs.

Figure 18. Mitochondrial Mass quantified by flow cytometry for Mitotracker Deep Red median fluorescence intensity (MFI) in MEFs **(a)** and AEFs **(b)** in their respective conditions (Empty and MGT) represented as the fold change in MGT over Empty at D6, D11 and D28 post transduction. Cells were cultured with 4:1 DMEM high glucose:M199 + 10% FBS + 1% Penicillin/Streptomycin.
Data is presented as Mean ± SD (n = 3/6 from 1 independent experiment); statistical significance was determined by One-way ANOVA with False Discovery Rate multiple comparisons test. *P < 0.05.

A preliminary evaluation of the mitochondrial membrane potential, which is generated during OXPHOS, was performed using TMRE (**Figure 19**). Despite MEFs-MGT presenting lower levels of TMRE

than corresponding MEFs Empty at initial time points (D11, D21), over time, there was an increase in TMRE staining in MGT-transduced MEFs, being the levels of TMRE at D28 significantly higher that previous time points (D21 and D11), (**Figure 19a**). For AEFs, there are no major differences between MGT and Empty transduced cells with a tendency to decrease TMRE staining in MGT-transduced AEFs over-time (**Figure 19b**).
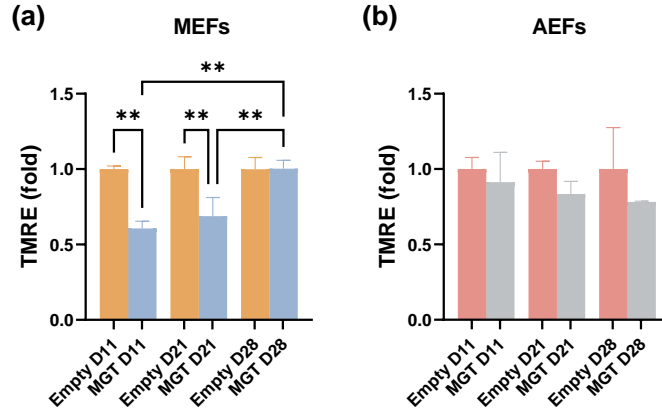
Figure 19. Mitochondrial Membrane Potential quantified by flow cytometry for TMRE MFI in MEFs (a) and AEFs (b) in their respective conditions (Empty and MGT) represented as the fold change in MGT over Empty at D11, D21 and D28 post transduction. Cells were cultured with 4:1 DMEM high glucose:M199 + 10% FBS + 1% Penicillin/Streptomycin. Data is presented as Mean ± SD (n = 3/6 from 1 independent experiment); statistical significance was determined by One-way ANOVA with False Discovery Rate multiple comparisons test. **$P < 0.01$.

Mitochondrial-derived ROS (superoxide anion), a byproduct of OXPHOS, was measured using Mitosox probe. A tendency to decrease Mitosox levels was observed in MGT-transduced cells compared to Empty for both MEFs and AEFs at D13 and D28 post-transduction (**Figure 20a, b**), being more pronounced for MGT-transduced MEFs. If comparing both cell types in the same time point, as expected, adult fibroblasts present overall higher levels than embryonic MEFs at both D13 and D28 (**Supplementary Figure 5a, b**), with both MGT and Empty conditions of AEFs presenting statistically significant higher Mitosox levels than the corresponding conditions of MEFs (**Supplementary Figure 5**). Additionally, we analyzed the alternative ROS probe, Cell ROX, which evaluates cellular ROS species, confirming a trend to decrease staining in MGT-transduced MEFs compared to Empty (**Supplementary Figure 6a**) whereas, on the contrary, the inducible reprogrammable fibroblast cell line icMEFs present significantly higher levels of Cell ROX upon addition of Dox for 3 days in both GFP negative and GFP positive cells, with the latter presenting the highest levels (**Supplementary Figure 6b**).
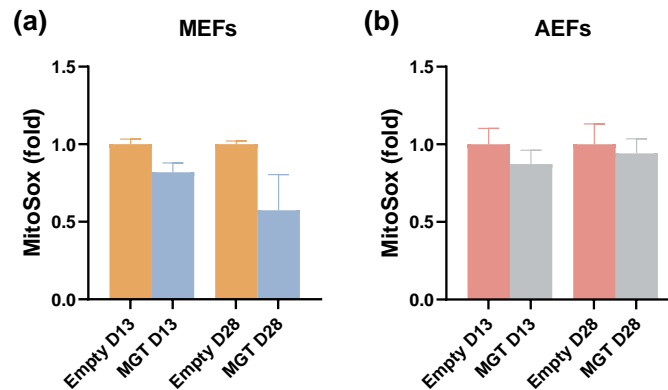
Figure 20. Mitochondrial ROS levels quantified by flow cytometry for Mitosox MFI in MEFs **(a)** and AEFs **(b)** in their respective conditions (Empty and MGT) represented as the fold change in MGT over Empty at D13 and D28 post transduction. Cells were cultured with 4:1 DMEM high glucose:M199 + 10% FBS + 1% Penicillin/Streptomycin.

Data is presented as Mean ± SD (n=3 from 1 independent experiment); statistical significance was determined by One-way ANOVA with False Discovery Rate multiple comparisons test.

With the switch from glycolysis to OXPHOS, cells can also undergo a change in energetic fuels. Indeed, with the fetal metabolic switch, cardiomyocytes start relying on fatty acids instead of glucose as their main substrate (Walejko et al., 2018). Therefore, we evaluated preliminarily if this change also happens during DCC through the levels of neutral fatty acids in the cell deposited in lipid droplets (**Figure 21**), measured using Bodipy 493/503. At the initial time point (D11), both MEFs and AEFs-MGT transduced cells present a marked increase in Bodipy levels, being significantly higher for AEFs at D11. At later time points (D21, D28), MGT-transduced AEFs maintained the higher levels of lipid droplets reservoir compared to Empty (**Figure 21b**), whereas for MEFs, no difference in Bodipy between MGT and Empty was observed (**Figure 21a**).
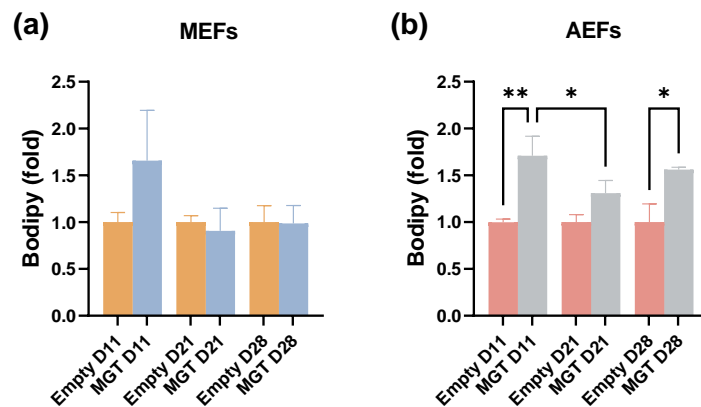
Figure 21. Lipid Droplets levels quantified by flow cytometry for Bodipy 493/503 MFI in MEFs **(a)** and AEFs **(b)** cells in their respective conditions (Empty and MGT) represented as the fold change in MGT over Empty at D11, D21 and D28 post transduction. Cells were cultured with 4:1 DMEM high glucose:M199 + 10% FBS + 1% Penicillin/Streptomycin (experiment 1) or 4:1 DMEM low glucose:M199 + 10% FBS + 1% Penicillin/Streptomycin (experiment 2).
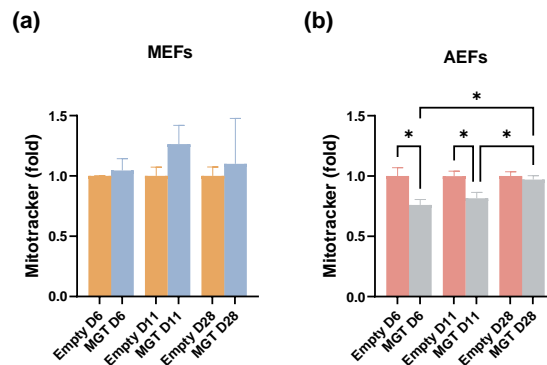Data is presented as Mean ± SD (n=3/6 from 2 independent experiments); statistical significance was determined by One-way ANOVA with False Discovery Rate multiple comparisons test. *P < 0.05; **P < 0.01.

Overall, these results demonstrate that there are clear metabolic differences between MEFs and AEFs during DCC, with embryonic iCLMs gaining mitochondrial mass and overtime increase mitochondrial transmembrane potential while decreasing ROS levels, whereas in adult iCLMs no significant differences were observed. This shows that, for the same time point, embryonic fibroblasts are approaching a cardiomyocyte characteristic metabolism, while adult fibroblasts seem to have more barriers to this process.

Some studies have suggested that manipulating fibroblast metabolism to resemble cardiomyocyte's, either by promoting mitochondrial OXPHOS or by inhibiting glycolysis, leads to increase of DCC efficiency (Ishida et al., 2021; Stone et al., 2019). Therefore, 2-Deoxi-d-glucose (2-DG), an inhibitor of the production of Glucose 6-phosphatase and widely used as a glycolytic inhibitor, was added to MEFs Empty and MGT transduced from D0-11 to test if, by blocking glycolysis could alter the reprogramming efficiency of MEFs. 2-DG treatment presented toxicity to the cells with a significant loss of cell population in both MEFs MGT and Empty with drug when compared to the populations without drug (**Supplementary Figure 7**). Moreover, 2-DG treated cells (both empty and MGT) present decrease mitochondrial mass by Mitotracker staining when compared to corresponding controls without the drug (**Figure 22a**). Determination of cTnT expression by flow cytometry at D11 (**Figure 22b**), revealed a non-significant increase in cTnT expression (detected in the FL1 channel) in MGT versus empty transduced cells. However, addition of 2-DG to MEFs empty also produced an increase in cTnT expression compared to no drug. Nevertheless, MEFs MGT supplemented with 2-DG present

increased cTnT expression compared to 2-DG treated empty MEFs and MGT-transduced MEFs with no drug, suggesting that 2-DG could be promoting cTnT expression despite the lower mitochondrial mass observed (**Figure 22**).

(a)　　　　　　　　　　　**(b)**
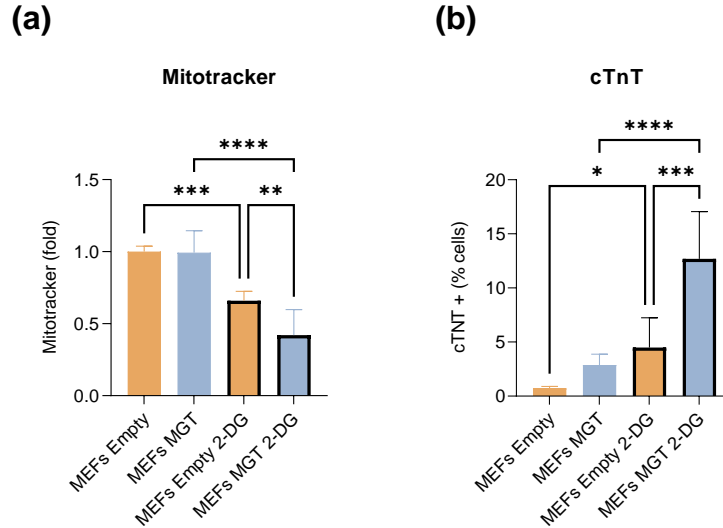
Figure 22. Mitochondrial mass and reprogramming efficiency quantified by flow cytometry for Mitotracker Deep Red MFI **(a)** and cardiac reporter cTnT intracellular staining (conjugated to anti-mouse Alexa 488 secondary anibody) detected in the FL1 channel **(b)**, respectively, of MEFs Empty and MGT without and with 2-DG (0,5 to 2mM from D0-D11) as the fold change in MGT over Empty **(a)** and percentage of cells **(b)** at D11 post transduction (pt). Cells were cultured with 4:1 DMEM high glucose:M199 + 10% FBS + 1% Penicillin/Streptomycin.
Data is presented as Mean ± SD (n=4/6 from 2 independent experiments); statistical significance was determined by One-way ANOVA with False Discovery Rate multiple comparisons test. $*P < 0.05$; $**P < 0.01$; $***P < 0.001$; $****P < 0.0001$.

We also tested the impact of glycolysis inhibition in the efficiency of DCC using the icMEFs line. As for primary MEFs, the drug produced toxicity, with a marked decrease in the percentage of alive cells in the flow cytometer of Dox 2-DG treated cells compared to no drug (**Supplementary Figure 8**). 2-DG addition to the inducible icMEFs at 1mM for 3 days together with Dox produced an increase in the level of Mitotracker (**Figure 23a**) compared to Dox only. As for the reprogramming efficiency, evaluated by GFP expression through flow cytometry (**Figure 23b**), supplementation of 2-DG lead to a marked increase in the percentage of cells expressing GFP from around 10% to 20%.

(a)　　　　　　　　　　　**(b)**
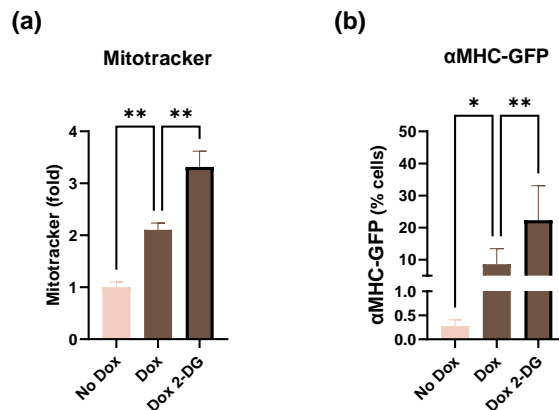
Figure 23. Mitochondrial mass and reprogramming efficiency quantified by flow cytometry for Mitotracker Deep Red MFI **(a)** and GFP from the cardiac αMHC-GFP reporter **(b)**, respectively, of icMEFs without or with doxycycline (Dox) supplementation for 3 days and with administration of 2-DG (1mM) represented as the fold change over No Dox **(a)** and percentage of cells **(b)**. For Dox supplemented cells, the entire population (GFP-negative and GFP-positive), was considered for the analysis. Cells were cultured with 4:1 DMEM high glucose + 10% FBS + 1% Penicillin/Streptomycin.

Data is presented as Mean ± SD (n=2/9 from 2 independent experiments); statistical significance was determined by One-way ANOVA with False Discovery Rate multiple comparisons test. *P < 0.05; **P < 0.01; ***P < 0.001; ****P < 0.0001.

These results confirm that inhibition of glycolysis is indeed a promising strategy to increase DCC efficiency, but due to the toxicity induced by 2-DG in fibroblasts, further supplementation regimens and alternatives to block glycolysis and/or promote OXPHOS should be tested.

Discussion

Direct Cardiac Conversion has become a very promising strategy to reestablish the cardiac tissue after injury. With the loss of cardiomyocytes, that retain a very limited regenerative capacity after birth, fibroblasts grow in their place and form a fibrotic scar (González et al., 2018). Therefore, DCC takes advantage of fibroblasts to generate induced Cardiac Like Myocytes (iCLMs), through infection with three cardiogenic factors (Mef2c, Gata4 and Tbx5 – MGT). These iCLMs have been shown to express cardiac genes, to contract spontaneously both *in vitro* and *in vivo*, and lead to an improved cardiac function *in vivo*, while reducing the fibrotic scar (Ieda et al., 2010; Qian et al., 2012). However, this process still presents low efficiency, as confirmed by our results (only 4% of MGT transduced MEFs were cTnT positive, **Figure 7**), with an even further decrease of efficiency reported when using adult fibroblasts (Chen et al., 2012), which are more clinically relevant. Accordingly, this work explores the differences between embryonic and adult fibroblasts that could be responsible for the decreased DCC efficiency in adult fibroblasts, focusing on the metabolism.

Our analysis to the endogenous expression of the *MGT* genes at D12 post-transduction revealed that both MEFs and AEFs underwent successful retroviral infection, with no significant differences between ages. However, when compared to MEFs, AEFs still expressed high levels of fibroblast markers and low levels of cardiac markers, suggesting that these have not yet been, respectively, deactivated and activated in the adult fibroblasts, which are both important steps for DCC progression (Liu et al., 2016).

Embryonic cells are known for having less epigenetic barriers than adult cells for cellular reprogramming (Rodrigues & Roelen, 2020), reason why they are often used for these experiments and present higher efficiency. These barriers include remodeling of the chromatin, post-translational modification of histones and modifications in patterns of DNA methylation (López-Otín et al., 2013). For example, H3K27me3, associated with inactive transcription, was found to gradually increase in fibroblast promoter sites during DCC (Liu et al., 2016). However, with aging, a global loss of H3K27me3 has been reported (López-Otín et al., 2013), which could explain why AEFs haven't achieved a decrease in the expression of fibroblast genes compared to MEFs at D12 post-transduction, as well as the lower levels of these genes' expression in AEFs Empty, when compared to MEFs Empty. Indeed, it was observed that a global loss of H3K27me3 reduces the efficiency of the reprogramming of iPSCs, demonstrating the need for the repression of the genes responsible for cell's original identity (Fragola et al., 2013). Moreover, other aging-related epigenetic barriers could be underlying the adult fibroblast's difficulty in activating the cardiac markers. Therefore, a further understanding of how aging affects the epigenetic barriers during DCC is needed.

The metabolism is an important element of DCC, with the cell's main supplier of energy switching from glycolysis to OXPHOS during the process (H. Wang et al., 2021). Interestingly, during the fetal metabolic switch (also from glycolysis to OXPHOS), the mitochondria of embryonic cardiomyocytes have been shown to evolve into a more elongated network (Hom et al., 2011). Therefore, a remodeling of the mitochondria is expected to occur during DCC, as an increased metabolic demand is associated with more fused organelles (Chi, 2020). Indeed, through analysis of the mitochondria network in MEFs at D11 post-transduction, we observed an increase in area, shape and branch parameters (approaching cardiac cell line HL-1), which are characteristic of a more filamentous phenotype, as reported by Tronstad and colleagues. Likewise, they also reported that while the mitochondrial mass increases, the number of organelles remains unchanged (or can even decrease) in this phenotype (Tronstad et al., 2014). Despite not being significant, MEFs MGT did present a tendency to increase mitochondrial mass over MEFs Empty (**Figure 18a**). A similar tendency has also been reported during DCC (by D12) using neonatal murine cardiac fibroblasts as well as an increase in mtDNA content at late time-points (D21) (Chi, 2020).

This remodeling of mitochondrial network is also present in other reprogramming processes. For example, in iPSCs differentiation, a metabolic switch occurs, also from glycolysis to OXPHOS, with

subsequent changes in the mitochondria from fragmented to more elongated (Choi et al., 2015). This highlights the importance of the mitochondria during cellular reprogramming, not only by providing energy to the growing demand of the cells, but also through its role in metaboloepigenetics. With the metabolic switch, an increase of mitochondrial metabolites occurs, which could be responsible for modifications in histone acetylation (citrate) and both histone and DNA methylation (αKG) patterns (Ryall et al., 2015), that can lead to the activation of cardiac markers and inactivation of fibroblast markers.

Regarding the mitochondrial network in adult fibroblasts, analysis of immunofluorescence detection of TOM20 (**Figure 11**) and HSP-60 (**Supplementary Figure 1**) provide different results, with AEFs MGT-transduced not showing alterations compared to their Empty counterparts in the TOM-20 staining and displaying an evolution similar to MEFs by HSP-60 analysis. HSP-60 is involved in the folding of proteins in the mitochondrial matrix, gaining a more prominent role when mitochondria detect stress due to a large quantity of unfolded or misfolded proteins (Pellegrino et al., 2013). This event happens mostly due to high ROS levels (Pellegrino et al., 2013), which increase with age (López-Otín et al., 2013), as confirmed by the higher Mitosox levels displayed by adult fibroblasts (**Supplementary Figure 5**). Therefore, as TOM20 is more ubiquitously expressed (as part of the TOM complex, which is involved in the import of proteins (Giacomello et al., 2020)), it is probably more suitable for mitochondria network analysis in adult fibroblasts. Our data shows that the network of AEFs only became more filamentous at D21, taking more time than MEFs, which can be explained by the presence of more barriers in adult cells, as mentioned previously. Accordingly, mitochondrial mass also increased overtime in AEFs MGT-transduced (**Figure 18**).

During DCC, several subpopulations arise due to not all fibroblasts undergoing reprogramming and some taking more time than others, making it a heterogenous and asynchronous process (Liu et al., 2017). Indeed, analysis of cTnT expression allowed us to divide the fibroblasts transduced with MGT into two subpopulations, with cTnT positive cells presenting a more filamentous mitochondrial network than cTnT negative (as well as Empty). This demonstrates the need of a more accurate analysis of the process, through the study of only the cells that undergo cardiac reprogramming and not the bulk MGT-transduced population. Taking this into account, we used the cell line icMEFs which allows for transdifferentiated fibroblasts to be easily detected through the expression of the GFP (Vaseghi et al., 2016). However, as this cell line is immortalized and no evidence of its ability to mature has yet been obtained, ideally, analysis would be conducted in primary cells with a cardiac reporter, as MEFs isolated from αMHC-GFP mice (Ieda et al., 2010).

Mitochondrial morphology is regulated by both fusion and fission, ranging from round organelles to more elongated ones. Therefore, as the network becomes more filamentous, an increase in fusion would be expected (Tronstad et al., 2014). However, no major conclusions can be drawn from the gene expression analysis of the mitochondrial dynamics-related genes evaluated. This could be due to the fact that the process is modulated by post-translational modifications of key effector proteins. For example, OMA1 protease was shown to inhibit Opa1, originating a decrease in fusion (Head et al., 2009); while several post-translational modifications, like phosphorylation and ubiquitination, have been described as regulators of Drp1 activity and, therefore, fission (Chang & Blackstone, 2010). Additionally, the proteins can also be involved in other processes. For example, Opa1 has been shown to be an important regulator of mitochondria cristae junction formation and maintenance in addition to its role in fusion (Giacomello et al., 2020).

Mitochondria homeostasis is important in the regulation of the mitochondrial content through the generation of new healthy organelles by biogenesis and the degradation of damaged ones by mitophagy (Tronstad et al., 2014). Biogenesis is seen as a long-term response, not fluctuating to short-term energetic needs, which are regulated through post-translational modifications (Tronstad et al., 2014). A decrease in mitophagy efficiency is expected to take place with age (Cavallini et al., 2007) which is only translated in our results in the *SQTM1* analysis. The expression of both *LC3* and *Parkin* appears to increase in AEFs, comparing to MEFs. This could reveal a potential deregulation of the process in adult fibroblasts that could be fostering

the lower mitochondrial mass presented by AEFs MGT-transduced compared to their Empty counterparts by D6 and D11 (**Figure 18**). Therefore, additional analysis is needed to understand mitochondrial dynamics and homeostasis, possibly at protein level, since it has been shown that these processes can impact reprogramming. Indeed, both Drp1 and Fis1 depletion or PGC1α overexpression were shown to be able to increase DCC efficiency (cTnT expression) in neonatal murine cardiac fibroblasts and MEFs, respectively (Chi, 2020).

With DCC progression, an increase in OXPHOS is expected to occur (H. Wang et al., 2021). Indeed, an increase in mitochondrial respiratory capacity by Seahorse oxygen consumption (at D8) was reported in neonatal murine cardiac fibroblasts during DCC (Chi, 2020). Our analysis of the mitochondrial membrane potential shows an increase overtime in MEFs' levels, whereas AEFs remains unchanged, which could reveal that the metabolic switch is yet to occur in adult fibroblasts. However, despite the increase overtime, MEFs transduced with MGT present lower levels than Empty at D11. This could be an artefact, since it has been reported that TMRE can interact unspecifically (Zorova et al., 2018). Therefore, additional analysis would be needed to clarify these results and the occurrence of a delayed metabolic switch in adult-derived iCLMs compared to embryonic.

With the increase of OXPHOS, an increase of the byproducts of this process, such as ROS, would be expected (H. Wang et al., 2021). However, our results show that ROS levels in MEFs tend to decrease as DCC progresses (**Figure 20**), concomitantly with the network becoming more filamentous and interconnected. Indeed, it has been reported that fragmented mitochondria produce more ROS (Giacomello et al., 2020), which would explain the decrease as the network becomes more filamentous. Additionally, it has also been shown that high levels of ROS can impede the progress of DCC (Wang et al., 2021), which could be one of the causes for the differences in efficiency of DCC between ages, since adult fibroblasts present much higher levels of ROS than embryonic fibroblasts (**Supplementary Figure 5**). This suggests that reducing ROS levels could lead to an increase in DCC efficiency. Indeed, several studies having shown that antioxidants (as selenium, ascorbic acid and vitamin E nicotinate) could lead to enhancement of the reprogramming (Suzuki & Shults, 2019; Talkhabi et al., 2015; X. Wang et al., 2016). However, in our lab we did not observe any differences in DCC efficiency using the ROS-scavenger NAC in icMEFs (data not shown), and similar results were obtained by treating murine cardiac fibroblasts with NAC (Chi, 2020). Therefore, it seems that the levels of ROS can be critical for DCC and lowering ROS levels in the cells (e.g NAC) is not an advantage for the DCC process in embryonic cells. It would be interesting to explore the impact of ROS scavenging in adult fibroblasts.

Moreover, while there is a tendency to decrease in ROS levels in primary MEFs MGT-transduced as DCC progresses, transduction of the icMEFs cell line (by Dox supplementation) lead to higher ROS levels. Primary and the immortalized icMEFs cell line have different proliferation potentials and are at different levels of DCC induction, raising the question of whether the icMEFs line, despite its advantages in monitoring and achieving a more synchronized DCC, might be a limited model for the study of DCC.

Fatty acids become the main substrate for ATP production in cardiomyocytes after the fetal metabolic switch (Lopaschuk & Jaswal, 2010), which is also expected to happen in DCC with the switch to the OXPHOS predominant metabolism (Zhou et al., 2017). In our analysis of lipid droplets, both MEFs and AEFs transduced with MGT present higher levels of Bodipy staining by D11, which indicates a higher storage of neutral fatty acids in lipid droplets. However, at D21, there is a decrease of their levels in MEFs, which could reveal an increased mobilization (possibly for beta-oxidation), while AEFs also decrease but increase again by D28. As this is an indirect measurement of fatty acid mobilization, a more direct approach to measure FAO is needed to confirm the results.

So far, the results discussed above reveal that there is a lot of potential in modulating mitochondria metabolism and dynamics in order to improve DCC efficiency. Indeed, blocking glycolysis, for example through the downregulation of HIF-1α (an important regulator of glycolysis) (Stone et al., 2019), or promoting OXPHOS, through upregulation of isocitrate dehydrogenase3α (Ishida et al., 2021), lead to enhanced DCC

reprogramming. Moreover, by using 2-DG, which blocks glycolysis and forces the cells to adopt OXPHOS, we were able to enhance reprogramming in both MEFs and icMEFs. The increase in cTnT positive cells (or signal in the FL4 flow cytometry channel) in 2-DG treated MEFs Empty compared to no drug could be due to either autofluorescence of the compound or induction of cTnT expression, however, those levels were still significantly lower than in 2-DG-treated MEFs MGT transduced. Nevertheless, the drug presented cell toxicity in both MEFs and icMEFs, even after reduction of the concentration, which could be due to fibroblast's high dependence in glycolysis. To overcome this, 2-DG addition should be made at a later stage of transduction when the fibroblasts have already started undergoing metabolic changes, in order to potentiate DCC without compromising fibroblast's viability.

Overall, our study shows that there are clear differences between embryonic and adult-derived iCLMs, which can be a starting point in improving the efficiency of the reprogramming for adult and old fibroblasts. Furthermore, modulating the metabolism seems very promising for improving DCC efficiency, given its role not only in meeting increased energetic demand of the cell, but also in regulating epigenetic modifications that underlie cell fate transitions taking place during the direct conversion of fibroblast into iCLMs.

Conclusion and Future Perspectives

Heart diseases are one of the most concerning public health problems. Due to the adult heart's limited ability to regenerate after injury, direct cardiac conversion arises as a promising strategy to replenish the lost cardiomyocyte population, while decreasing the fibrotic scar.

With this work, we confirm the loss of DCC efficiency in adult fibroblasts, compared to embryonic fibroblasts. Further studies need to be made to understand how aging and epigenetics impacts the fibroblasts' ability to transdifferentiate.

Our studies of the mitochondrial network reveal that extensive mitochondrial remodeling takes place during DCC of embryonic and adult fibroblasts into iCLMs, with the latter progressing slower. However, no major conclusions could be drawn from our work on the mechanisms that regulate this remodeling since we only evaluated gene expression. Therefore, a deepening of the knowledge of the mitochondrial dynamics and homeostasis through evaluation of the proteins involved in these processes is required. This will allow not only to explain the slower progress of adult cells but also enlighten possible modulating targets for the enhancement of the reprogramming.

Furthermore, we were able to increase the efficiency of the DCC in embryonic fibroblasts through modulation of the metabolism, confirming its potential. For future work, a refinement of the 2-DG protocol, as well as usage of alternative drugs that modulate bioenergetics, and their applicability in adult cells is a priority. Moreover, it would also be interesting to further explore the link between the energetic metabolism, mitochondrial network and the availability of epigenetic remodeling metabolites, in facilitating epigenetic landscape transitions driving DCC in embryonic and adult fibroblasts.

References

André, E., lia De Pauw, A., Verdoy, R., Brusa, D., Bouzin, C., lie Timmermans, A., Bertrand, L., & Balligand, J.-L. (2019). Changes of Metabolic Phenotype of Cardiac Progenitor Cells During Differentiation: Neutral Effect of Stimulation of AMP-Activated Protein Kinase. *STEM CELLS AND DEVELOPMENT*, *28*(22), 1498–1513. https://doi.org/10.1089/scd.2019.0129

Bacmeister, L., Schwarzl, M., Warnke, S., Stoffers, B., Blankenberg, S., Westermann, D., & Lindner, D. (2019). Inflammation and fibrosis in murine models of heart failure. *Basic Research in Cardiology 2019 114:3*, *114*(3), 1–35. https://doi.org/10.1007/S00395-019-0722-5

Brade, T., Pane, L. S., Moretti, A., Chien, K. R., & Laugwitz, K. L. (2013). Embryonic heart progenitors and cardiogenesis. *Cold Spring Harbor Perspectives in Medicine, 3*(10), 1–17. https://doi.org/10.1101/cshperspect.a013847

Cardiovascular diseases. (n.d.). Retrieved 11 October 2022, from https://www.who.int/health-topics/cardiovascular-diseases#tab=tab_1

Cardoso, A. C., Lam, N. T., Savla, J. J., Nakada, Y., Helena Pereira, A. M., Elnwasany, A., Menendez-Montes, I., Ensley, E. L., Bezan Petric, U., Sharma, G., Dean Sherry, A., Malloy, C. R., Khemtong, C., Kinter, M. T., Lek Wen Tan, W., George Anene-Nzelu, C., Sik-Yin Foo, R., Uyen Nhi Nguyen, N., Li, S., … Sadek, H. A. (2020). Mitochondrial Substrate Utilization Regulates Cardiomyocyte Cell Cycle Progression. *Nat Metab.*, *2*(2), 167–178. https://doi.org/10.1038/s42255-020-0169-x

Cavallini, G., Donati, A., Taddei, M., & Bergamini, E. (2007). Evidence for selective mitochondrial autophagy and failure in aging. *Autophagy*, *3*(1), 26–27. https://doi.org/10.4161/AUTO.3268

Chang, C. R., & Blackstone, C. (2010). Dynamic regulation of mitochondrial fission through modification of the dynamin-related protein Drp1. *Annals of the New York Academy of Sciences*, *1201*(1), 34–39. https://doi.org/10.1111/J.1749-6632.2010.05629.X

Chaudhry, A., Shi, R., & Luciani, D. S. (2020). A pipeline for multidimensional confocal analysis of mitochondrial morphology, function, and dynamics in pancreatic-cells. *Am J Physiol Endocrinol Metab*, *318*(2), 87–101. https://doi.org/10.1152/ajpendo.00457.2019.-Live-cell

Chen, J. X., Krane, M., Deutsch, M. A., Wang, L., Rav-Acha, M., Gregoire, S., Engels, M. C., Rajarajan, K., Karra, R., Abel, E. D., Wu, J. C., Milan, D., & Wu, S. M. (2012). Inefficient reprogramming of fibroblasts into cardiomyocytes using Gata4, Mef2c, and Tbx5. *Circulation Research*, *111*(1), 50–55. https://doi.org/10.1161/CIRCRESAHA.112.270264

Chi, H. R. (2020). *Molecular Mechanisms of Direct Cardiac Reprogramming* [Doctoral thesis, University of North Carolina]. https://doi.org/https://doi.org/10.17615/5z9g-pe63

Choi, H. W., Kim, J. H., Chung, M. K., Hong, Y. J., Jang, H. S., Seo, B. J., Jung, T. H., Kim, J. S., Chung, H. M., Byun, S. J., Han, S. G., Seo, H. G., & Do, J. T. (2015). Mitochondrial and metabolic remodeling during reprogramming and differentiation of the reprogrammed cells. *Stem Cells and Development*, *24*(11), 1366–1373. https://doi.org/10.1089/SCD.2014.0561

Claycomb, W. C., Lanson, N. A., Stallworth, B. S., Egeland, D. B., Delcarpio, J. B., Bahinski, A., & Izzo, N. J. (1998). HL-1 cells: a cardiac muscle cell line that contracts and retains phenotypic characteristics of the adult cardiomyocyte. *Proceedings of the National Academy of Sciences of the United States of America*, *95*(6), 2979–2984. www.pnas.org.

Correia, M., Santos, F., Da, R., Ferreira, S., Ferreira, R., Bernardes De Jesus, B., & Nóbrega-Pereira, S. (2022). Metabolic Determinants in Cardiomyocyte Function and Heart Regenerative Strategies. *Metabolites 2022, Vol. 12, Page 500*, *12*(6), 500. https://doi.org/10.3390/METABO12060500

di Fonso, A., Pietrangelo, L., D'onofrio, L., Michelucci, A., Boncompagni, S., & Protasi, F. (2021). Ageing causes ultrastructural modification to calcium release units and mitochondria in cardiomyocytes. *International Journal of Molecular Sciences*, *22*(16), 8364. https://doi.org/10.3390/IJMS22168364/S1

Fragola, G., Germain, P.-L., Laise, P., Cuomo, A., & Blasimme, A. (2013). Cell Reprogramming Requires Silencing of a Core Subset of Polycomb Targets. *PLOS Genetics*, *9*(2), 1003292. https://doi.org/10.1371/journal.pgen.1003292

Fu, Y., Huang, C., Xu, X., Gu, H., Ye, Y., Jiang, C., Qiu, Z., & Xie, X. (2015). Direct reprogramming of mouse fibroblasts into cardiomyocytes with chemical cocktails. *Cell Research*, *25*(9), 1013–1024. https://doi.org/10.1038/CR.2015.99

Giacomello, M., Pyakurel, A., Glytsou, C., & Scorrano, L. (2020). The cell biology of mitochondrial membrane dynamics. *Nature Reviews Molecular Cell Biology*, *21*(4), 204–224. https://doi.org/10.1038/S41580-020-0210-7

González, A., Schelbert, E. B., Díez, J., & Butler, J. (2018). Myocardial Interstitial Fibrosis in Heart Failure: Biological and Translational Perspectives. *Journal of the American College of Cardiology*, *71*(15), 1696–1706. https://doi.org/10.1016/J.JACC.2018.02.021

Head, B., Griparic, L., Amiri, M., Gandre-Babbe, S., & van der Bliek, A. M. (2009). Inducible proteolytic inactivation of OPA1 mediated by the OMA1 protease in mammalian cells. *The Journal of Cell Biology*, *187*(7), 959–966. https://doi.org/10.1083/JCB.200906083

Hirai, H., & Kikyo, N. (2014). Inhibitors of suppressive histone modification promote direct reprogramming of fibroblasts to cardiomyocyte-like cells. *Cardiovascular Research*, *102*(1), 188–190. https://doi.org/10.1093/CVR/CVU023

Hom, J. R., Quintanilla, R. A., Hoffman, D. L., de Mesy Bentley, K. L., Molkentin, J. D., Sheu, S. S., & Porter, G. A. (2011). The Permeability Transition Pore Controls Cardiac Mitochondrial Maturation and Myocyte Differentiation. *Developmental Cell*, *21*(3), 469–478. https://doi.org/10.1016/J.DEVCEL.2011.08.008

Hwang, I. Y., Kwak, S., Lee, S., Kim, H., Lee, S. E., Kim, J. H., Kim, Y. A., Jeon, Y. K., Chung, D. H., Jin, X., Park, S., Jang, H., Cho, E. J., & Youn, H. D. (2016). Psat1-Dependent Fluctuations in α-Ketoglutarate Affect the Timing of ESC Differentiation. *Cell Metabolism*, *24*(3), 494–501. https://doi.org/10.1016/j.cmet.2016.06.014

Ieda, M., Fu, J. D., Delgado-Olguin, P., Vedantham, V., Hayashi, Y., Bruneau, B. G., & Srivastava, D. (2010). Direct reprogramming of fibroblasts into functional cardiomyocytes by defined factors. *Cell*, *142*(3), 375–386. https://doi.org/10.1016/j.cell.2010.07.002

Intlekofer, A. M., & Finley, L. W. S. (2019). Metabolic signatures of cancer cells and stem cells. *Nature Metabolism, 1*(2), 177–188. https://doi.org/10.1038/s42255-019-0032-0

Ishida, T., Ueyama, T., Baba, A., Hasegawa, K., & Kawamura, T. (2021). The Role of Isocitrate Dehydrogenases in Direct Reprogramming to Cardiomyocytes. *European Cardiology Review*, *16*. https://doi.org/10.15420/ECR.2021.16.PO8

Jayawardena, T. M., Finch, E. A., Zhang, L., Zhang, H., Hodgkinson, C. P., Pratt, R. E., Rosenberg, P. B., Mirotsou, M., & Dzau, V. J. (2015). MicroRNA induced cardiac reprogramming in vivo: evidence for mature cardiac myocytes and improved cardiac function. *Circulation Research*, *116*(3), 418–424. https://doi.org/10.1161/CIRCRESAHA.116.304510

Johnson, J., Mohsin, S., & Houser, S. R. (2021). Cardiomyocyte Proliferation as a Source of New Myocyte Development in the Adult Heart. *International Journal of Molecular Sciences*, *22*(15), 7764. https://doi.org/10.3390/IJMS22157764

Karakikes, I., Ameen, M., Termglinchan, V., & Wu, J. C. (2015). Human Induced Pluripotent Stem Cell-Derived Cardiomyocytes: Insights into Molecular, Cellular, and Functional Phenotypes. In *Circulation Research* (Vol. 117, Issue 1, pp. 80–88). https://doi.org/10.1161/CIRCRESAHA.117.305365

Kojima, H., & Ieda, M. (2017). Discovery and progress of direct cardiac reprogramming. *Cellular and Molecular Life Sciences 2017 74:12*, *74*(12), 2203–2215. https://doi.org/10.1007/S00018-017-2466-4

Li, A., Gao, M., Jiang, W., Qin, Y., & Gong, G. (2020). Mitochondrial Dynamics in Adult Cardiomyocytes and Heart Diseases. *Frontiers in Cell and Developmental Biology*, *8*, 584800. https://doi.org/10.3389/FCELL.2020.584800/BIBTEX

Li, Y., Zheng, W., Lu, Y., Zheng, Y., Pan, L., Wu, X., Yuan, Y., Shen, Z., Ma, S., Zhang, X., Wu, J., Chen, Z., & Zhang, X. (2021). BNIP3L/NIX-mediated mitophagy: molecular mechanisms and implications for human disease. *Cell Death & Disease 2021, 13*(1), 1–11. https://doi.org/10.1038/s41419-021-04469-y

Liu, Z., Chen, O., Zheng, M., Wang, L., Zhou, Y., Yin, C., Liu, J., & Qian, L. (2016). Re-patterning of H3K27me3, H3K4me3 and DNA methylation during fibroblast conversion

into induced cardiomyocytes. *Stem Cell Res*, *16*(2), 507–518. https://doi.org/10.1016/j.scr.2016.02.037

Liu, Z., Wang, L., Welch, J. D., Ma, H., Zhou, Y., Vaseghi, H. R., Yu, S., Wall, J. B., Alimohamadi, S., Zheng, M., Yin, C., Shen, W., Prins, J. F., Liu, J., & Qian, L. (2017). Single-cell transcriptomics reconstructs fate conversion from fibroblast to cardiomyocyte. *Nature 2017, 551*(7678), 100–104. https://doi.org/10.1038/nature24454

Lopaschuk, G. D., & Jaswal, J. S. (2010). Energy metabolic phenotype of the cardiomyocyte during development, differentiation, and postnatal maturation. *Journal of Cardiovascular Pharmacology*, *56*(2), 130–140. https://doi.org/10.1097/FJC.0B013E3181E74A14

López-Otín, C., Blasco, M. A., Partridge, L., Serrano, M., & Kroemer, G. (2013). The Hallmarks of Aging. *Cell*, *153*(6), 1194–1217. https://doi.org/10.1016/J.CELL.2013.05.039

Malliaras, K., Zhang, Y., Seinfeld, J., Galang, G., Tseliou, E., Cheng, K., Sun, B., Aminzadeh, M., & Marbán, E. (2013). Cardiomyocyte proliferation and progenitor cell recruitment underlie therapeutic regeneration after myocardial infarction in the adult mouse heart. *EMBO Molecular Medicine*, *5*(2), 191–209. https://doi.org/10.1002/EMMM.201201737

Mann, D. L. (1999). Mechanisms and models in heart failure: A combinatorial approach. *Circulation*, *100*(9), 999–1008. https://doi.org/10.1161/01.CIR.100.9.999

Moussaieff, A., Rouleau, M., Kitsberg, D., Cohen, M., Levy, G., Barasch, D., Nemirovski, A., Shen-Orr, S., Laevsky, I., Amit, M., Bomze, D., Elena-Herrmann, B., Scherf, T., Nissim-Rafinia, M., Kempa, S., Itskovitz-Eldor, J., Meshorer, E., Aberdam, D., & Nahmias, Y. (2015). Glycolysis-Mediated Changes in Acetyl-CoA and Histone Acetylation Control the Early Differentiation of Embryonic Stem Cells. *Cell Metabolism*, *21*(3), 392–402. https://doi.org/10.1016/J.CMET.2015.02.002

Nam, Y. J., Song, K., Luo, X., Daniel, E., Lambeth, K., West, K., Hill, J. A., di Maio, J. M., Baker, L. A., Bassel-Duby, R., & Olson, E. N. (2013). Reprogramming of human fibroblasts toward a cardiac fate. *Proceedings of the National Academy of Sciences of the United States of America*, *110*(14), 5588–5593. https://doi.org/10.1073/pnas.1301019110

Ng, S.-C., & Ng, H.-H. (2017). The metabolic programming of stem cells. *GENES & DEVELOPMENT*, *31*(4), 336–346. https://doi.org/10.1101/gad.293167

Olson, E. N. (2006). Gene regulatory networks in the evolution and development of the heart. In *Science, 313*(5795), 1922–1927. https://doi.org/10.1126/science.1132292

Orrenius, S., Gogvadze, V., & Zhivotovsky, B. (2007). Mitochondrial Oxidative Stress: Implications for Cell Death. *Https://Doi.Org/10.1146/Annurev.Pharmtox.47.120505.105122*, *47*, 143–183. https://doi.org/10.1146/ANNUREV.PHARMTOX.47.120505.105122

Pellegrino, M. W., Nargund, A. M., & Haynes, C. M. (2013). Signaling the mitochondrial unfolded protein response. *Biochimica et Biophysica Acta - Molecular Cell Research*, *1833*(2), 410–416. https://doi.org/10.1016/J.BBAMCR.2012.02.019

Pushp, P., Nogueira, D. E. S., Rodrigues, C. A. V., Ferreira, F. C., Cabral, J. M. S., & Gupta, M. K. (2021). A Concise Review on Induced Pluripotent Stem Cell-Derived Cardiomyocytes for Personalized Regenerative Medicine. *Stem Cell Reviews and Reports*, *17*(3), 748–776. https://doi.org/10.1007/S12015-020-10061-2

Qian, L., Huang, Y., Spencer, C. I., Foley, A., Vedantham, V., Liu, L., Conway, S. J., Fu, J. D., & Srivastava, D. (2012). In vivo reprogramming of murine cardiac fibroblasts into induced cardiomyocytes. *Nature*, *485*(7400), 593–598. https://doi.org/10.1038/nature11044

Rodrigues, G., & Roelen, B. (2020). *Concepts and Applications of Stem Cell Biology* (G. Rodrigues & B. A. J. Roelen, Eds.). Springer International Publishing. https://doi.org/10.1007/978-3-030-43939-2

Ryall, J. G., Cliff, T., Dalton, S., & Sartorelli, V. (2015). Metabolic Reprogramming of Stem Cell Epigenetics. *Cell Stem Cell*, *17*(6), 651–662. https://doi.org/10.1016/J.STEM.2015.11.012

Senyo, S. E., Steinhauser, M. L., Pizzimenti, C. L., Yang, V. K., Cai, L., Wang, M., Wu, T. di, Guerquin-Kern, J. L., Lechene, C. P., & Lee, R. T. (2013). Mammalian Heart Renewal by Preexisting Cardiomyocytes. *Nature*, *493*(7432), 433–436. https://doi.org/10.1038/NATURE11682

Song, K., Nam, Y. J., Luo, X., Qi, X., Tan, W., Huang, G. N., Acharya, A., Smith, C. L., Tallquist, M. D., Neilson, E. G., Hill, J. A., Bassel-Duby, R., & Olson, E. N. (2012). Heart repair by reprogramming non-myocytes with cardiac transcription factors. *Nature*, *485*(7400), 599–604. https://doi.org/10.1038/nature11139

Stone, N. R., Gifford, C. A., Thomas, R., B Pratt, K. J., Samse-Knapp, K., A Mohamed, T. M., Radzinsky, E. M., Schricker, A., Ye, L., Yu, P., van Bemmel, J. G., Ivey, K. N., Pollard, K. S., Srivastava, D., & performed experiments NRS, P. (2019). Context-Specific Transcription Factor Functions Regulate Epigenomic and Transcriptional Dynamics During Cardiac Reprogramming HHS Public Access. *Cell Stem Cell*, *25*(1), 87–102. https://doi.org/10.1016/j.stem.2019.06.012

Suzuki, Y. J., & Shults, N. v. (2019). Antioxidant Regulation of Cell Reprogramming. *Antioxidants*, *8*(8), 323. https://doi.org/10.3390/ANTIOX8080323

Talkhabi, M., Pahlavan, S., Aghdami, N., & Baharvand, H. (2015). Ascorbic acid promotes the direct conversion of mouse fibroblasts into beating cardiomyocytes. *Biochemical and Biophysical Research Communications*, *463*(4), 699–705. https://doi.org/10.1016/J.BBRC.2015.05.127

Tang, Y. L., Zhu, W., Cheng, M., Chen, L., Zhang, J., Sun, T., Kishore, R., Phillips, M. I., Losordo, D. W., & Qin, G. (2009). Hypoxic preconditioning enhances the benefit of cardiac progenitor cell therapy for treatment of myocardial infarction by inducing CXCR4 expression. *Circulation Research*, *104*(10), 1209–1216. https://doi.org/10.1161/CIRCRESAHA.109.197723

Tronstad, K., Nooteboom, M., Nilsson, L., Nikolaisen, J., Sokolewicz, M., Grefte, S., Pettersen, I., Dyrstad, S., Hoel, F., Willems, P., & Koopman, W. (2014). Regulation and quantification of cellular mitochondrial morphology and content. *Current Pharmaceutical Design*, *20*(35), 5634–5652. https://doi.org/10.2174/1381612820666140305230546

Vaseghi, H. R., Yin, C., Zhou, Y., Wang, L., Liu, J., & Qian, L. (2016). Generation of an inducible fibroblast cell line for studying direct cardiac reprogramming. *Genesis*, *54*(7), 398–406. https://doi.org/10.1002/dvg.22947

Vásquez-Trincado, C., García-Carvajal, I., Pennanen, C., Parra, V., Hill, J. A., Rothermel, B. A., & Lavandero, S. (2016). Mitochondrial dynamics, mitophagy and cardiovascular disease. *Journal of Physiology*, *594*(3), 509–525. https://doi.org/10.1113/JP271301

Wada, R., Muraoka, N., Inagawa, K., Yamakawa, H., Miyamoto, K., Sadahiro, T., Umei, T., Kaneda, R., Suzuki, T., Kamiya, K., Tohyama, S., Yuasa, S., Kokaji, K., Aeba, R., Yozu, R., Yamagishi, H., Kitamura, T., Fukuda, K., & Ieda, M. (2013). Induction of human cardiomyocyte-like cells from fibroblasts by defined factors. *Proceedings of the National Academy of Sciences of the United States of America*, *110*(31), 12667–12672. https://doi.org/10.1073/pnas.1304053110

Walejko, J. M., Koelmel, J. P., Garrett, T. J., Edison, A. S., & Keller-Wood, M. (2018). Multiomics approach reveals metabolic changes in the heart at birth. *American Journal of Physiology. Endocrinology and Metabolism*, *315*(6), 1212–1223. https://doi.org/10.1152/AJPENDO.00297.2018

Wang, H., Yang, Y., Liu, J., & Qian, L. (2021). Direct cell reprogramming: approaches, mechanisms and progress. In *Nature Reviews Molecular Cell Biology, 22*(6), 410–424. Nature Research. https://doi.org/10.1038/s41580-021-00335-z

Wang, L., Liu, Z., Yin, C., Asfour, H., Chen, O., Li, Y., Bursac, N., Liu, J., & Qian, L. (2015). Stoichiometry of Gata4, Mef2c, and Tbx5 influences the efficiency and quality of induced cardiac myocyte reprogramming. *Circulation Research*, *116*(2), 237–244. https://doi.org/10.1161/CIRCRESAHA.116.305547

Wang, X., Hodgkinson, C. P., Lu, K., Payne, A. J., Pratt, R. E., & Dzau, V. J. (2016). Selenium Augments microRNA Directed Reprogramming of Fibroblasts to Cardiomyocytes via Nanog. *Scientific Reports*, *6*, 23017. https://doi.org/10.1038/SREP23017

Zhou, Y., Wang, L., Liu, Z., Alimohamadi, S., Yin, C., Liu, J., & Qian, L. (2017). Comparative Gene Expression Analyses Reveal Distinct Molecular Signatures between Differentially Reprogrammed Cardiomyocytes. *Cell Reports*, *20*(13), 3014–3024. https://doi.org/10.1016/J.CELREP.2017.09.005

Zhou, Y., Wang, L., Vaseghi, H. R., Liu, Z., Lu, R., Alimohamadi, S., Yin, C., Fu, J.-D., Wang, G. G., Liu, J., & Qian, L. (2016). Bmi1 Is a Key Epigenetic Barrier to Direct Cardiac Reprogramming HHS Public Access. *Cell Stem Cell*, *18*(3), 382–395. https://doi.org/10.1016/j.stem.2016.02.003

Zorova, L. D., Popkov, V. A., Plotnikov, E. Y., Silachev, D. N., Pevzner, I. B., Jankauskas, S. S., Babenko, V. A., Zorov, S. D., Balakireva, A. v., Juhaszova, M., Sollott, S. J., & Zorov, D.

B. (2018). Mitochondrial membrane potential. *Analytical Biochemistry*, *552*, 50–59. https://doi.org/10.1016/J.AB.2017.07.009

Supplementary Figures
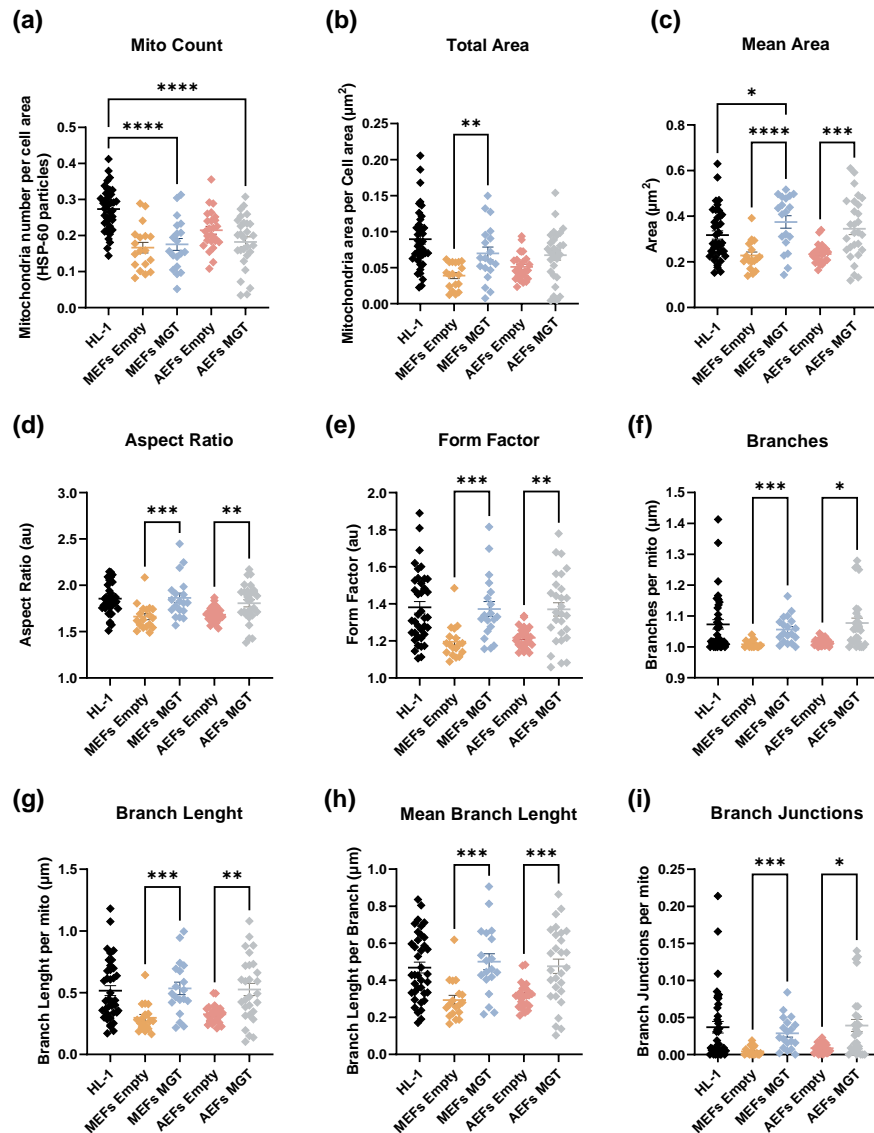
Supplementary Figure 1. Quantitative analysis and comparison of HSP-60 stained mitochondria number **(a)**, area **(b-c)**, shape **(d-e)** and network **(f-i)** parameters (briefly summarized in table 3), between MEFs and AEFs groups in their respective conditions (Empty and MGT), D11 post-transduction. Cells were cultured with DMEM high glucose + 10% FBS + 1% Penicillin/Streptomycin.
Data is presented as Mean ± SEM (n=18/38 from 1 independent experiment); statistical significance was determined by One-way ANOVA or Kruskal-Wallis with False Discovery Rate multiple comparisons test. *P < 0.05; **P < 0.01; ***P < 0.001; ****P < 0.0001.

Fluorescence Intensity
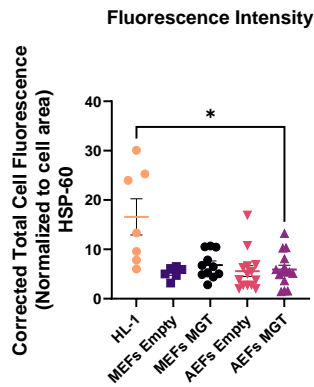
Supplementary Figure 2. Quantitative analysis and comparison of HSP-60 fluorescence intensity between HL-1, MEFs and AEFs Empty and MGT groups in their respective conditions (Empty and MGT), at D11 post-transduction. Cells were cultured with DMEM high glucose + 10% FBS + 1% Penicillin/Streptomycin.
Data is presented as Mean ± SEM (n =6/17 from 1 independent experiment); statistical significance was determined by Kruskal-Wallis with False Discovery Rate multiple comparisons test. *$P < 0.05$.
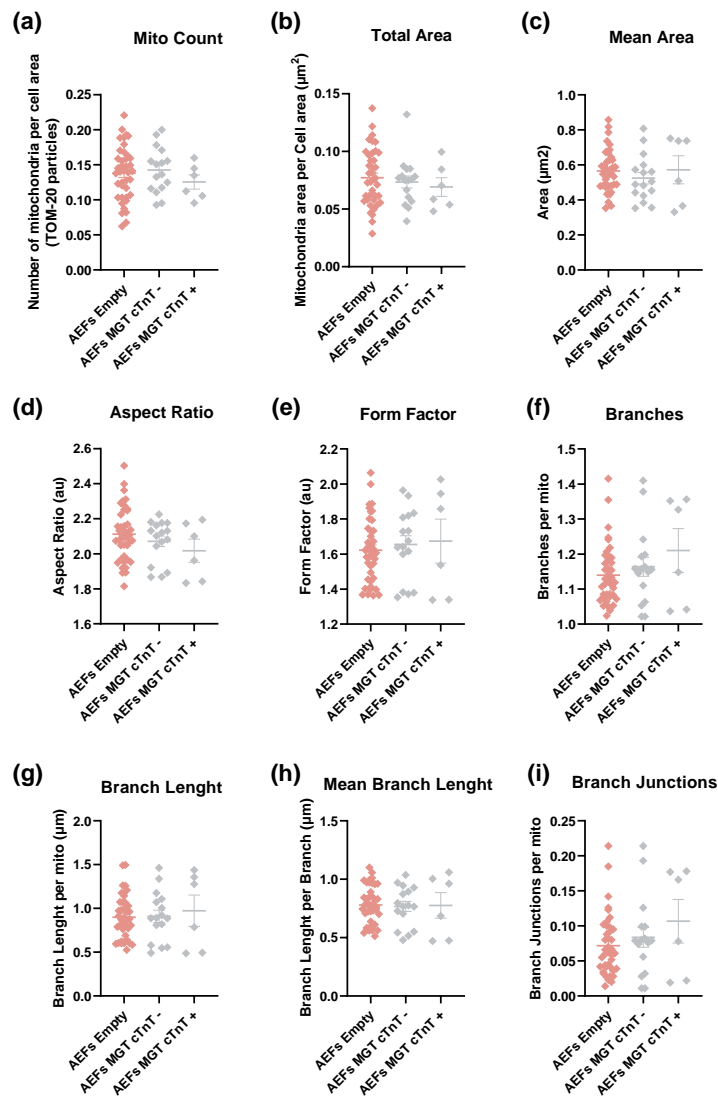
Supplementary Figure 3. Quantitative analysis and comparison of TOM-20 stained mitochondria number **(a)**, area **(b-c)**, shape **(d-e)** and network **(f-i)** parameters (briefly summarized in Table 3), between AEFs Empty and MGT, divided in cTNT-negative and cTNT-positive, at D11 post-transduction. Cells were cultured with 4:1 DMEM low glucose:M199 + 10% FBS + 1% Penicillin/Streptomycin.

Data is presented as Mean ± SEM (n = 6 (AEFs MGT cTnT+), 16 (AEFs MGT cTnT-) and 40 (AEFs Empty) from 1 independent experiment); statistical significance was determined by One-way ANOVA or Kruskal-Wallis with False Discovery Rate multiple comparisons test.
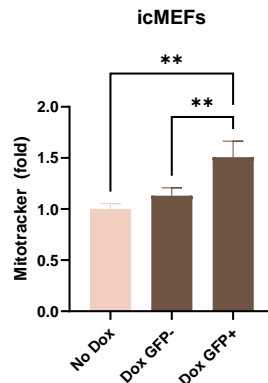
icMEFs

Supplementary Figure 4. Mitochondrial Mass quantified by flow cytometry for Mitotracker Deep Red MFI in icMEFs without or with doxycycline (Dox) supplementation for 3 days represented as the fold change to No Dox in Dox-supplemented GFP-negative and GFP-positive cells. Cells were cultured with 4:1 DMEM high glucose:M199 + 10% FBS + 1% Penicillin/Streptomycin.
Data is presented as Mean ± SD (n = 3 from 1 independent experiments); statistical significance was determined by One-way ANOVA with False Discovery Rate multiple comparisons test. **P < 0.01.

(a) D13   **(b) D28**
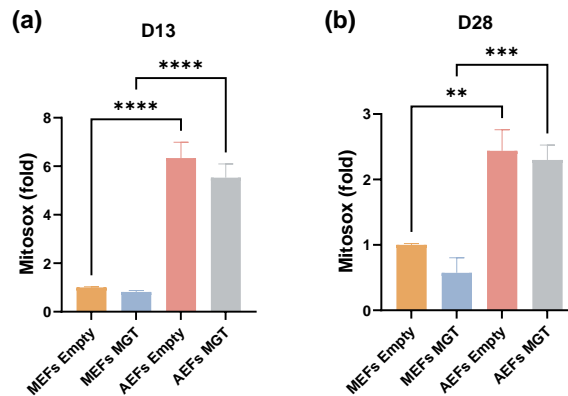
Supplementary Figure 5. Mitochondrial ROS levels quantified by flow cytometry for Mitosox MFI in MEFs and AEFs in their respective conditions (Empty and MGT) represented as the fold change over MEFs Empty at D13 **(a)** and D28 **(b)** post transduction. Cells were cultured with 4:1 DMEM high glucose:M199 + 10% FBS + 1% Penicillin/Streptomycin.
Data is presented as Mean ± SD (n=3 from 1 independent experiment); statistical significance was determined by One-way ANOVA with False Discovery Rate multiple comparisons test. **P < 0.01; ***P < 0.001; ****P < 0.0001.

(a) MEFs   **(b) icMEFs**
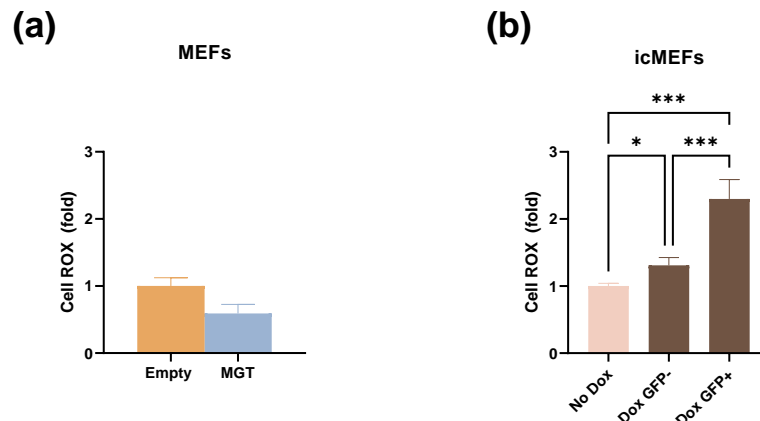
Supplementary Figure 6. ROS levels quantified by flow cytometry for CellROX MFI in MEFs Empty and MGT represented as the fold change over MEFs Empty at 11 days post-transduction (a) and icMEFs without or with doxycycline (Dox) supplementation for 3 days represented as the fold change to No Dox in Dox-supplemented GFP-

negative and GFP-positive cells (b). MEFs were cultured with 4:1 DMEM high glucose + 10% FBS + 1% Penicillin/Streptomycin. icMEFs were cultured with 4:1 DMEM high glucose:M199 + 10% FBS + 1% Penicillin/Streptomycin.

Data is presented as Mean ± SD (n=3 from 1 independent experiment); statistical significance was determined by Student *t*-test and One-way ANOVA with False Discovery Rate multiple comparisons test. *P < 0.05; ***P < 0.001.

MEFs Empty	MEFs MGT
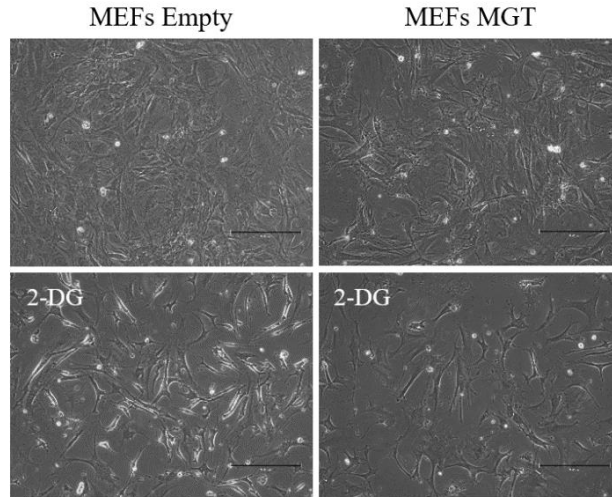
Supplementary Figure 7. Representative phase-contrast images of MEFs Empty and MGT, with and without 2-DG (0,5 to 2mM from D0-D11) at D11 post transduction. The magnification used was 10x and scale bar equals 300 μm.
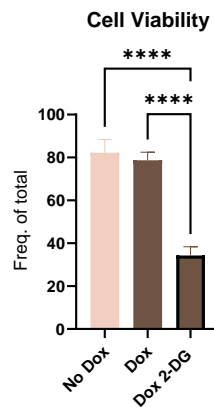
Supplementary Figure 8. Cell viability determined by flow cytometry as percentage of alive cells of icMEFs without or with doxycycline (Dox) supplementation for 3 days and with administration of 2-DG (1mM). For Dox supplemented cells, the entire population (GFP-negative and GFP-positive), was considered for the analysis. Cells were cultured with 4:1 DMEM high glucose + 10% FBS + 1% Penicillin/Streptomycin.

Data is presented as Mean ± SD (n=2/9 from 2 independent experiments); statistical significance was determined by One-way ANOVA with False Discovery Rate multiple comparisons test. ****P < 0.0001.

Annex

Review

# Metabolic Determinants in Cardiomyocyte Function and Heart Regenerative Strategies

Magda Correia [1,†], Francisco Santos [1,†], Rita da Silva Ferreira [1,†], Rita Ferreira [2,*], Bruno Bernardes de Jesus [1,*] and Sandrina Nóbrega-Pereira [1,*]

1 Department of Medical Sciences, Institute of Biomedicine—iBiMED, University of Aveiro, 3810-193 Aveiro, Portugal; tcorreiapm@ua.pt (M.C.); franciscojfsantos@ua.pt (F.S.); ritasferreira@live.ua.pt (R.d.S.F.)

2 Associated Laboratory for Green Chemistry—LAQV, Department of Chemistry, University of Aveiro, 3810-193 Aveiro, Portugal

* Correspondence: ritaferreira@ua.pt (R.F.); brunob.jesus@ua.pt (B.B.d.J.); sandrina.pereira@ua.pt (S.N.-P.)

† These authors contributed equally to this work.

Abstract: Heart disease is the leading cause of mortality in developed countries. The associated pathology is characterized by a loss of cardiomyocytes that leads, eventually, to heart failure. In this context, several cardiac regenerative strategies have been developed, but they still lack clinical effectiveness. The mammalian neonatal heart is capable of substantial regeneration following injury, but this capacity is lost at postnatal stages when cardiomyocytes become terminally differentiated and transit to the fetal metabolic switch. Cardiomyocytes are metabolically versatile cells capable of using an array of fuel sources, and the metabolism of cardiomyocytes suffers extended reprogramming after injury. Apart from energetic sources, metabolites are emerging regulators of epigenetic programs driving cell pluripotency and differentiation. Thus, understanding the metabolic determinants that regulate cardiomyocyte maturation and function is key for unlocking future metabolic interventions for cardiac regeneration. In this review, we will discuss the emerging role of metabolism and nutrient signaling in cardiomyocyte function and repair, as well as whether exploiting this axis could potentiate current cellular regenerative strategies for the mammalian heart.

Keywords: cell reprogramming; pluripotency; metabolism; nutrient signaling; cardiomyocytes; cardiac regeneration; mitochondria

1. Introduction

Cardiovascular diseases are the leading cause of morbidity and mortality worldwide [1]. This is largely due to the inability of the adult mammalian heart to replenish the lost myocardial tissue following injury, which results in the progressive weakening of the heart muscle and the development of heart failure [2]. Although, currently, there is a large range of pharmaceutical drugs and surgical options that prevent further deterioration or restore function to the failing heart, the only long-term solution for end-stage heart failure is heart transplantation [3]. Several regenerative strategies to repair the injured heart and improve heart function have been pursued, including post-injury activation of cardiomyocyte proliferation, recruitment of cardiac progenitor cells, delivery of embryonic stem cells (ESCs) or induced pluripotent stem cells (iPSCs)-derived cardiomyocytes, and direct reprogramming of somatic cells into induced cardiomyocytes (for a revision, see [3,4]). Besides holding great promise, most cardiac regenerative strategies still lack effective clinical outcomes [3,4]. Thus, understanding the molecular mechanisms and players governing cardiomyocyte function is warranted for improving the efficiency of cardiac regenerative strategies and the patient's welfare. Following an injury, the capacity for regeneration of the adult mammalian heart is limited, with an estimation of only 1% De Novo cardiomyogenesis per year [5], while the neonatal heart is capable of substantial

regeneration, but this capacity is lost by postnatal day (P) 7 [6]. The transition from neonatal to adult heart is accompanied by profound cellular and metabolic changes. Interestingly, this loss of proliferative potential is accompanied by a bioenergetic shift in cardiomyocytes, from glucose-driven anaerobic glycolysis to oxygen-dependent oxidative phosphorylation of pyruvate and fatty acids (FAs), in the mitochondria [7,8]: the so-called fetal metabolic switch (Figure 1). The healthy heart is the most energetically demanding and metabolically versatile organ [9–11], and upon injury, metabolic reprogramming compensates for impaired fuel utilization and loss of mitochondrial functionality in the diseased heart [12]. Apart from energetic sources, metabolites, including those that are mitochondria-derived, are key regulators of gene expression programs by acting as essential substrates or cofactors for chromatin-modifying enzymes [13] and regulating histone landscape transitions that drive adult stem cell regeneration [14–16]. Understanding the impact of systemic metabolism and nutrient signaling in cardiomyocytes' self-renewal, differentiation, and maturation may bring new opportunities for cardiac regeneration.
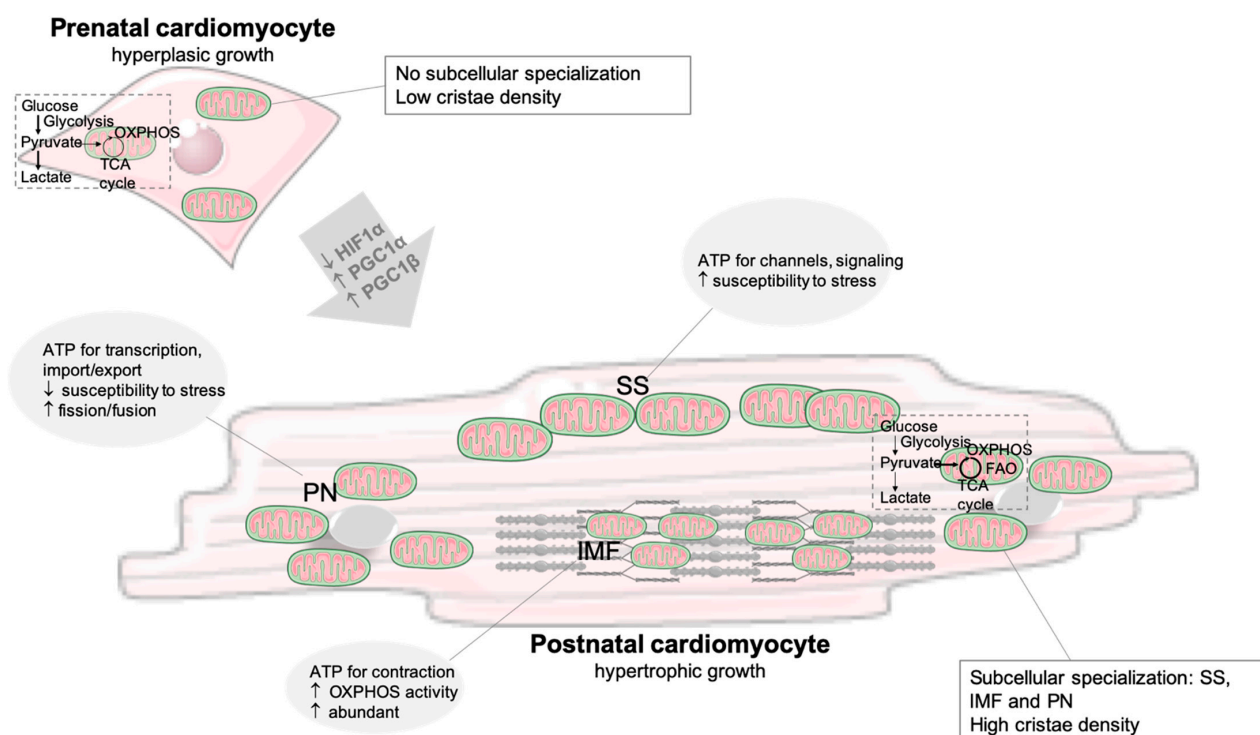
Figure 1. Connection between cardiomyocyte development and mitochondria usage and maturation, highlighting mitochondria specialization according to the spacial arrangement in postnatal cardiomyocytes. After birth, a bioenergetic shift from glucose-driven anaerobic glycolysis to the oxidation of fuels in the mitochondria occurs. Mitochondria increase in size and density, and cristae become denser. The upregulation of PGC coactivators and the downregulation of HIF1α regulate mitochondria biogenesis. Abbreviations: FAO, fatty acid oxidation; HIF, hypoxia-inducible factor; IMF, intermyofibrillar; OXPHOS, oxidative phosphorylation; PGC, peroxisome proliferator-activated receptor-gamma coactivator; PN, perinuclear mitochondria; SS, subsarcolemmal; TCA, tricarboxylic acid cycle; up arrow: increase; low arrow: decrease.

In this review, we highlight major studies of metabolism and nutrient signaling in cardiomyocyte function, including insights into metabolic reprogramming during development and in the injured heart. We also discuss key metabolic determinants and manipulations that drive cellular pluripotency and cardiac differentiation, which have been shown to improve current heart regenerative strategies.

2. Metabolism in the Adult Heart: Mitochondria and Fuels

The healthy adult heart is highly reliant on fatty acid oxidation (FAO, 50–70%) for ATP generation, while the remaining percentage is mostly assured by glucose oxidation. Ketone bodies, mainly β-hydroxybutyrate (βOHB), are the third main supplier of the tricarboxylic acid (TCA) cycle (10–15%), whereas amino acids only contribute 1–2% for energetic purposes [17]. The heart can use a variety of amino acids as fuel sources, including branched-chain amino acids (BCAAs), glutamate, cysteine, histidine, and lysine [18]. The contribution of these substrates as energetic suppliers highly depends on their circulating levels, hormonal status, and cardiac workload [17]. Mitochondria are the ultimate fate of fatty acyl-CoA and pyruvate, products of lipolysis or free fatty acids (FFAs) uptake and glycolysis, respectively, and they are the place in the cell where ketone bodies are converted into acetyl-CoA and amino acids undergo transamination [17,19].

Mitochondria occupy around 30% of cardiomyocytes' volume to accommodate the high ATP demands that drive cardiac contraction/relaxation (around 90%) and ionic homeostasis. In fact, cardiomyocytes, out of all the cell types, exhibit the highest mitochondrial density, which reflect the key role of this organelle in the cardiac remodeling, induced by several pathophysiological conditions [12,19–21]. The organization of mitochondria within cardiomyocytes is determined to support heart function [22]. In adult cardiomyocytes, mitochondria are spatially arranged in three different subpopulations: intermyofibrillar (IMF), subsarcolemmal (SS), and perinuclear (PN) mitochondria (Figure 1). IMF mitochondria, the most abundant subpopulation, energetically support the contractile activity of cardiomyocytes, whereas the SS subpopulation provides ATP for membrane activities (channel and signaling functions), and the PN mitochondria provide energy for transcription and import/export processes [19,23,24].

Regardless of the cellular location, the major function of mitochondria is to support ATP generation through the OXPHOS process, which is primarily reliant on the reducing equivalents obtained from the oxidation of long-chain fatty acids (LCFAs). Circulating FA (lipoprotein-derived and albumin-derived FAs) are taken up by a family of transporters, including FA translocase (FAT/CD36), plasma membrane fatty acid-binding protein (FABP), and FA transport protein 1 (FATP1), with FAT/CD36 showing greater efficiency [25–27] (Figure 2). The translocation of these transporters to the sarcolemma is crucial for FA uptake and oxidation, and it is regulated by contraction, insulin, and AMP-activated protein kinase (AMPK). In fact, changes in the relocation of these transporters have great impact on the use of FA for energetic purposes [26] since the energetic stores (such as triglycerides, TG) are limited, supporting only a few heart beats [19] (Figure 2).

FAO is co-regulated with other metabolic pathways to assure homeostasis when the environmental conditions change. Such reciprocal regulation in the heart is mostly noticeable between FAO and glucose oxidation [26,28]. Glucose, the second main fuel, is translocated into cardiomyocytes through the glucose transporters (GLUTs)—mainly GLUT4 (Figure 2). This glucose transporter resides in intracellular storage vesicles, being translocated to the sarcolemma in response to stimuli, such as insulin, increased workload, and catecholamines [29]. Glucose is converted into pyruvate through glycolysis, and pyruvate is then oxidized in mitochondria. Regarding ATP generation efficiency, glucose oxidation is more cost-effective compared to FAO (2.58 vs. 2.33 P/O ratio) [11]. Glycolysis contributes with a small percentage of ATP (less than 10%), which is mostly used to energetically support ion pumps [30]. However, the role of glycolysis goes beyond the energy supply. This metabolic pathway feeds other pathways with intermediate metabolites, such as glycogen synthesis, hexosamine biosynthetic, polyol, and pentose phosphate pathways that regulate cell proliferation, redox balance, and transcription. The deregulation of these pathways has been reported in conditions that lead to cardiac dysfunction [31].
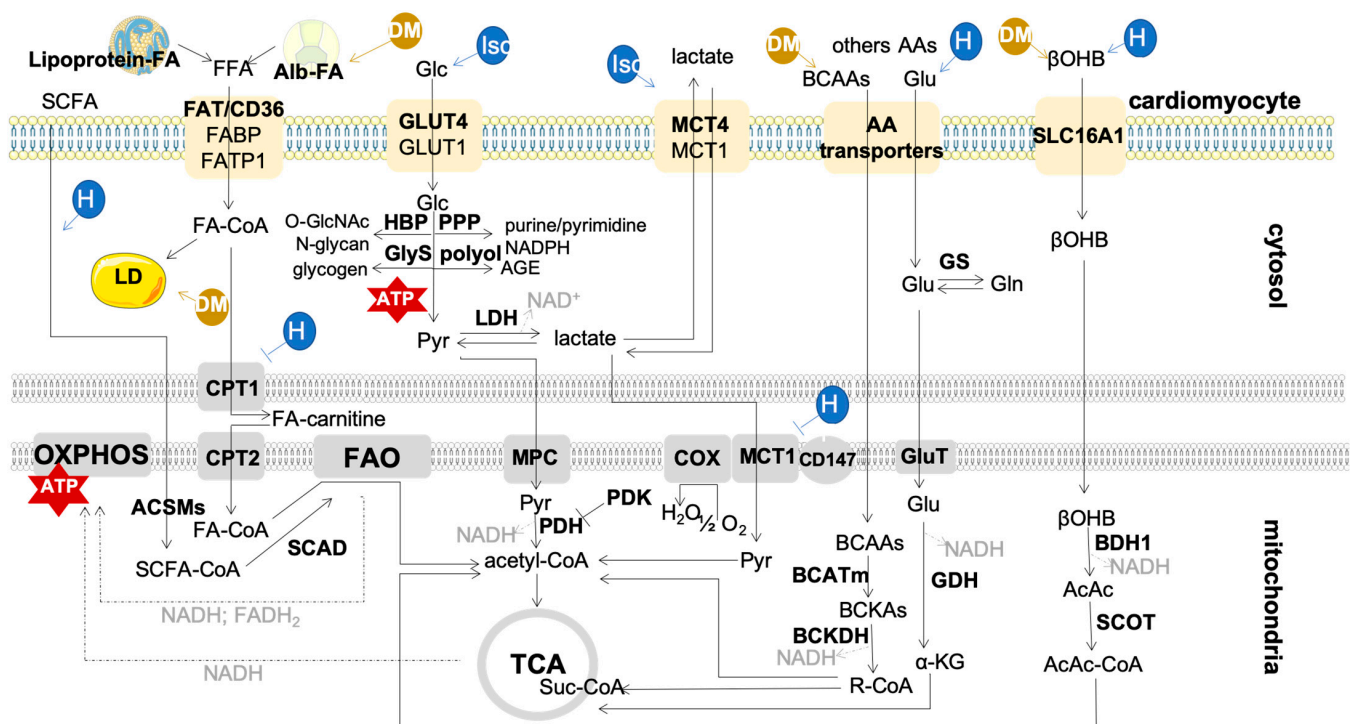
Figure 2. Energetic metabolism of cardiomyocytes. FFAs (free fatty acids), the main energetic fuel, are converted into long-chain acyl-CoA esters by fatty acyl CoA synthetase, and then, into long-chain acylcarnitine by CPT1, the rate limiting enzyme of long-chain FAO. Inside the mitochondria, long-chain acylcarnitine is converted back to long-chain acyl-CoA by CPT2, and then, several isoforms of acyl-CoA dehydrogenase, enoyl-CoA hydratase, 3-hydroxyacyl CoA dehydrogenase, and 3-ketoacyl CoA thiolase (specific for different chain lengths) mediate the shortening of the fatty acyl moiety, generating acetyl-CoA, FADH2, and NADH. Glc is transported by GLUTs (GLUT4 in adult heart) into cardiomyocytes, and, in the cytosol, Glc is converted into pyruvate through glycolysis. Pyruvate may be oxidized in mitochondria or converted into lactate by LDH in the cytosol. Lactate uptake and secretion is mediated by MCTs (MCT4 in the adult heart). MCT1 makes part of the mtLOC, which is also composed of CD147, LDH, and COX. Lactate may be oxidized in the mitochondria by this complex. Ketones, mostly βOHB, may feed TCA after being metabolized by the enzymes β-hydroxybutyrate dehydrogenase 1 (BDH1, the enzyme that interconverts β-hydroxybutyrate into acetoacetate) and succinyl-CoA:3-ketoacid CoA transferase (SCOT, the rate-limiting enzyme of ketone oxidation). SCFAs (including acetate, propanoate, and butyrate) can cross the mitochondrial membrane by diffusion, and enter FAO through SCAD, after being activated via ACSMs. BCAA and other amino acids, such as Glu, may be used for energetic purposes by feeding the TCA cycle. BCATm and BCKDH catalyze the first two enzymatic steps in BCAA metabolism. The contribution of these metabolic pathways changes in the injured heart. In ischemia (Isc), the reliance on glucose and lactate increases, but when insulin signaling is repressed, FAO is upregulated. During heart failure (HF) glucose oxidation prevails until mitochondria functionality is impaired, which happens at advanced stages of disease. In diabetes mellitus (DM), glucose uptake and oxidation decrease, inducing a higher reliance of cardiac metabolism on lipids for energetic purposes. Abbreviations: α-KG, α-ketoglutarate; βOHB, β-hydroxybutyrate; AA, amino acid; AcAc, acetoacetate; ACSMs, acyl-coenzyme A synthetase medium chain family members; AGE, advanced glycation end products; Alb, albumin; ATP, adenosine-5′-triphosphate; BCAA, branched chain amino acids; BCATm, mitochondrial branched-chain aminotransferase; BCKDH, branched-chain α-ketoacid dehydrogenase complex; BDH1, 3-hydroxybutyrate dehydrogenase 1; CD147, cluster of differentiation 147; COX, cytochrome c oxidase; CPT, carnitine palmitoyl transferase; DM, diabetes mellitus; FA-carnitine, acyl-carnitine; FA-CoA, long-chain acyl-CoA; FABP, fatty acid binding protein;

FAO, fatty acid oxidation; FAT/CD36, fatty acid translocase; FATP, fatty acid transport protein; $FADH_2$, reduced flavin adenine dinucleotide; GDH, glutamate dehydrogenase; Glc, glucose; Gln, glutamine; Glu, glutamate; GLUT, glucose transporter; GluT, glutamate transporter; GlyS, glycogen synthesis; GS, glutamine synthase; HBP, hexosamine biosynthetic pathway; HF, heart failure; Isc, ischemia; LD, lipid droplet; LDH, lactate dehydrogenase; MCT, monocarboxylate transporter; MPC, mitochondrial pyruvate carrier; NAD^+, oxidized nicotinamide adenine dinucleotide; NADH, reduced nicotinamide adenine dinucleotide; O-GlcNAc, O-linked β-N-acetylglucosamine; OXPHOS, oxidative phosphorylation; PDH, pyruvate dehydrogenase; PDK, pyruvate dehydrogenase kinase; PPP, pentose phosphate pathway; Pyr, pyruvate; R-CoA, branched-chain acyl CoAs; SCOT, succinyl-CoA: 3-oxoacid-CoA transferase; SCAD, short chain acyl-CoA dehydrogenase; SCFA, short chain fatty acids; SLC16A, solute carrier family 16 member 1; Suc-CoA, succinyl-CoA; TCA, tricarboxylic acid cycle.

2.1. Developmental Changes and the Fetal Metabolic Switch

The human heart starts pumping blood in the fourth week of fetal development [32]. The fetal heart relies on glucose and lactate for energetic purposes, and these metabolites are obtained from the mother via the placenta [33]. Glucose is the chosen fuel not only due to hypoxia in utero but also due to substrate availability. Low oxygen levels activate the hypoxia-inducible factor (HIF)1α, which is a transcription factor that regulates the expression of genes involved in glucose metabolism, particularly in glycolysis [32]. The higher reliance on glycolysis is reflected in the expression of specific gene isoforms of glycolytic enzymes, such as hexokinase I, pyruvate kinase 4, fetal phosphofructokinase (PFK), and lactate dehydrogenase (LDH) isoform LDHA [34]. The uptake of glucose is assured by GLUT1, whereas in the adult heart, GLUT4 is the most represented isoform [31] (Figure 2). The cardiac expression of hexokinase I, HIF, and LDHA has been reported to be uniform during the late first and early second trimester in human fetuses. This glycolytic environment supports the biosynthesis of biomolecules, such as lipids and nucleotides, sustaining fetal development [35]. In utero, the heart also seems very dependent on BCAA degradation compared to that of newborns, given the significant overexpression of 17 genes associated with BCAA metabolism [33]. The expression of genes from fatty acid metabolism (e.g., fatty acid binding protein 4 (FABP4), FABP2, and retinol-binding protein (RBP)) was reported to increase as the heart matures [35]. The energetic metabolism changes, from glycolysis to FAO, during the first weeks after birth (Figure 1). The upregulation of CPT1A transcripts suggests an elevation in medium and long-chain FA oxidation in the newborn heart [33]. The increased levels of oxygen and decreased activity of HIF1α are key determinants for this metabolic remodeling of the myocardium [34].

The metabolic switch towards OXPHOS is dependent on the mitochondrial oxidative capacity, which increases in mature and terminally differentiated cardiomyocytes. In humans, cardiomyocytes proliferate during the first months of the postnatal life, after which these cells are only capable of hypertrophic growth (Figure 1). Mitochondria are small and round in the fetus, but in the neonatal heart, mitochondria fuse, increasing in size, and the cristae become denser. Increased biogenesis, together with the overexpression of peroxisome proliferator-activated receptor-gamma coactivator (PGC)-1α, occurs in the early phases of postnatal life, doubling the mitochondrial mass [34,36] (Figure 1). PGC-1β is also essential for mitochondrial maturation and dynamics during postnatal development. Both PGC-1α and PGC-1β regulate the expression of genes involved in fusion and fission processes [37]. The downregulation of HIF1α is also essential for mitochondrial maturation and, consequently, for increasing OXPHOS activity [38] (Figure 1).

2.2. Metabolic Changes in the Injured Heart

In the pathological remodeling of the heart, metabolic changes occur to compensate for impaired fuel utilization and loss of mitochondrial functionality that may occur at advanced stages. This remodeling is characterized by a shift in the energetic fuel, from FFAs to glucose (towards a fetal phenotype), with impact on cardiomyocytes function [12].

Nevertheless, there are discrepancies in the literature regarding the energetic choices of the failing heart, which seems to depend on the animal model, duration of cardiac disease, and on the availability of energetic substrates [11].

Ischemic heart is more reliant on glycolysis due to an oxygen deficit; however, the glycolysis rate is not enough to cope with ATP decline. Increased glucose uptake and glycolysis seems to be regulated by AMPK and not by insulin-dependent phosphoinositide 3-kinase (PI3K) signaling. AMPK phosphorylates and activates PFK2 during ischemia, leading to increased production of fructose-2,6-biphosphate and, consequently, to the activation of PFK1 [39]. AMPK-dependent mechanisms are also implicated in the translocation of GLUT4 to the cell membrane during ischemia, increasing glucose uptake [26]. However, increased glycolysis becomes uncoupled from pyruvate oxidation. The decrease in mitochondrial pyruvate metabolism seems to be due, at least in part, to the diminished activities of mitochondrial pyruvate carrier (MPC) and pyruvate dehydrogenase (PDH) [40,41]. The cytosolic pyruvate that accumulates is converted into lactate by the bidirectional enzyme LDH (Figure 2). Increased expression of LDHA, the isoform more likely to produce lactate from pyruvate, was reported in the Dahl salt-sensitive rat model of heart failure with a preserved ejection fraction (HFpEF) [40]. The relative abundance of lactate is higher than pyruvate, so lactate turns out to be the main supplier of acetyl-CoA, and lactate consumption decreases [41]. Increased lactate uptake was also reported in the heart from patients with HFrEF [25]. Monocarboxylate transporter (MCT) isoforms 1 and 4 are key lactate transporters in cardiac muscle (Figure 2), and enhanced expression of MCT4 was observed following ischemia; however, this isoform is mainly associated with lactate efflux [42]. In fact, cardiomyocytes seem to release and consume lactate at the same time [43]; endogenously produced lactate is mainly released, whereas most of the consumed lactate is oxidized, as it is an important source of energy for the heart [44]. Lactate is oxidized by the mitochondrial lactate oxidation complex (mtLOC) [40,43] (Figure 2). Impaired activity of mtLOC may occur in a failing heart, leading to intracellular lactate overload that is accompanied by enhanced H$^+$ levels and a pH decrease. Subsequently, ATP is consumed by ion channels to reestablish pH, and cardiac muscle contractibility becomes impaired [40].

Decrease in fatty acid uptake and oxidation (Figure 2) was reported in late-stage heart failure due to increased phosphorylation and ubiquitination of CD36. This leads to the reduced activation of peroxisome proliferator-activated receptor alpha (PPARα; the cardiac abundant isoform of PPAR family), as FFAs are endogenous ligands of this transcription factor, and, thus, CD36 expression is limited [45]. Moreover, PGC-1α/PPARα downregulation suppresses FAO activity [12]. The decrease in CPT1 activity aggravates the lack of a fatty acyl supply for OXPHOS, and LCFA can be converted into the cardiotoxic species. The decline in CPT1 activity is related to a shift from CPT1B to CPT1A expression (the predominant fetal isoform). Short chain fatty acids (SCFAs) can overcome the lack of CPT1 activity and represent an important fuel for OXPHOS in the failing heart [46] (Figure 2). SCFAs are mainly produced by gut microbiota, with acetate being the most abundantly produced metabolite that can be used as energetic fuel and in epigenetic regulation [25,46]. Nevertheless, the downregulation of PGC1α impairs mitochondrial biogenesis and, consequently, reduces mitochondrial density and worsens the energy crisis, by being PGC1α expression fine-tuning critical for cardiac homeostasis.

In the insulin-resistant state of heart failure, glucose uptake and oxidation decrease [11]. Being a typical insulin-targeted cell, cardiomyocyte metabolism is affected by failure in insulin signaling. The increased content of circulating FFAs further inhibits insulin signaling by targeting insulin receptor substrate 1 (IRS1) and AMPK [47], reducing glucose uptake and inducing a higher reliance of cardiac metabolism on lipids for energetic purposes (approximately 90% of energy) [48]. Still, increased FAO may not be enough to compensate for FFAs uptake by cardiomyocytes, resulting in an ectopic lipid accumulation (a condition known as cardiac steatosis) of TG and other forms of lipids, such as ceramides and diacylglycerols (DAG). Lipotoxicity results in the loss of proton gradient and, therefore, in decreased ATP generation. Ultimately, the loss of mitochondrial membrane potential and

the release of cytochrome c activates apoptosis, contributing to cardiomyopathy in obese and diabetic patients [22,49,50]. However, the heart has mechanisms to control lipotoxicity. For example, cardiac progesterone receptor membrane component 1 (PGRMC1) enhances mitochondrial respiration and FAO rates, preventing the accumulation of toxic lipids [50]. Increased circulating levels of BCAAs (i.e., Val, Leu, Ile) have also been related to insulin resistance through the BCAA-induced activation of the mechanistic target of rapamycin (mTOR) in the muscle and the direct toxicity of BCAA products, such as branched-chain ketoacids (BCKA) [51] (Figure 2). BCAA oxidation rates were reported to decrease and contribute with only around 1%, for ATP generation in the heart of insulin-resistant obese rats, which is accompanied by increased production of BCKA [52]. Still, the impact of BCAA on cardiac maladaptive remodeling is unclear. Other amino acids can be used as metabolic substrates. For example, glutamate uptake was reported to increase in heart failure as a response to increased circulating levels and lower rates of cardiac perfusion [25] (Figure 2). However, the heart not only consumes but also secretes amino acids—mainly glutamine and alanine—which is a way to remove amino groups from the working heart, and it is a sign of proteolysis and impaired cardiac function [25,53].

The diabetic and failing heart can be exposed to increased ketone concentrations, which are mainly produced in the liver. Increased availability is synonymous with enhanced use, with ketones becoming a major fuel of the heart (approximately 20% of energy). However, ketone oxidation does not replace that of FFAs and glucose, thus acting as an extra source of energy [9,10]. Indeed, increased reliance on ketone oxidation leads to enhanced TCA cycle activity, oxygen consumption, and, consequently, to higher cardiac work with no change in cardiac function [10]. The role of ketone bodies in heart failure goes beyond energy supply, acting as signaling molecules (e.g., βOHB inhibits histone deacetylases) and regulators of inflammation and immune cell function with an impact on heart homeostasis [54,55].

Taken together, energetic substrates are involved in the development and progression of cardiac dysfunction. Changes in the metabolic choice have an impact on energy generation and other regulatory functions, and, as a result, on cardiac remodeling and functionality.

3. Metabolic Control of Stem Cells Pluripotency with Implications for Cardiac Regeneration

There is a growing interest in understanding the mechanisms of ESCs and iPSCs self-renewal and differentiation, given their potential application for cell therapy, including heart regeneration [56]. Metabolites play many roles beyond serving as substrates for energy generation and anabolic growth, such contributing to intracellular redox balance and activation of intracellular signaling cascades [14]. Moreover, several metabolites can directly regulate histone marks by serving as substrates or cofactors for chromatin-modifying enzymes. For instance, acetylation and demethylation of histones relies on the availability of the TCA cycle intermediates, citrate-derived acetyl-CoA and α-ketoglutarate [14], coupling mitochondrial metabolism to transcriptional regulation.

The energetic metabolism is a key regulator of ESCs and iPSCs self-renewal, pluripotency, and differentiation (for a review, see [13,57,58]). In rodents, naïve and primed ESCs display key differences, including signaling requirements for self-renewal and central carbon metabolism [58,59]. In particular, naïve ESCs use more OXPHOS, whereas primed ESCs rely almost entirely on glycolysis [60,61]. In contrast to a mouse, human naïve ESCs exhibit increased glycolysis compared to primed ESCs [62], reflecting species-specific differences, such as dependence on FGF signaling [13]. The adoption of a predominant glycolytic metabolism, highly dependent on glucose and glutamine, irrespective of oxygen, is shared by transformed cancer cells and is known as the Warburg effect [63], which is a cancer hallmark with relevance for therapy [64–67]. The major function of aerobic glycolysis seems to be the provision of glycolytic intermediates for anabolic reactions required during proliferation [64,68], highlighting the intricate relationship between proliferation and bioenergetics.

Mitochondria are essential regulators of stem cell function [69]. Reactive oxygen species (ROS), a secondary product of mitochondrial respiration, regulate the transcription and proliferation of stem cells [69]. Despite the dominant glycolytic metabolism, mouse primed ESCs can engage in the oxidation of substrates in the mitochondria (as glutamine) [70,71]. Naïve and primed mouse ESCs present significant differences in the mitochondria dynamics, with naïve ESCs exhibiting fragmented, perinuclear mitochondrial morphology with underdeveloped cristae, whereas primed ESCs mitochondria appear elongated, with relatively more developed cristae [72]. The predominant elongated mitochondrial network of mouse primed ESCs is not accompanied by an expected reliance on mitochondrial respiration, suggesting other regulatory roles, other than bioenergetics, for mitochondria. As for ESCs, the reprogramming of somatic cells into iPSCs is accompanied by a shift from OXPHOS to glycolysis [57,73]. In iPSC reprogramming, an early fragmentation of mitochondria governed by Drp1 occurs, and the reprogramming-induced mitochondria fission is required for the full activation of pluripotency [74].

Apart from energy, intracellular FAs and acetyl-CoA pools regulate stem cell self-renewal and differentiation by epigenetic modulation [13,14,75]. Acetyl-CoA-driven histone H3 acetylation, together with H3K4me3, results in an open euchromatin state that promotes ESCs pluripotency and self-renewal [76,77]. De novo FA synthesis is critical for stem cell pluripotency and cellular reprogramming by promoting mitochondrial fission in an ACC1-dependent manner [78]. The balance between exogenous lipids and de novo lipogenesis is key for the metabolic programming of epigenetics [79,80]. Lipid free culture conditions shift human stem cells towards a naïve to primed intermediate state, resulting in markedly de novo lipogenesis and endogenous ERK inhibition. Increased lipogenesis raises acetyl-CoA and α-ketoglutarate levels, promoting histone acetylation and DNA hypomethylation [79]. ESCs' and iPSCs' exits from pluripotency are generally accompanied by a metabolic switch from glycolysis to OXPHOS-dependency [62,81,82]. High glycolytic fluxes contribute to elevated acetyl-CoA pools, which drive a highly-acetylated, open chromatin landscape in proliferating stem cells, in deep contrast to differentiated cells that exhibit compacted chromatin [77,81].

Most adult endogenous progenitor/stem cells reside quiescent in hypoxic niches, unless activated by stress or injury, and have an intrinsically glycolytic mode of metabolism [13, 83], minimizing ROS production and entry into proliferation. Several reports have highlighted the importance of glucose and lipid metabolism in adult stem and progenitor cells including skeletal muscle stem cells (MuSCs) (for a review, see [13,16]). Glucose is dispensable for mitochondrial respiration in proliferating MuSCs, thus becoming available for acetyl-Co-dependent histone acetylation and chromatin accessibility of genes that must be silenced upon differentiation [84]. Conversely, quiescent and differentiating MuSCs increase glucose oxidation in the mitochondria, with reduction in histone acetylation. FAO usage is also necessary for preserving MuSCs' self-renewal, where SIRT1 deacetylates and activates PGC-1α, promoting FAO and repressing glycolysis [85]. During the exit from quiescence, MuSCs deactivate FAO in favor of glucose catabolism, decreasing NAD+, SIRT1, and its histone H4K16 deacetylation activity, leading to the activation of a myogenic transcription program and differentiation [86]. Moreover, lipid availability can also determine skeletal progenitor cells' potential of chondrogenesis over osteogenic differentiation [87]. When lipids are scarce, skeletal progenitors activate FOXO that suppress FAO in a SOX9-depedent manner, adapting cells to an avascular life [87].

In conclusion, the balance between intrinsic metabolic needs and extrinsic metabolic constraints regulates stem cell metabolism and self-renewal, highlighting the importance of nutritional systemic factors in modulating pluripotency during development and regeneration.

4. Metabolic Reprogramming to Enhance Cardiac Regenerative Strategies

In order to minimize the distressing outcomes of heart failure, several regenerative strategies have been proposed (Figure 3a). Current protocols of cardiomyocyte regenera-

tion have been developed based on activating the embryonic cardiomyogenesis-induced signaling pathways and gene regulatory networks. Most studies of cardiomyocyte regeneration are focusing on the contributions of transcriptional mechanisms, including gene programming, epigenetic chromatin modifications, and biochemical differentiation cues (for review, see [88,89]). Energy metabolism is central to mammalian heart development and function, and metabolic processes can be modulated to support the contractile apparatus of regenerated cardiomyocytes. Moreover, metabolism impacts the ability of stem cell self-renewal, differentiation, and cell fate decision. Although the coordination of genetic networks with developmental bioenergetics is critical to cardiomyocyte specification, the underlying metabolic mechanisms that drive cardiac induction and differentiation, in the context of heart regeneration, are only just beginning to be appreciated (summarized in Table 1 and Figure 3b).
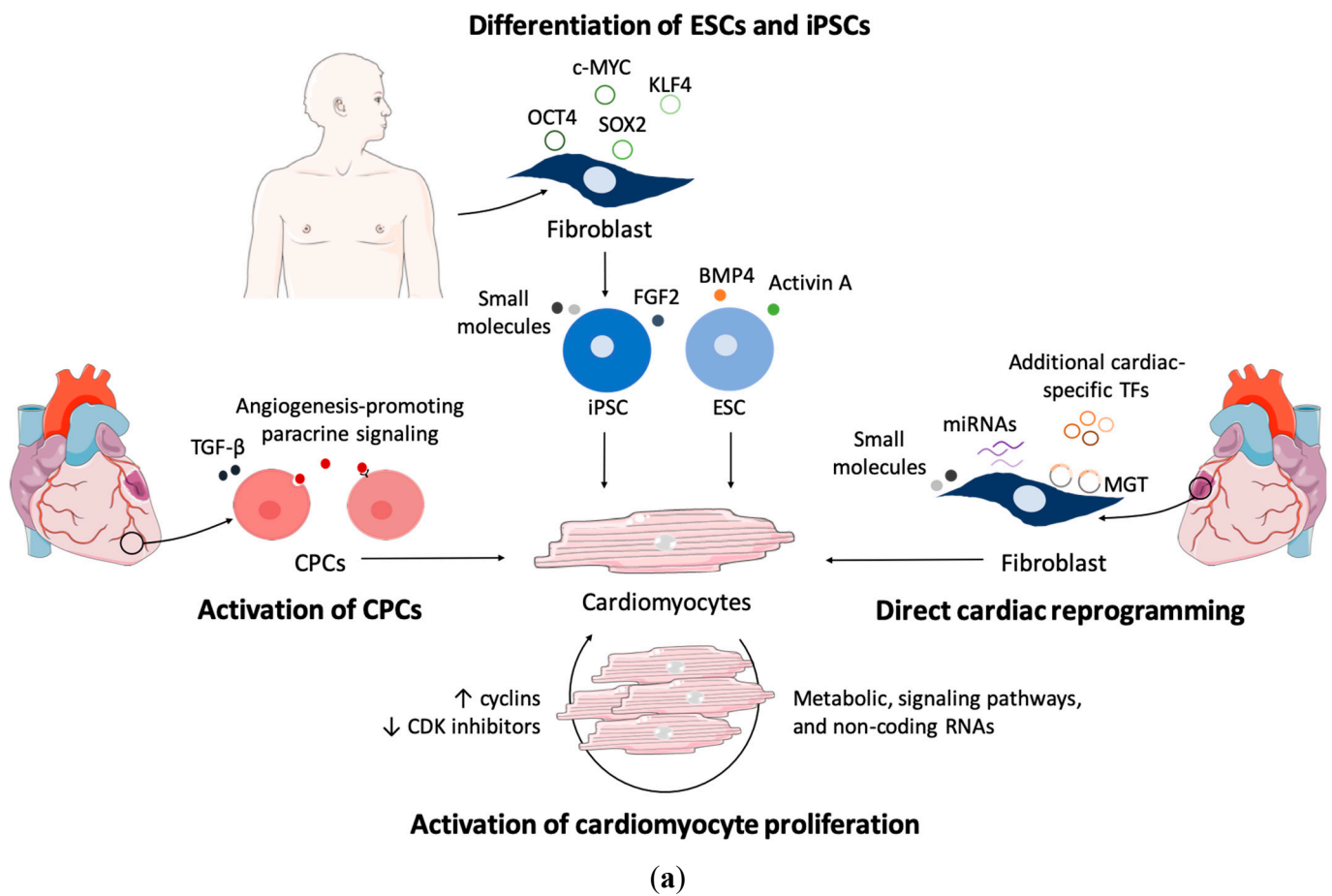
Figure 3. *Cont.*
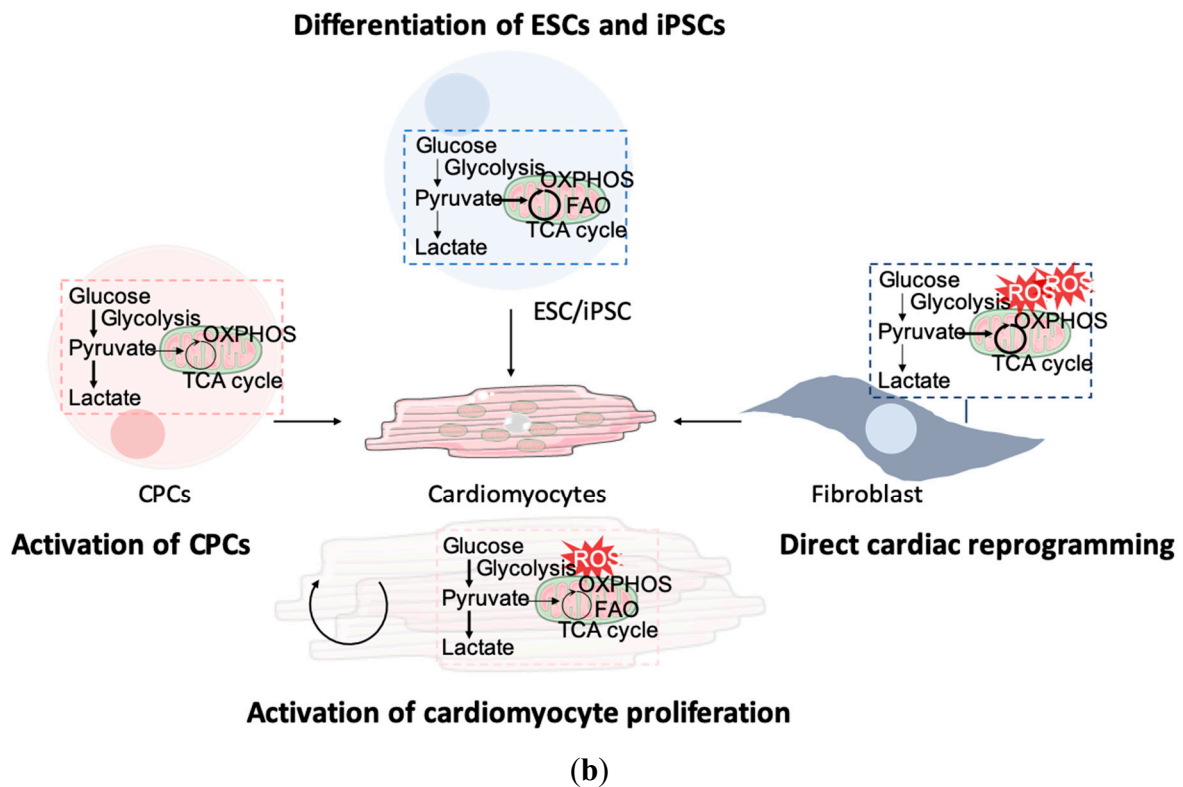
Figure 3. Heart regeneration strategies and metabolic manipulations to increase cardiac regeneration. (**a**) Approaches for replacing lost cardiomyocytes. By modulating factors that either promote (overexpression of cyclins) or repress (silencing of CDK inhibitors) cell cycle activity, adult cardiomyocytes, can be forced to proliferate. Metabolic and signaling pathways, as well as the expression of non-coding RNAs, can also be modulated to induce cardiomyocyte proliferation. Stimulating the differentiation of CPCs into cardiomyocytes can be achieved by treatment with TGF-β or paracrine signaling, for example. ESCs and iPSCs have been used to generate cardiomyocytes, which can be transplanted to replace cells that were lost upon cardiac injury. Direct cardiac reprogramming can be achieved by overexpressing the cardiac factors Mef2c, Gata4, and Tbx5 (termed MGT) into resident fibroblasts. The addition of additional transcription factors and small molecules, and manipulation of miRNAs, can improve reprograming efficiency. (**b**) Metabolic reprogramming to increase cardiac regenerative potential. The stimulation of glycolysis, inhibition of FAO, and decrease in oxygen increase cardiomyocyte proliferation. Activation of CPCs can be induced with high concentrations of glucose and glutamine in the media, hypoxia, and reduction in ROS levels. Differentiation of ESCs and iPSCs into cardiomyocytes can be improved by increasing FAO, decreasing glucose, and increasing exogenous lipids and galactose. For direct cardiac reprogramming, stimulation of OXPHOS and inhibition of glycolysis increases the efficiency of the process. Abbreviations: CPCs, cardiac progenitor cells; ESCs, embryonic stem cells; FAO, fatty acid oxidation; iPSCs, induced pluripotent stem cells; OXPHOS, oxidative phosphorylation; ROS, reactive oxygen species; TCA, Tricarboxylic acid cycle; up arrow: increase; low arrow: decrease.

4.1. Activation of Cardiomyocyte Proliferation

The re-entry of cardiomyocytes into the cell cycle has become one of the employed strategies to regenerate cardiac tissue (for review, see [90,91]) (Figure 3a). Indeed, fetal, neonatal, and adult hearts exhibit very specific expression patterns of cardiomyocyte proliferation regulators, including gene expression, cell cycle regulators, metabolic and signaling pathways, extracellular matrix proteins and growth factors. As expected, manipulating these factors has become a strategy to force adult cardiomyocytes to re-enter the cell cycle [90,91]. Several studies have focused on the overexpression of cyclins to force mammalian (particularly mouse) cardiomyocytes to re-enter the cell cycle. For example,

overexpression of cyclins D1, D2, and A2 were shown to induce cardiomyocyte proliferation, upon and in the absence of injury [92–95]. Similarly, the inhibition of cyclin-dependent kinase inhibitors, such as p21, p27, and p57, have also been shown to promote cardiomyocyte proliferation [96]. The Hippo signaling pathway has been extensively studied in cardiomyocyte proliferation, and the modulation of Hippo pathway components has been shown to promote cardiomyocyte proliferation. Indeed, activation of YAP or the depletion of Hippo or Salvador all exhibit promising results in pushing cardiomyocytes to re-enter the cell cycle [97,98]. Other signaling pathways that stimulate cardiomyocytes to proliferate and induce cardiac regeneration upon injury include the neuregulin/ERBB2/ERBB4, PI3K/AKT/CDK7, Wnt/β-catenin, PDGFR-β, and Notch signaling pathways [91,92]. Non-coding RNAs, such as microRNAs (miRNAs) and long non-coding RNAs (lncRNAs), have gained special attention over the last few years, given their potential to regulate gene expression at various levels, revealing very particular spatiotemporal profiles. In fact, several miRNAs, such as miR-128, and lncRNAs, namely *CAREL*, have been associated with cardiomyocyte proliferation and cardiac regeneration (for review, see [99–101]).

Table 1. Metabolic manipulations that potentiate cardiac regenerative strategies.

Cardiac Regenerative Approach	Metabolic Target	Strategy	Species	Cell Type	Impact	References
Activation of cardiomyocyte proliferation	Glycolysis	Glut 1 overexpression in vivo	Mouse	Neonatal cardiomyocytes	Increases proliferation and decreases fibrosis post-injury	[90]
	Glycolysis	PDK4 knockout in vivo	Mouse	Adult cardiomyocytes	Increases proliferation and improves heart function	[91]
	FAO	FAs -deficient milk in vivo	Mouse	Neonatal cardiomyocytes	Extends the post-natal regenerative window	[91]
	CPT1	Etomoxir supplementation in vivo	Mouse Rat	Neonatal and adult cardiomyocytes	Enhances cardiac efficiency post-injury	[92,93]
	Lactate	Supplementation in vitro	Mouse	Cardiac fibroblasts	Pro-regenerative environment for cardiomyocytes post-injury	[94]
	ROS	NAC, malonate supplementation in vivo	Mouse	Neonatal and adult cardiomyocytes	Extends the post-natal regenerative window	[95,96]
Recruitment of cardiac stem or progenitor cells	HIF-1α	Hypoxia in vivo and in vitro	Mouse	CPCs	Promotes migration and recruitment	[97,98]
	Glucose, glutamine	Supplementation in vitro	Mouse	CPCs	Increases proliferation and prevents cell death induced by oxidative stress	[99,100]
	ROS	Ascorbic acid supplementation in vitro	Mouse	CPCs	Increases proliferation	[101]
Delivery of De Novo cardiomyocytes from differentiated ESCs/iPSCs	Glucose	Low	Human	ESCs-CMs iPSCs-CMs	Physiological support for cardiac development	[102]
	Glucose	High	Mouse	ESCs-CMs	Suppresses mesoderm and cardiac transcription genes	[103]
	mTOR AMPK	Torin1 AICAR supplementation in vitro	Human	iPSCs-CMs	Cardiomyocyte maturation	[104,105]
	Galactose, FAs	Supplementation in vitro	Human	iPSCs-CMs ESCS-CMs	Improves contractile capacity and maturation	[106,107]
	FAO	MM in vitro	Human Mouse	iPSCs-CMs	Metabolic maturation	[107]
Direct reprogramming of fibroblasts into iCMs	Glycolysis	HIF-1α knockdown in vitro	Mouse	Neonatal cardiac fibroblasts	Enhances reprogramming efficiency	[108]
	OXPHOS TCA cycle	Rotenone, IDH3A knockdown in vitro	Mouse	Embryonic fibroblasts	Decreases reprogramming efficiency	[109]
	ROS	Selenium, ascorbic acid supplementation in vitro	Mouse	Embryonic, neonatal cardiac and tail tip fibroblasts	Enhances reprogramming efficiency	[101,110]
	ROS	Vitamin E nicotinate supplementation in vivo	Rat	Cardiac fibroblasts	Improves heart damage repair through reprogramming	[111]

Table 1. *Cont.*

Cardiac Regenerative Approach	Metabolic Target	Strategy	Species	Cell Type	Impact	References
Nutrient signaling	AMPK	Metformin supplementation in vitro	Rat	H9C2 cardiomyoblasts	Nitrate-dependent decrease in oxidative damage	[112]
	SIRT1	Resveratrol supplementation in vivo	Mouse	Neonatal cardiomyocytes	Ejection fraction preservation, decreases cardiac stiffness and oxidative stress	[113]
Gene therapy	Mitochondria	AAV9- Tert overexpression in vivo	Mouse	Adult heart	Improves mitochondrial fitness and activity, protects against heart failure after MI	[114–116]
	Mitochondria	Ad5-CMV-Sirt1 overexpression in vitro	Rat	Neonatal cardiomyocytes	Protects against oxidative stress, FAO inhibition and cell size enlargement	[117]
	Mitochondria	Malat1 knockdown in vitro knockout in vivo	Mouse	CMECs	Mitochondrial dysfunction, apoptosis and microvascular injuries	[118]
	Mitochondria	AAV9- LARP7 overexpression in vivo	Mouse	Adult heart	Protects against heart failure, improves pump function	[119]
	ROS	lncDACH1 knockdown in vitro knockout in vivo	Mouse	NMCVs Adult heart	SIRT3-mediated attenuation of mitochondrial oxidative stress	[120]
	ROS	AAV9-Nrf1 overexpression in vivo	Mouse	Adult heart	Protects against I/R injury by activating ROS scavengers	[121]

Abbreviations: AAV9, Adeno-associated virus serotype 9; AICAR, 5-Aminoimidazole-4-carboxamide ribonucleo-side; AMP, 5′ adenosine monophosphate; AMPK, AMP-activated protein kinase; CMECs, Cardiac microvascular endothelial cells; CPCs, cardiac progenitor cells; CPT1, carnitine palmitoyltransferase 1; ESCs, embryonic stem cells; ESCs-CMs, embryonic stem cells-derived cardiomyocytes; FAs, fatty acids; FAO, fatty acid oxidation; Glut 1, Glucose transporter 1; HIF-1α, Hypoxia-inducible factor-1α; iCMs, induced cardiomyocytes; IDH3A, Isocitrate dehydrogenase 3α; iPSCs, induced pluripotent stem cells; iPSCs-CMs, induced pluripotent stem cells-derived cardiomyocytes; I/R, ischemia/reperfusion; LARP7, la ribonucleoprotein domain family member 7; MI, myocardial infarction; MM, maturation media; mTOR, mechanistic target of rapamycin; NAC, N-acetyl-cysteine; NMCVs, neonatal mouse ventricular cardiomyocytes; Nrf1, nuclear respiratory factor 1; OXPHOS, oxidative phosphorylation; PDK4, pyruvate dehydrogenase kinase 4; ROS, reactive oxygen species; Sirt, sirtuin; TCA, Tricarboxylic acid cycle; Tert, Telomerase reverse transcriptase.

Another important aspect to be considered for cardiomyocyte proliferation is the fetal metabolic switch (Figures 1 and 3b). Shortly after birth, mammalian cardiomyocytes lose proliferative and regenerative capacities, highlighting a connection between metabolism and cardiac differentiation. The consequence of increased exposure to oxygen leads to an intensification of OXPHOS and increased levels of ROS [20], contributing to postnatal cardiomyocyte cell cycle arrest, oxidative DNA damage, and the activation of DNA damage response [102,103]. FA utilization by the mitochondria induces a significant increase in ROS at the chromatin level compared to other nuclear compartments, highlighting chromatin as the main target of the prooxidant effect of FA utilization by the mitochondria [103]. Puente et al. investigated the influence of both hyperoxia and hypoxia in neonatal mice and reported that, while a high oxygen environment led to cardiomyocyte cell cycle arrest, lower oxygen extended the regenerative window [102]. Moreover, hypoxia was also shown to inhibit OXPHOS and reactivate mitosis in cardiomyocytes [104,105]. To extend the neonatal regenerative window, the ROS levels can be decreased, by either targeting one of its sources—for example, succinate accumulation (with the use of malonate)—or through the administration of ROS scavengers, such as N-acetylcysteine (NAC) [102,106] (Table 1). The decrease in ROS has also been shown to stimulate proliferation in adult cardiomyocytes [106].

During regeneration, cardiomyocytes, located in the border zones of the injured area, switch back to glycolytic metabolism [107]. Stimulation of glycolysis by overexpressing Glut1 leads to increased glucose uptake, which is sufficient to enhance the neonatal regenerative capacity [108]. Similarly, the deletion of PDK4, a PDH inhibitor whose normal

expression is upregulated at P7, enhances cardiomyocyte proliferation and heart regeneration after myocardial infarction [109]. Inhibition of FAO also offers some promising results. Cardoso et al. demonstrated that the consumption of FA-deficient milk expanded the regenerative window up until post-natal day 21, yet this does not apply to 10-week-old mice [109]. Inhibition of CPT1 with etomoxir leads to decreased FAO and the proliferation of neonatal mouse/rat cardiomyocyte proliferation [110,111]. However, this effect does not appear to extend to adult cardiomyocytes, and etomoxir usage for extended periods of time can lead to hepatic steatosis and glucose intolerance [112,113]. Ordoño et al. have demonstrated that lactate induces changes in gene expression, which leads to cardiomyocyte proliferation. Additionally, lactate can have an impact on the surrounding environment after injury, reducing the secretion of inflammatory cytokines by cardiac fibroblasts and promoting a pro-regenerative environment for cardiomyocytes [114]. With these findings, it becomes clear that mimicking the fetal metabolic environment represents a promising strategy to activate cardiomyocyte proliferation and to increase regeneration. However, most of the studies report positive outcomes on neonatal cardiomyocytes only, and further evidence from adult hearts is needed.

4.2. Recruitment of Cardiac Stem or Progenitor Cells

In the normal heart, the replenishment of the cardiomyocyte population is mostly made through the proliferation of existing cardiomyocytes [115,116]. However, after injury, the recruitment and differentiation of endogenous progenitor cells have gained a more prominent role [116]. Cardiac progenitor cells (CPCs) are multipotent cells that can differentiate into both cardiomyocytes and non-myocyte cells in the heart [117] (Figure 3a). Upon activation during tissue regeneration, CPCs contribute to a newly generated pool of both cardiomyocytes and endothelial cells [118]. Reactivating pathways that are involved in cardiac lineage specification can provide a potential means to attenuate the loss of cardiomyocytes after injury [119]. In vitro differentiation of CPCs into cardiomyocytes has been demonstrated upon treatment with TGF-β. Further, paracrine signaling appears to play an important role in CPC-mediated cardiac regeneration. Smits and colleagues demonstrated that the transplantation of CPCs into the hearts of mice, after myocardial infarction, improved cardiac function [120,121]. Interestingly, the improved cardiac function, observed after CPC transplantation, has been attributed to paracrine signaling promoting angiogenesis. Enhancing angiogenesis by CPCs has been shown to promote cardiac regeneration by reducing infarcted myocardium [122,123].

CPCs niches were found in the adult mammalian heart, with these cells relying mostly on glycolytic metabolism in a low oxygen microenvironment [107] (Figure 3b). Hypoxia has been shown to increase CPCs migration in vitro and recruitment in vivo in mice, and to induce HIF-1α, which stimulates the activation of CPCs [124,125] (Table 1). The proliferation of CPCs is also important in the recruitment process and seems to be dependent on glucose and glutamine, with the latter also shown to prevent cell death induced by oxidative stress [126,127]. However, other metabolic substrates, such as lactate and pyruvate, as well as hypoxia, do not show a clear impact on CPC numbers [126,127]. The use of the antioxidant ascorbic acid has been reported to increase CPCs proliferation [128], although the impact of ROS in CPCs recruitment needs further clarification. Ultimately, CPCs recruitment seems a very promising, but under researched, strategy, and further studies are warranted.

4.3. Delivery of De Novo Cardiomyocytes from Differentiated ESCs/iPSCs

Several protocols were developed to generate ESCs-derived cardiomyocytes (ESCs-CMs) (reviewed in [129,130]). In vitro, cardiac differentiation of human ESCs initially involved the formation of embryoid bodies, whose cells spontaneously differentiate into derivatives of all three germ layers. This type of differentiation results in beating areas within the embryoid body, which correspond to cardiomyocytes [131,132]. Several studies have shown that ESCs-CMs exhibit typical cardiac gene and protein expressions patterns,

develop an organized sarcomeric structure, and exhibit electrophysiological properties typical of cardiac muscles [133,134]. To avoid problems associated with a lack of reproducibility, serum-free protocols containing growth factors, such as BMP4, activin A, FGF2, Wnt agonists and antagonists, and vascular endothelial growth factor, were developed [130] (Figure 3a). Embryoid bodies exhibit diffusional barriers that prevent the penetration of extracellular factors [130]. As such, monolayer differentiations of human ESCs into cardiomyocytes were developed, and they aimed at being more controlled and reproducible. In a study carried out by Laflamme and colleagues, H7 human ESCs were cultured on Matrigel, in the presence of mouse embryonic fibroblast conditioned media, and subsequently differentiated upon sequential treatment, with activin A and BMP4, in serum-free conditions [135]. An alternative monolayer approach requires the use of extracellular matrix proteins, which are critical players in development and can complement responses to soluble cytokines [136]. Inductive co-cultures have also been described in cardiac differentiation protocols. Co-culture of human ESCs with mouse cell line END-2 (with features of visceral endoderm) resulted in beating cardiomyocytes, which is in agreement with the role of visceral endoderm in the differentiation of cardiogenic precursor cells in the adjacent mesoderm in developing embryos [137,138].

Despite their potential, there are a several concerns regarding the use of ESCs in research and clinics: namely, immune rejection and ethical issues [139]. Mouse and human fibroblasts can be successfully converted into iPSCs by the overexpression of pluripotency-related transcription factors Oct4, Sox2, Klf4, and c-Myc [139,140] (Figure 3a). As iPSCs are generated from cells derived from patients' own body, iPSCs-derived cardiomyocytes (iPSCs-CM) are less prone to immune rejection, and there are no ethical concerns involved [141]. Under in vitro conditions, iPSCs can be pushed towards a cardiac fate the same way as ESCs, either through the formation of embryoid bodies or monolayer culture [141]. The use of small molecules has also been extensively exploited to increase the efficiency of cardiac differentiation. For instance, inhibiting the TGF-β [142] or activating the Wnt/β-catenin [143] signaling pathways has proven to improve this process. Furthermore, small molecules, alone, such as CHIR99021 and Wnt-C59, have been used to differentiate iPSCs into cardiomyocytes [144].

Mouse and human ESCs-CMs have higher mitochondrial OXPHOS, and inhibition causes reduction and abnormal translocation of mitochondria, which results in impaired sarcomere organization and a reduced beating rate [145]. In ESCs-CMs, glucose inhibits maturation through the pentose phosphate pathway, and permanent hyperglycemic culture conditions suppress mesoderm and cardiac transcription genes and induce poor cardiomyocyte contractility [146] (Figure 3b and Table 1). The usage of galactose and FAs instead of glucose promoted a fast maturation of human ESCs-CMs, presenting higher oxidative metabolism and improved contractile capacity [147].

Despite their advantages, the physiological immaturity of iPSCs-CMs limits their utility for cardiac regeneration [148,149]. As the commonly used RPMI/B27-based media has high glucose and low oxidative substrate levels, iPSCs-CMs fail to effectively activate FAO, and lipid availability in cultures became limited during differentiation [150]. A maturation media (MM) capable of providing oxidative substrates adjusted to the metabolic demand of human iPSCs-CMs was recently proposed [151]. MM could enhance FAO, which is reinforced with a supplementation of FAs, and exacerbated electrophysiological and mechanical maturation features [151]. Exogenous supplementation of lipids, such as palmitate, improved cardiomyocyte morphology, mitochondrial function, and promoted increased FAO in human iPSCs-derivatives [150,152]. Human iPSCs-CMs present a substantial increase in the mitochondria number and activity during the differentiation process [153]. As for ESCs-CMs, glucose exclusion is necessary to induce iPSCs-CMs maturation and the switch from glycolysis to OXPHOS [154]. BCAAs can stimulate mTOR activation, which promotes metabolic reprogramming to glycolysis from FAO through HIF-1α [155]. Both the inhibition of mTOR and activation of AMPK by AICAR promote human iPSCs-CMs

maturation via p53-induced quiescence [156,157], suggesting that downstream pathways of BCAAs can regulate cardiomyocyte maturation.

Together, these findings indicate that ESCs and iPSCs-CMs immaturity can be overcome by the modulation of the intracellular metabolism driving cardiomyocyte differentiation, promoting FAO, improvement of mitochondrial function, and reducing glucose metabolism.

4.4. Direct Reprogramming of Fibroblasts into Induced Cardiomyocytes

Most of the human heart is composed of cardiac fibroblasts, accounting for more than 50% of all the cells, and upon cardiac injury, these cells play an important role in scar formation [158]. Therefore, the substantial population of cardiac fibroblasts has emerged as a potential source of cardiomyocytes for regenerative medicine. Cardiomyocytes can be generated directly from fibroblasts without having to pass through a pluripotent state, giving rise to induced cardiomyocytes (iCMs) [159] (Figure 3a). This type of cell reprogramming—direct cell reprogramming, or transdifferentiation—offers some advantages in relation to iPSC-based differentiation, in the sense that iPSC generation is a time-consuming process with risk of tumor formation from residual undifferentiated cells [160]. A pioneer study, in 2010, identified the cardiomyocyte-inducing factors Gata4, Mef2c, Tbx5 (termed GMT), which, upon overexpression in cardiac fibroblasts, isolated from αMHC (myosin heavy chain) promoter-driven EGFP-IRES-puromycin transgenic mice (αMHC-GFP), led to an increased expression of cardiac markers: namely, αMHC (reported by GFP expression), cardiac troponin T (cTnT), and α-actinin [159]. Furthermore, iCMs resulting from the transduction of fibroblasts with GMT presented epigenetic alterations and genetic expression patterns similar to those of postnatal cardiomyocytes and spontaneous contraction, as evidenced by intracellular Ca^{2+} flux. Importantly, the possibility that these iCMs were derived either from a subpopulation of stem-like cells or cardiac progenitors was excluded, as GMT-transduced tail-tip dermal fibroblasts also exhibited the same characteristics as cardiac fibroblasts [159]. In vivo cardiac reprogramming has been achieved, with the in situ delivery of retroviruses expressing GMT, after myocardial infarction in the mouse, leading to a conversion of 15% of cardiac fibroblasts into iCMs, decreasing scar size and improving cardiac function [161].

In order to enhance reprogramming efficiency, many subsequent studies aimed at testing additional transcription factors. The addition of Hand2 (GHMT), for instance, was shown to improve cardiac conversion efficiency [162]. Additionally, 5-factor (GHMT + Nkx2.5) [163] and 7-factor (GMT + Myocd + Srf + Mesp1 + Smarcd3) cocktails were shown to further enhance cardiac reprogramming [164]. Chemical generation of iCMs has been made possible due to the use of small molecules, which function, mainly, by regulating specific signaling pathways, as well as epigenetic and metabolic processes (reviewed in [165]). Indeed, human fibroblasts were also subjected to direct reprogramming studies, although GMT transduction proved to be insufficient to induce cardiac conversion, and additional factors were simultaneously required [166,167]. Many protocols depend on retroviral and lentiviral vectors for gene delivery. Because they integrate into the host genome, endogenous gene expression destabilization and insertional mutagenesis could hinder clinical application [168]. Non-integrative viruses, such as Sendai virus, expressing cardiac reprogramming factors have been shown to reduce fibrosis after myocardial infarction and improve cardiac function [169].

Cardiac reprogramming factors function in a combinatorial way by co-occupying regulatory elements, thus inducing the activation of cardiac-specific gene expression [170]. In fact, each transcription factor plays different roles by activating cardiac-specific enhancers, with Mef2c playing a key role in initializing this process, compared to Gata4 and Tbx5. The balance and stoichiometry between transcription factors play an important role in cardiac fate commitment. The transduction of polycistronic MGT into fibroblasts resulted in the expression of Mef2c at relatively high levels and Gata4 and Tbx5 at low levels, which promoted reprogramming efficiency [171]. Owing to several intrinsic barriers, direct cardiac reprogramming is still a very inefficient process. For fibroblasts to be directly

reprogrammed, significant epigenetic alterations must occur in order to repress fibroblast identity and activate the cardiomyocyte program [172,173]. Another important issue is the heterogeneity and asynchronous nature of the reprogramming process. Using single-cell RNA sequencing, Liu and colleagues discovered molecularly distinct subpopulations of cells during the reprogramming process, and they further identified *Ptbp1* as a barrier of direct cardiac conversion [174]. Another reprogramming barrier worth noting is aging [175], as age-related inflammation, and possibly senescence, can hamper direct cardiac reprogramming [176].

Fibroblasts are metabolically different from cardiomyocytes, and during direct cardiac reprogramming, a shift from glycolysis to OXPHOS has been reported [174] (Figure 3b). Therefore, manipulating fibroblast metabolism to resemble that of cardiomyocytes seems to be a good strategy to improve direct cardiac reprogramming efficiency (Table 1). Fibroblasts with downregulation of HIF-1α, an important regulator of glycolysis, are more successfully reprogrammed [177]. Conversely, the use of rotenone, an inhibitor of mitochondria respiration, and knockdown of the TCA cycle enzyme isocitrate dehydrogenase 3α (IDH3A) decreases reprograming efficiency, while IDH3A upregulation led to increased reprogramming [178]. High ROS levels can also affect the efficiency of the process, and the use of antioxidants could boost this process. Selenium and ascorbic acid (vitamin C) supplementation have been shown to enhance reprogramming efficiency, in vitro, by increasing cardiac gene expression [128,179], and vitamin E nicotinate promotes heart damage repair through reprogramming in vivo [180]. However, ROS signaling is required for direct reprograming, so a delicate balance of ROS levels seems imperative for the success of direct cardiac conversion [181]. The specific culture conditions can also impact transdifferentiation of fibroblasts in vitro, which may not be translated into significant improvements in vivo. Differential culture methods and reagents, as fetal bovine serum, have been implied in the inefficiency of this process, and serum-free conditions were reported to improve transdifferentiation [182,183].

4.5. Systemic Metabolic Strategies for Heart Regeneration

4.5.1. Nutrient Signaling

A variety of caloric and dietary restriction regimens have been demonstrated to improve overall health and promote tissue regeneration [184]. Additionally, supplementation of metformin, resveratrol, and certain nutrients have been shown to favor cardiac tissue regeneration and remodeling in rodents. Nutritional and pharmacological modulators (e.g., vitamin E, ascorbic acid, selenium, taurine, and tocopherol) also promote mild to moderate cardioprotective effects after reperfusion injury [185,186], although substantial limitations, such as fast clearance, limit its activity. Metformin acts, both directly and indirectly, through the activation of AMPK and inhibition of mTORC1 and by improving mitophagy and overall mitochondrial homeostasis [187]. A postconditioning effect for metformin in experimental ischemia has been described (Table 1). Metformin maintained both cell viability and membrane stability of rat H9C2 cardiomyoblast cells after induced ischemic injury by alleviating the decrease in nitrate levels [188]. The increased levels of nitrate provided by metformin led to nitrate oxidative species (NOS)-independent nitrate oxide (NO) production and decrease in intracellular oxidative damage after ischemic cell injury [188]. A cardioprotective role for resveratrol was reported in a mouse model of HFpEF [189]. Resveratrol activates SIRT1, which prevents cardiac fibrosis and ROS production in cardiomyocytes [190]. Excessive myocardial ROS has a crucial role in ejection fraction preservation, leading to collagen uncoupling and formation of oxidative stress, decreased nitric oxide bioavailability, and heart failure. Resveratrol exerts a protective action against HFpEF-induced adverse cardiac remodeling, alleviating cardiac stiffness and oxidative stress by decreasing Smad3 acetylation and transcriptional activity via SIRT1 activation [189]. Whether systemic metabolic fuels can directly impact cardiomyocytes' cell fate specification and proliferation, as well as potentiating cardiac regeneration, are exciting possibilities that need further investigation.

4.5.2. Gene Therapy

Gene therapy strategies have been used to treat age-related diseases, including heart failure where documented targeted genes are involved, directly or indirectly, in metabolic-signaling pathways. Overall, the metabolic decay with age is accompanied by disrupted mitochondrial fitness, as a result of the activity decline of the master regulators PGC-1α/β [191]. Hearts from telomerase-deficient mice present deregulation of PGC-1α/β-related gene networks, mitochondria with defective electron transport chain activity, decreased ATP production, and low expression of ROS detoxifying enzymes [191]. Enforced telomerase reverse transcriptase (Tert), PGC-1α expression or germline deletion of p53 in telomerase-deficient mice restores PGC network expression, mitochondrial respiration, cardiac function, and gluconeogenesis [191]. Moreover, aged wild-type mice, infected with AAV9-Tert, present improved mitochondrial fitness, with partial rescue of PGC-1α, ATP synthase, and ERRα expression in the heart [192], and they are protected from heart failure after myocardial infarction (MI), with restored metabolic activity in the infarcted hearts [192,193] (Table 1). Overall, telomerase activation, and its impact on metabolism remodeling, could be a therapeutic strategy to prevent heart failure after myocardial infarction [193]. Under stress conditions, SIRT1 deacetylates FOXO1/3, activating the expression of the manganese-dependent superoxide dismutase and catalase anti-oxidant enzymes, protecting the heart against oxidative stress and apoptosis in ischemia/reperfusion (I/R) injury [194–196]. Adenoviral-mediated overexpression of Sirt1 blunted the increase in the atrial natriuretic factor and α-skeletal actin expression, and it inhibited cell size enlargement and FAO repression of phenylephrine-stimulated neonatal rat cardiomyocytes [197]. The mitochondrial deacetylase SIRT3 can also potentiate the mitochondria to eliminate excessive ROS through deacetylation and activation of superoxide dismutase [198]. The lncRNA lncDACH1 is highly expressed in high glucose-treated or diabetic cardiomyopathy mouse hearts, and its knockdown in neonatal mouse ventricular cardiomyocytes (NMCVs) attenuates mitochondrial oxidative stress and apoptosis. Additionally, the lncDACH1 knockout mouse has enhanced cardiac function due to the prevention of SIRT3 degradation through ubiquitination-related degradation of SERCA2a [199]. Similarly, SIRT1 increases SERCA2 pump activity during heart failure by SERCA2 acetylation at lysine 492 [200]. Additional lncRNAs have been reported to modulate mitochondrial dynamics in the heart [101]. Malat1 has increased expression in cardiac tissues and isolated endothelial cells in the peri-infarct region, and cardiac microvascular endothelial cells (CMECs)-specific knockout, in vivo, leads to persistent mitochondrial dysfunction, priming hypoxia-induced endothelial cell damage, apoptosis, capillary destruction, and cardiac microvascular injuries [201]. Malat1 silencing, both in vivo and its knockdown in CMECs, results in decreased Mfn1 through the regulation of miR-26b-5p, which leads to disrupted mitochondrial dynamics and activation of apoptosis [201]. These emerging insights highlight the possibility to explore lncRNAs-mediated-metabolism as a strategy to improve cardiac regeneration and heart function [101].

LARP7 was recently shown to preserve mitochondrial homeostasis and cardiac function. When the ataxia telangiectasia mutated (ATM)-mediated DNA damage response pathway is activated, oxidative stress leads to the decline of LARP7 and compromises the homeostasis and deacetylase activity of SIRT1, which leads to disruption of mitochondrial biogenesis. The cardiac-specific NKX2.5[Cre]:LARP7[f/f] and Myh6[Cre]:LARP7[f/f] conditional knockout mice developed heart failure with disturbed mitochondria function and morphology. Rescue of LARP7 expression by the AAV9- mediated gene delivery remarkably had a protective role against heart failure, improving the pump function of the infarcted heart [202]. Nrf1 is considered a master regulator of redox balance and a core component of stress adaptation in the heart [203]. Overexpression of Nrf1 confers protection to I/R injury in the adult mouse heart by activating ROS scavengers, including the detoxifying enzyme Hmox1, glutathione, and NADPH metabolism, as well as increasing proteasomal activity in the heart [203].

Overall, gene targeting seems promising to rescue impaired metabolism and mitochondria function in response to cardiac injury or heart pathologies.

5. Conclusions

Cellular metabolism and nutrient signaling are determinant for cardiomyocyte function in the adult heart, and extensive metabolic reprogramming takes place at developmental stages and in the injured heart. In fact, a hallmark of heart failure is the metabolic remodeling, characterized by a shift in energetic fuels and pathways towards a fetal phenotype (from FAO to glycolysis), which compensate for the loss of cardiomyocyte function. Understanding the key metabolic signals that drive cardiac regeneration post-injury, in vivo, is warranted for metabolically treating the diseased heart. Due to the extended impact of metabolites in cell signaling and epigenetic remodeling, changes in the metabolic fuel impact energy generation, other regulatory functions, and, as a result, cardiac remodeling and functionality. Several cellular strategies have been designed for regenerating the adult mammalian heart, with stem cells-based therapy and direct conversion of cardiac fibroblasts showing promising results. In this context, metabolic adaptations, mainly involving fuels (glucose, FAs), energetic pathways (glycolysis, OXPHOS), and the remodeling of mitochondria function (including dynamics and ROS) can promote self-renewal, differentiation, and cell lineage conversion events that are driving cardiac regeneration (Table 1 and Figure 3b). Cellular metabolism represents the balance of intrinsic metabolic needs and extrinsic metabolic constrains. Understanding how global shifts in nutrient availability (such as lipids) translate into specific gene expression programs, controlling cellular events with relevance for cardiac regeneration, is a major area for future investigation.

Conflicts of Interest: The authors declare no conflict of interest.

References

1. Virani, S.S.; Alonso, A.; Aparicio, H.J.; Benjamin, E.J.; Bittencourt, M.S.; Callaway, C.W.; Carson, A.P.; Chamberlain, A.M.; Cheng, S.; Delling, F.N.; et al. Heart Disease and Stroke Statistics 2021 Update. *Circulation* **2021**, *143*, e254–e743. [CrossRef] [PubMed]
2. Laflamme, M.A.; Murry, C.E. Heart regeneration. *Nature* **2011**, *473*, 326–335. [CrossRef] [PubMed]
3. Hashimoto, H.; Olson, E.N.; Bassel-Duby, R. Therapeutic approaches for cardiac regeneration and repair. *Nat. Rev. Cardiol.* **2018**, *15*, 585–600. [CrossRef] [PubMed]
4. Ghiroldi, A.; Piccoli, M.; Cirillo, F.; Monasky, M.M.; Ciconte, G.; Pappone, C.; Anastasia, L. Cell-Based Therapies for Cardiac Regeneration: A Comprehensive Review of Past and Ongoing Strategies. *Int. J. Mol. Sci.* **2018**, *19*, 3194. [CrossRef] [PubMed]
5. Neidig, L.E.; Weinberger, F.; Palpant, N.J.; Mignone, J.; Martinson, A.M.; Sorensen, D.W.; Bender, I.; Nemoto, N.; Reinecke, H.; Pabon, L.; et al. Evidence for minimal cardiogenic potential of stem cell antigen 1-positive cells in the adult mouse heart. *Circulation* **2018**, *138*, 2960–2962. [CrossRef] [PubMed]
6. Soonpaa, M.H.; Kim, K.K.; Pajak, L.; Franklin, M.; Field, L.J. Cardiomyocyte DNA synthesis and binucleation during murine development. *Am. J. Physiol. Circ. Physiol.* **1996**, *271*, H2183–H2189. [CrossRef]
7. Lehman, J.J.; Kelly, D.P. Transcriptional Activation of Energy Metabolic Switches in the Developing and Hypertrophied Heart. *Clin. Exp. Pharmacol. Physiol.* **2002**, *29*, 339–345. [CrossRef]
8. Lopaschuk, G.D.; Collins-Nakai, R.L.; Itoi, T. Developmental changes in energy substrate use by the heart. *Cardiovasc. Res.* **1992**, *26*, 1172–1180. [CrossRef]

9. Ho, K.L.; Zhang, L.; Wagg, C.; Al Batran, R.; Gopal, K.; Levasseur, J.; Leone, T.; Dyck, J.R.B.; Ussher, J.R.; Muoio, D.M.; et al. Increased ketone body oxidation provides additional energy for the failing heart without improving cardiac efficiency. *Cardiovasc. Res.* **2019**, *115*, 1606–1616. [CrossRef]

10. Ho, K.L.; Karwi, Q.G.; Wagg, C.; Zhang, L.; Vo, K.; Altamimi, T.; Uddin, G.M.; Ussher, J.R.; Lopaschuk, G.D. Ketones can become the major fuel source for the heart but do not increase cardiac efficiency. *Cardiovasc. Res.* **2020**, *117*, 1178–1187. [CrossRef]

11. Karwi, Q.G.; Uddin, G.M.; Ho, K.L.; Lopaschuk, G.D. Loss of Metabolic Flexibility in the Failing Heart. *Front. Cardiovasc. Med.* **2018**, *5*, 68. [CrossRef] [PubMed]

12. Ritterhoff, J.; McMillen, T.S.; Villet, O.; Young, S.; Kolwicz, S.C.; Senn, T.; Caudal, A.; Tian, R. Increasing fatty acid oxidation elicits a sex-dependent response in failing mouse hearts. *J. Mol. Cell. Cardiol.* **2021**, *158*, 1–10. [CrossRef] [PubMed]

13. Shyh-Chang, N.; Ng, H.-H. The metabolic programming of stem cells. *Genes Dev.* **2017**, *31*, 336–346. [CrossRef] [PubMed]

14. Intlekofer, A.M.; Finley, L.W.S. Metabolic signatures of cancer cells and stem cells. *Nat. Metab.* **2019**, *1*, 177–188. [CrossRef] [PubMed]

15. Nguyen, J.H.; Chung, J.D.; Lynch, G.S.; Ryall, J.G. The Microenvironment Is a Critical Regulator of Muscle Stem Cell Activation and Proliferation. *Front. Cell Dev. Biol.* **2019**, *7*, 254. [CrossRef] [PubMed]

16. Clémot, M.; Demarco, R.S.; Jones, D.L. Lipid Mediated Regulation of Adult Stem Cell Behavior. *Front. Cell Dev. Biol.* **2020**, *8*, 115. [CrossRef]

17. Karwi, Q.G.; Biswas, D.; Pulinilkunnil, T.; Lopaschuk, G.D. Myocardial Ketones Metabolism in Heart Failure. *J. Card. Fail.* **2020**, *26*, 998–1005. [CrossRef]

18. Karwi, Q.G.; Lopaschuk, G.D. Branched-Chain Amino Acid Metabolism in the Failing Heart. *Cardiovasc. Drugs Ther.* **2022**, 1–8. [CrossRef]

19. Brown, D.A.; Perry, J.B.; Allen, D.A.B.J.B.P.M.E.; Sabbah, H.N.; Stauffer, B.L.; Shaikh, S.R.; Cleland, J.G.F.; Colucci, W.S.; Butler, J.; Voors, A.A.; et al. Mitochondrial function as a therapeutic target in heart failure. *Nat. Rev. Cardiol.* **2017**, *14*, 238–250. [CrossRef]

20. Lopaschuk, G.D.; Jaswal, J.S. Energy Metabolic Phenotype of the Cardiomyocyte during Development, Differentiation, and Postnatal Maturation. *J. Cardiovasc. Pharmacol.* **2010**, *56*, 130–140. [CrossRef]

21. Kolwicz, S.C., Jr.; Purohit, S.; Tian, R. Cardiac Metabolism and its Interactions with Contraction, Growth, and Survival of Cardiomyocytes. *Circ. Res.* **2013**, *113*, 603–616. [CrossRef] [PubMed]

22. Haffar, T.; Bérubé-Simard, F.; Bousette, N. Impaired fatty acid oxidation as a cause for lipotoxity in cardiomyocytes. *Biochem. Biophys. Res. Commun.* **2015**, *468*, 73–78. [CrossRef] [PubMed]

23. Lu, X.; Thai, P.N.; Lu, S.; Pu, J.; Bers, D.M. Intrafibrillar and perinuclear mitochondrial heterogeneity in adult cardiac myocytes. *J. Mol. Cell. Cardiol.* **2019**, *136*, 72–84. [CrossRef] [PubMed]

24. Ong, S.-B.; Kalkhoran, S.B.; Hernández-Reséndiz, S.; Samangouei, P.; Hausenloy, D.J. Mitochondrial-Shaping Proteins in Cardiac Health and Disease—The Long and the Short of It! *Cardiovasc. Drugs Ther.* **2017**, *31*, 87–107. [CrossRef]

25. Murashige, D.; Jang, C.; Neinast, M.; Edwards, J.J.; Cowan, A.; Hyman, M.C.; Rabinowitz, J.D.; Frankel, D.S.; Arany, Z. Comprehensive quantification of fuel use by the failing and nonfailing human heart. *Science* **2020**, *370*, 364–368. [CrossRef]

26. Heather, L.C.; Pates, K.M.; Atherton, H.J.; Cole, M.A.; Ball, D.R.; Evans, R.D.; Glatz, J.F.; Luiken, J.J.; Griffin, J.L.; Clarke, K. Differential Translocation of the Fatty Acid Transporter, FAT/CD36, and the Glucose Transporter, GLUT4, Coordinates Changes in Cardiac Substrate Metabolism during Ischemia and Reperfusion. *Circ. Heart Fail.* **2013**, *6*, 1058–1066. [CrossRef]

27. Sorrentino, D.; Stump, D.; Potter, B.J.; Robinson, R.B.; White, R.; Kiang, C.L.; Berk, P.D. Oleate uptake by cardiac myocytes is carrier mediated and involves a 40-kD plasma membrane fatty acid binding protein similar to that in liver, adipose tissue, and gut. *J. Clin. Investig.* **1988**, *82*, 928–935. [CrossRef]

28. Pettersen, I.K.N.; Tusubira, D.; Ashrafi, H.; Dyrstad, S.E.; Hansen, L.; Liu, X.-Z.; Nilsson, L.I.H.; Løvsletten, N.G.; Berge, K.; Wergedahl, H.; et al. Upregulated PDK4 expression is a sensitive marker of increased fatty acid oxidation. *Mitochondrion* **2019**, *49*, 97–110. [CrossRef]

29. Bertrand, L.; Auquier, J.; Renguet, E.; Angé, M.; Cumps, J.; Horman, S.; Beauloye, C. Glucose transporters in cardiovascular system in health and disease. *Pflugers Arch.* **2020**, *472*, 1385–1399. [CrossRef]

30. Kolwicz, S.C.; Tian, R. Glucose metabolism and cardiac hypertrophy. *Cardiovasc. Res.* **2011**, *90*, 194–201. [CrossRef]

31. Tran, D.H.; Wang, Z.V. Glucose Metabolism in Cardiac Hypertrophy and Heart Failure. *J. Am. Heart Assoc.* **2019**, *8*, e012673. [CrossRef] [PubMed]

32. Ritterhoff, J.; Tian, R. Metabolism in cardiomyopathy: Every substrate matters. *Cardiovasc Res.* **2017**, *113*, 411–421. [CrossRef] [PubMed]

33. Walejko, J.M.; Koelmel, J.P.; Garrett, T.J.; Edison, A.S.; Keller-Wood, M. Multiomics approach reveals metabolic changes in the heart at birth. *Am. J. Physiol.-Endocrinol. Metab.* **2018**, *315*, E1212–E1223. [CrossRef] [PubMed]

34. Cerychova, R.; Pavlinkova, G. HIF-1, Metabolism, and Diabetes in the Embryonic and Adult Heart. *Front. Endocrinol.* **2018**, *9*, 460. [CrossRef]

35. Iruretagoyena, J.I.; Davis, W.; Bird, C.; Olsen, J.; Radue, R.; Broman, A.T.; Kendziorski, C.; Bondurant, S.S.; Golos, T.; Bird, I.; et al. Metabolic gene profile in early human fetal heart development. *Mol. Hum. Reprod.* **2014**, *20*, 690–700. [CrossRef]

36. Goffart, S.; Von Kleist-Retzow, J.-C.; Wiesner, R.J. Regulation of mitochondrial proliferation in the heart: Power-plant failure contributes to cardiac failure in hypertrophy. *Cardiovasc. Res.* **2004**, *64*, 198–207. [CrossRef]

37. Martin, O.J.; Lai, L.; Soundarapandian, M.M.; Leone, T.C.; Zorzano, A.; Keller, M.P.; Attie, A.D.; Muoio, D.M.; Kelly, D.P. A Role for Peroxisome Proliferator-Activated Receptor γ Coactivator-1 in the Control of Mitochondrial Dynamics during Postnatal Cardiac Growth. *Circ. Res.* **2014**, *114*, 626–636. [CrossRef]

38. Menendez-Montes, I.; Escobar, B.; Palacios, B.; Gómez, M.J.; Izquierdo-Garcia, J.L.; Flores, L.; Jiménez-Borreguero, L.J.; Aragones, J.; Ruiz-Cabello, J.; Torres, M.; et al. Myocardial VHL-HIF Signaling Controls an Embryonic Metabolic Switch Essential for Cardiac Maturation. *Dev. Cell* **2016**, *39*, 724–739. [CrossRef]

39. Russell, R.R.; Li, J.; Coven, D.L.; Pypaert, M.; Zechner, C.; Palmeri, M.; Giordano, F.J.; Mu, J.; Birnbaum, M.J.; Young, L.H. AMP-activated protein kinase mediates ischemic glucose uptake and prevents postischemic cardiac dysfunction, apoptosis, and injury. *J. Clin. Investig.* **2004**, *114*, 495–503. [CrossRef]

40. Fillmore, N.; Levasseur, J.L.; Fukushima, A.; Wagg, C.S.; Wang, W.; Dyck, J.R.B.; Lopaschuk, G.D. Uncoupling of glycolysis from glucose oxidation accompanies the development of heart failure with preserved ejection fraction. *Mol. Med.* **2018**, *24*, 3. [CrossRef]

41. Cluntun, A.A.; Badolia, R.; Lettlova, S.; Parnell, K.M.; Shankar, T.S.; Diakos, N.A.; Olson, K.A.; Taleb, I.; Tatum, S.M.; Berg, J.A.; et al. The pyruvate-lactate axis modulates cardiac hypertrophy and heart failure. *Cell Metab.* **2020**, *33*, 629–648.e10. [CrossRef] [PubMed]

42. Zhu, Y.; Soto, J.; Anderson, B.; Riehle, C.; Zhang, Y.; Wende, A.; Jones, D.; McClain, D.; Abel, E.D. Regulation of fatty acid metabolism by mTOR in adult murine hearts occurs independently of changes in PGC-1α. *Am. J. Physiol. Circ. Physiol.-Heart* **2013**, *305*, H41–H51. [CrossRef] [PubMed]

43. Dong, S.; Qian, L.; Cheng, Z.; Chen, C.; Wang, K.; Hu, S.; Zhang, X.; Wu, T. Lactate and Myocadiac Energy Metabolism. *Front. Physiol.* **2021**, *12*, 715081. [CrossRef] [PubMed]

44. Chatham, J.C.; Rosiers, C.D.; Forder, J.R. Evidence of separate pathways for lactate uptake and release by the perfused rat heart. *Am. J. Physiol.-Endocrinol. Metab.* **2001**, *281*, E794–E802. [CrossRef] [PubMed]

45. Pfleger, J.; Gross, P.; Johnson, J.; Carter, R.L.; Gao, E.; Tilley, D.G.; Houser, S.R.; Koch, W.J. G protein-coupled receptor kinase 2 contributes to impaired fatty acid metabolism in the failing heart. *J. Mol. Cell. Cardiol.* **2018**, *123*, 108–117. [CrossRef]

46. Carley, A.N.; Maurya, S.K.; Fasano, M.; Wang, Y.; Selzman, C.H.; Drakos, S.G.; Lewandowski, E.D. Short-Chain Fatty Acids Outpace Ketone Oxidation in the Failing Heart. *Circulation* **2021**, *143*, 1797–1808. [CrossRef] [PubMed]

47. Han, L.; Liu, J.; Zhu, L.; Tan, F.; Qin, Y.; Huang, H.; Yu, Y. Free fatty acid can induce cardiac dysfunction and alter insulin signaling pathways in the heart. *Lipids Health Dis.* **2018**, *17*, 185. [CrossRef]

48. Karwi, Q.G.; Sun, Q.; Lopaschuk, G.D. The Contribution of Cardiac Fatty Acid Oxidation to Diabetic Cardiomyopathy Severity. *Cells* **2021**, *10*, 3259. [CrossRef]

49. Wang, L.-Y.; Chen, C. Energy metabolism homeostasis in cardiovascular diseases. *J. Geriatr. Cardiol.* **2021**, *18*, 1044–1057. [CrossRef]

50. Lee, S.R.; Heo, J.H.; Jo, S.L.; Kim, G.; Kim, S.J.; Yoo, H.J.; Lee, K.-P.; Kwun, H.-J.; Shin, H.-J.; Baek, I.-J.; et al. Progesterone receptor membrane component 1 reduces cardiac steatosis and lipotoxicity via activation of fatty acid oxidation and mitochondrial respiration. *Sci. Rep.* **2021**, *11*, 8781. [CrossRef]

51. Lynch, C.J.; Adams, S.H. Branched-chain amino acids in metabolic signalling and insulin resistance. *Nat. Rev. Endocrinol.* **2014**, *10*, 723–736. [CrossRef] [PubMed]

52. Fillmore, N.; Wagg, C.S.; Zhang, L.; Fukushima, A.; Lopaschuk, G.D. Cardiac branched-chain amino acid oxidation is reduced during insulin resistance in the heart. *Am. J. Physiol.-Endocrinol. Metab.* **2018**, *315*, E1046–E1052. [CrossRef] [PubMed]

53. Drake, K.J.; Sidorov, V.Y.; Mcguinness, O.P.; Wasserman, D.H.; Wikswo, J.P. Amino acids as metabolic substrates during cardiac ischemia. *Exp. Biol. Med.* **2012**, *237*, 1369–1378. [CrossRef] [PubMed]

54. Puchalska, P.; Crawford, P.A. Multi-dimensional Roles of Ketone Bodies in Fuel Metabolism, Signaling, and Therapeutics. *Cell Metab.* **2017**, *25*, 262–284. [CrossRef] [PubMed]

55. Newman, J.C.; Verdin, E. Ketone bodies as signaling metabolites. *Trends Endocrinol. Metab.* **2013**, *25*, 42–52. [CrossRef]

56. Yamanaka, S. Pluripotent Stem Cell-Based Cell Therapy—Promise and Challenges. *Cell Stem Cell* **2020**, *27*, 523–531. [CrossRef]

57. Wu, J.; Ocampo, A.; Belmonte, J.C.I. Cellular Metabolism and Induced Pluripotency. *Cell* **2016**, *166*, 1371–1385. [CrossRef]

58. Tsogtbaatar, E.; Landin, C.; Minter-Dykhouse, K.; Folmes, C.D.L. Energy Metabolism Regulates Stem Cell Pluripotency. *Front. Cell Dev. Biol.* **2020**, *8*, 87. [CrossRef]

59. Davidson, K.C.; Mason, E.; Pera, M.F. The pluripotent state in mouse and human. *Development* **2015**, *142*, 3090–3099. [CrossRef]

60. Takashima, Y.; Guo, G.; Loos, R.; Nichols, J.; Ficz, G.; Krueger, F.; Oxley, D.; Santos, F.; Clarke, J.; Mansfield, W.; et al. Resetting Transcription Factor Control Circuitry toward Ground-State Pluripotency in Human. *Cell* **2014**, *158*, 1254–1269. [CrossRef]

61. Sperber, H.; Mathieu, J.; Wang, Y.; Ferreccio, A.; Hesson, J.; Xu, Z.; Fischer, K.A.; Devi, A.; Detraux, D.; Gu, H.; et al. The metabolome regulates the epigenetic landscape during naive-to-primed human embryonic stem cell transition. *Nat. Cell Biol.* **2015**, *17*, 1523–1535. [CrossRef] [PubMed]

62. Gu, W.; Gaeta, X.; Sahakyan, A.; Chan, A.B.; Hong, C.S.; Kim, R.; Braas, D.; Plath, K.; Lowry, W.E.; Christofk, H.R. Glycolytic Metabolism Plays a Functional Role in Regulating Human Pluripotent Stem Cell State. *Cell Stem Cell* **2016**, *19*, 476–490. [CrossRef] [PubMed]

63. Warburg, O. On the Origin of Cancer Cells. *Science* **1956**, *123*, 309–314. [CrossRef] [PubMed]

64. Vander Heiden, M.G.; Cantley, L.C.; Thompson, C.B. Understanding the Warburg Effect: The Metabolic Requirements of Cell Proliferation. *Science* **2009**, *324*, 1029–1033. [CrossRef] [PubMed]
65. Hanahan, D.; Weinberg, R.A. Hallmarks of cancer: The next generation. *Cell* **2011**, *144*, 646–674. [CrossRef]
66. Nóbrega-Pereira, S.; Caiado, F.; Carvalho, T.; Matias, I.; Graça, G.; Gonçalves, L.G.; Silva-Santos, B.; Norell, H.; Dias, S. VEGFR2–Mediated Reprogramming of Mitochondrial Metabolism Regulates the Sensitivity of Acute Myeloid Leukemia to Chemotherapy. *Cancer Res.* **2018**, *78*, 731–741. [CrossRef]
67. Nobrega-Pereira, S.; Dias, S. VEGF signaling in acute leukemia: Mitochondrial connections. *Oncoscience* **2018**, *5*, 54–56. [CrossRef]
68. Lunt, S.Y.; Vander Heiden, M.G. Aerobic Glycolysis: Meeting the Metabolic Requirements of Cell Proliferation. *Annu. Rev. Cell Dev. Biol.* **2011**, *27*, 441–464. [CrossRef]
69. Bahat, A.; Gross, A. Mitochondrial plasticity in cell fate regulation. *J. Biol. Chem.* **2019**, *294*, 13852–13863. [CrossRef]
70. Carey, B.W.; Finley, L.W.S.; Cross, J.; Allis, C.D.; Thompson, C.B. Intracellular α-ketoglutarate maintains the pluripotency of embryonic stem cells. *Nature* **2015**, *518*, 413–416. [CrossRef]
71. Tohyama, S.; Fujita, J.; Hishiki, T.; Matsuura, T.; Hattori, F.; Ohno, R.; Kanazawa, H.; Seki, T.; Nakajima, K.; Kishino, Y.; et al. Glutamine Oxidation Is Indispensable for Survival of Human Pluripotent Stem Cells. *Cell Metab.* **2016**, *23*, 663–674. [CrossRef] [PubMed]
72. Zhou, W.; Choi, M.; Margineantu, D.; Margaretha, L.; Hesson, J.; Cavanaugh, C.; Blau, C.A.; Horwitz, M.S.; Hockenbery, D.; Ware, C.; et al. HIF1α induced switch from bivalent to exclusively glycolytic metabolism during ESC-to-EpiSC/hESC transition. *EMBO J.* **2012**, *31*, 2103–2116. [CrossRef] [PubMed]
73. Panopoulos, A.D.; Yanes, O.; Ruiz, S.; Kida, Y.S.; Diep, D.; Tautenhahn, R.; Herrerías, A.; Batchelder, E.M.; Plongthongkum, N.; Lutz, M.; et al. The metabolome of induced pluripotent stem cells reveals metabolic changes occurring in somatic cell reprogramming. *Cell Res.* **2012**, *22*, 168–177. [CrossRef] [PubMed]
74. Prieto, J.; León, M.; Ponsoda, X.; Sendra, R.; Bort, R.; Ferrer-Lorente, R.; Raya, A.; López-García, C.; Torres, J. Early ERK1/2 activation promotes DRP1-dependent mitochondrial fission necessary for cell reprogramming. *Nat. Commun.* **2016**, *7*, 11124. [CrossRef] [PubMed]
75. Van Winkle, L.J.; Ryznar, R. One-Carbon Metabolism Regulates Embryonic Stem Cell Fate Through Epigenetic DNA and Histone Modifications: Implications for Transgenerational Metabolic Disorders in Adults. *Front. Cell Dev. Biol.* **2019**, *7*, 300. [CrossRef] [PubMed]
76. Azuara, V.; Perry, P.; Sauer, S.; Spivakov, M.; Jørgensen, H.; John, R.; Gouti, M.; Casanova, M.; Warnes, G.; Merkenschlager, M.; et al. Chromatin signatures of pluripotent cell lines. *Nat. Cell Biol.* **2006**, *8*, 532–538. [CrossRef]
77. Gaspar-Maia, A.; Alajem, A.; Meshorer, E.; Ramalho-Santos, M. Open chromatin in pluripotency and reprogramming. *Nat. Rev. Mol. Cell Biol.* **2010**, *12*, 36–47. [CrossRef]
78. Wang, L.; Zhang, T.; Wang, L.; Cai, Y.; Zhong, X.; He, X.; Hu, L.; Tian, S.; Wu, M.; Hui, L.; et al. Fatty acid synthesis is critical for stem cell pluripotency via promoting mitochondrial fission. *EMBO J.* **2017**, *36*, 1330–1347. [CrossRef]
79. Cornacchia, D.; Zhang, C.; Zimmer, B.; Chung, S.Y.; Fan, Y.; Soliman, M.A.; Tchieu, J.; Chambers, S.M.; Shah, H.; Paull, D.; et al. Lipid Deprivation Induces a Stable, Naive-to-Primed Intermediate State of Pluripotency in Human PSCs. *Cell Stem Cell* **2019**, *25*, 120–136.e10. [CrossRef]
80. Jiang, Z.; Guang, L.; Li, L.; Shyh-Chang, N. Putting Stem Cells on a Low-Fat Diet Switches Their Pluripotent State. *Cell Stem Cell* **2019**, *25*, 3–5. [CrossRef]
81. Moussaieff, A.; Rouleau, M.; Kitsberg, D.; Cohen, M.; Levy, G.; Barasch, D.; Nemirovski, A.; Shen-Orr, S.; Laevsky, I.; Amit, M.; et al. Glycolysis-Mediated Changes in Acetyl-CoA and Histone Acetylation Control the Early Differentiation of Embryonic Stem Cells. *Cell Metab.* **2015**, *21*, 392–402. [CrossRef] [PubMed]
82. Zhang, J.; Khvorostov, I.; Hong, J.S.; Oktay, Y.; Vergnes, L.; Nuebel, E.; Wahjudi, P.N.; Setoguchi, K.; Wang, G.; Do, A.; et al. UCP2 regulates energy metabolism and differentiation potential of human pluripotent stem cells. *EMBO J.* **2011**, *30*, 4860–4873. [CrossRef] [PubMed]
83. Cai, C.-L.; Molkentin, J.D. The Elusive Progenitor Cell in Cardiac Regeneration: Slip Slidin' Away. *Circ. Res.* **2017**, *120*, 400–406. [CrossRef] [PubMed]
84. Yucel, N.; Wang, Y.X.; Mai, T.; Porpiglia, E.; Lund, P.J.; Markov, G.; Garcia, B.A.; Bendall, S.C.; Angelo, M.; Blau, H.M. Glucose Metabolism Drives Histone Acetylation Landscape Transitions that Dictate Muscle Stem Cell Function. *Cell Rep.* **2019**, *27*, 3939–3955.e6. [CrossRef] [PubMed]
85. Gerhart-Hines, Z.; Rodgers, J.T.; Bare, O.; Lerin, C.; Kim, S.-H.; Mostoslavsky, R.; Alt, F.W.; Wu, Z.; Puigserver, P. Metabolic control of muscle mitochondrial function and fatty acid oxidation through SIRT1/PGC-1α. *EMBO J.* **2007**, *26*, 1913–1923. [CrossRef] [PubMed]
86. Ryall, J.G.; Dell'Orso, S.; Derfoul, A.; Juan, A.; Zare, H.; Feng, X.; Clermont, D.; Koulnis, M.; Gutierrez-Cruz, G.; Sartorelli, V.; et al. The NAD+-Dependent SIRT1 Deacetylase Translates a Metabolic Switch into Regulatory Epigenetics in Skeletal Muscle Stem Cells. *Cell Stem Cell* **2015**, *16*, 171–183. [CrossRef]
87. van Gastel, N.; Stegen, S.; Eelen, G.; Schoors, S.; Carlier, A.; Daniëls, V.W.; Baryawno, N.; Przybylski, D.; Depypere, M.; Stiers, P.-J.; et al. Lipid availability determines fate of skeletal progenitor cells via SOX9. *Nature* **2020**, *579*, 111–117. [CrossRef]
88. Cahill, T.J.; Choudhury, R.P.; Riley, P.R. Heart regeneration and repair after myocardial infarction: Translational opportunities for novel therapeutics. *Nat. Rev. Drug Discov.* **2017**, *16*, 699–717. [CrossRef]

89. Testa, G.; Di Benedetto, G.; Passaro, F. Advanced Technologies to Target Cardiac Cell Fate Plasticity for Heart Regeneration. *Int. J. Mol. Sci.* **2021**, *22*, 9517. [CrossRef]

90. Payan, S.M.; Hubert, F.; Rochais, F. Cardiomyocyte proliferation, a target for cardiac regeneration. *Biochim. Biophys. Acta-Mol. Cell Res.* **2020**, *1867*, 118461. [CrossRef]

91. Johnson, J.; Mohsin, S.; Houser, S. Cardiomyocyte Proliferation as a Source of New Myocyte Development in the Adult Heart. *Int. J. Mol. Sci.* **2021**, *22*, 7764. [CrossRef] [PubMed]

92. Tane, S.; Kubota, M.; Okayama, H.; Ikenishi, A.; Yoshitome, S.; Iwamoto, N.; Satoh, Y.; Kusakabe, A.; Ogawa, S.; Kanai, A.; et al. Repression of Cyclin D1 Expression Is Necessary for the Maintenance of Cell Cycle Exit in Adult Mammalian Cardiomyocytes. *J. Biol. Chem.* **2014**, *289*, 18033–18044. [CrossRef] [PubMed]

93. Pasumarthi, K.B.; Nakajima, H.; Nakajima, H.O.; Soonpaa, M.H.; Field, L.J. Targeted Expression of Cyclin D2 Results in Cardiomyocyte DNA Synthesis and Infarct Regression in Transgenic Mice. *Circ. Res.* **2005**, *96*, 110–118. [CrossRef] [PubMed]

94. Chaudhry, H.W.; Dashoush, N.H.; Tang, H.; Zhang, L.; Wang, X.; Wu, E.X.; Wolgemuth, D.J. Cyclin A2 Mediates Cardiomyocyte Mitosis in the Postmitotic Myocardium. *J. Biol. Chem.* **2004**, *279*, 35858–35866. [CrossRef] [PubMed]

95. Shapiro, S.D.; Ranjan, A.K.; Kawase, Y.; Cheng, R.K.; Kara, R.J.; Bhattacharya, R.; Guzman-Martinez, G.; Sanz, J.; Garcia, M.J.; Chaudhry, H.W. Cyclin A2 Induces Cardiac Regeneration After Myocardial Infarction Through Cytokinesis of Adult Cardiomyocytes. *Sci. Transl. Med.* **2014**, *6*, 224ra27. [CrossRef] [PubMed]

96. Di Stefano, V.; Giacca, M.; Capogrossi, M.C.; Crescenzi, M.; Martelli, F. Knockdown of Cyclin-dependent Kinase Inhibitors Induces Cardiomyocyte Re-entry in the Cell Cycle. *J. Biol. Chem.* **2011**, *286*, 8644–8654. [CrossRef]

97. Bersell, K.; Arab, S.; Haring, B.; Kühn, B. Neuregulin1/ErbB4 Signaling Induces Cardiomyocyte Proliferation and Repair of Heart Injury. *Cell* **2009**, *138*, 257–270. [CrossRef]

98. D'Uva, G.; Aharonov, A.; Lauriola, M.; Kain, D.; Yahalom-Ronen, Y.; Carvalho, S.; Weisinger, K.; Bassat, E.; Rajchman, D.; Yifa, O.; et al. ERBB2 triggers mammalian heart regeneration by promoting cardiomyocyte dedifferentiation and proliferation. *Nat. Cell Biol.* **2015**, *17*, 627–638. [CrossRef]

99. Abbas, N.; Perbellini, F.; Thum, T. Non-coding RNAs: Emerging players in cardiomyocyte proliferation and cardiac regeneration. *Basic Res. Cardiol.* **2020**, *115*, 52. [CrossRef]

100. Santos, F.; Correia, M.; Nóbrega-Pereira, S.; de Jesus, B.B. Age-Related Pathways in Cardiac Regeneration: A Role for lncRNAs? *Front. Physiol.* **2021**, *11*, 583191. [CrossRef]

101. Correia, M.; de Jesus, B.B.; Nobrega-Pereira, S. Novel Insights Linking lncRNAs and Metabolism with Implications for Cardiac Regeneration. *Front. Physiol.* **2021**, *12*, 586927. [CrossRef] [PubMed]

102. Puente, B.N.; Kimura, W.; Muralidhar, S.A.; Moon, J.; Amatruda, J.F.; Phelps, K.L.; Grinsfelder, D.; Rothermel, B.A.; Chen, R.; Garcia, J.A.; et al. The Oxygen-Rich Postnatal Environment Induces Cardiomyocyte Cell-Cycle Arrest through DNA Damage Response. *Cell* **2014**, *157*, 565–579. [CrossRef] [PubMed]

103. Menendez-Montes, I.; Abdisalaam, S.; Xiao, F.; Lam, N.T.; Mukherjee, S.; Szweda, L.I.; Asaithamby, A.; Sadek, H.A. Mitochondrial fatty acid utilization increases chromatin oxidative stress in cardiomyocytes. *Proc. Natl. Acad. Sci. USA* **2021**, *118*, 3–5. [CrossRef] [PubMed]

104. Lalowski, M.M.; Björk, S.; Finckenberg, P.; Soliymani, R.; Tarkia, M.; Calza, G.; Blokhina, D.; Tulokas, S.; Kankainen, M.; Lakkisto, P.; et al. Characterizing the Key Metabolic Pathways of the Neonatal Mouse Heart Using a Quantitative Combinatorial Omics Approach. *Front. Physiol.* **2018**, *9*, 365. [CrossRef]

105. Nakada, Y.; Canseco, D.C.; Thet, S.; Abdisalaam, S.; Asaithamby, A.; Santos, C.X.; Shah, A.M.; Zhang, H.; Faber, J.E.; Kinter, M.T.; et al. Hypoxia induces heart regeneration in adult mice. *Nature* **2017**, *541*, 222–227. [CrossRef] [PubMed]

106. Bae, J.; Salamon, R.J.; Brandt, E.B.; Paltzer, W.G.; Zhang, Z.; Britt, E.C.; Hacker, T.A.; Fan, J.; Mahmoud, A.I. Malonate Promotes Adult Cardiomyocyte Proliferation and Heart Regeneration. *Circulation* **2021**, *143*, 1973–1986. [CrossRef] [PubMed]

107. Honkoop, H.; de Bakker, D.E.; Aharonov, A.; Kruse, F.; Shakked, A.; Nguyen, P.D.; de Heus, C.; Garric, L.; Muraro, M.J.; Shoffner, A.; et al. Single-cell analysis uncovers that metabolic reprogramming by ErbB2 signaling is essential for cardiomyocyte proliferation in the regenerating heart. *eLife* **2019**, *8*, e50163. [CrossRef]

108. Fajardo, V.M.; Feng, I.; Chen, B.Y.; Perez-Ramirez, C.A.; Shi, B.; Clark, P.; Tian, R.; Lien, C.-L.; Pellegrini, M.; Christofk, H.; et al. GLUT1 overexpression enhances glucose metabolism and promotes neonatal heart regeneration. *Sci. Rep.* **2021**, *11*, 8669. [CrossRef]

109. Cardoso, A.C.; Lam, N.T.; Savla, J.J.; Nakada, Y.; Pereira, A.H.M.; Elnwasany, A.; Menendez-Montes, I.; Ensley, E.L.; Petric, U.B.; Sharma, G.; et al. Mitochondrial substrate utilization regulates cardiomyocyte cell-cycle progression. *Nat. Metab.* **2020**, *2*, 167–178. [CrossRef]

110. Cao, T.; Liccardo, D.; Lacanna, R.; Zhang, X.; Lu, R.; Finck, B.N.; Leigh, T.; Chen, X.; Drosatos, K.; Tian, Y. Fatty Acid Oxidation Promotes Cardiomyocyte Proliferation Rate but Does Not Change Cardiomyocyte Number in Infant Mice. *Front. Cell Dev. Biol.* **2019**, *7*, 42. [CrossRef]

111. Wang, W.; Zhang, L.; Battiprolu, P.K.; Fukushima, A.; Nguyen, K.; Milner, K.; Gupta, A.; Altamimi, T.; Byrne, N.; Mori, J.; et al. Malonyl CoA Decarboxylase Inhibition Improves Cardiac Function Post-Myocardial Infarction. *JACC: Basic Transl. Sci.* **2019**, *4*, 385–400. [CrossRef] [PubMed]

112. Roy, R.; Leigh, T.; Gao, E.; Zhang, X.; Tian, Y. Activation or Inhibition of PPARα-Mediated Fatty Acid β-Oxidation Does Not Active Cardiomyocyte Proliferation in Normal or Infarcted Adult Mice. *bioRxiv* **2019**, 667964. [CrossRef]

113. Lundsgaard, A.-M.; Fritzen, A.M.; Nicolaisen, T.S.; Carl, C.S.; Sjøberg, K.A.; Raun, S.H.; Klein, A.B.; Quant, E.S.S.; Langer, J.; Ørskov, C.; et al. Glucometabolic consequences of acute and prolonged inhibition of fatty acid oxidation. *J. Lipid Res.* **2020**, *61*, 10–19. [CrossRef] [PubMed]

114. Ordoño, J.; Pérez-Amodio, S.; Ball, K.; Aguirre, A.; Engel, E. Lactate Promotes Cardiomyocyte Dedifferentiation through Metabolic Reprogramming. *bioRxiv* **2020**. [CrossRef]

115. Bergmann, O.; Bhardwaj, R.D.; Bernard, S.; Zdunek, S.; Barnabé-Heider, F.; Walsh, S.; Zupicich, J.; Alkass, K.; Buchholz, B.A.; Druid, H.; et al. Evidence for Cardiomyocyte Renewal in Humans. *Science* **2009**, *324*, 98–102. [CrossRef] [PubMed]

116. Malliaras, K.; Zhang, Y.; Seinfeld, J.; Galang, G.; Tseliou, E.; Cheng, K.; Sun, B.; Aminzadeh, M.; Marbán, E. Cardiomyocyte proliferation and progenitor cell recruitment underlie therapeutic regeneration after myocardial infarction in the adult mouse heart. *EMBO Mol. Med.* **2013**, *5*, 191–209. [CrossRef]

117. Brade, T.; Pane, L.S.; Moretti, A.; Chien, K.R.; Laugwitz, K.-L. Embryonic Heart Progenitors and Cardiogenesis. *Cold Spring Harb. Perspect. Med.* **2013**, *3*, a013847. [CrossRef]

118. Urbanek, K.; Torella, D.; Sheikh, F.; De Angelis, A.; Nurzynska, D.; Silvestri, F.; Beltrami, C.A.; Bussani, R.; Beltrami, A.P.; Quaini, F.; et al. Myocardial regeneration by activation of multipotent cardiac stem cells in ischemic heart failure. *Proc. Natl. Acad. Sci. USA* **2005**, *102*, 8692–8697. [CrossRef]

119. Xin, M.; Kim, Y.; Sutherland, L.B.; Murakami, M.; Qi, X.; McAnally, J.; Porrello, E.R.; Mahmoud, A.I.; Tan, W.; Shelton, J.M.; et al. Hippo pathway effector Yap promotes cardiac regeneration. *Proc. Natl. Acad. Sci. USA* **2013**, *110*, 13839–13844. [CrossRef]

120. Smits, A.M.; van Vliet, P.; Metz, C.H.; Korfage, T.; Sluijter, J.P.; Doevendans, P.A.; Goumans, M.-J. Human cardiomyocyte progenitor cells differentiate into functional mature cardiomyocytes: An in vitro model for studying human cardiac physiology and pathophysiology. *Nat. Protoc.* **2009**, *4*, 232–243. [CrossRef]

121. Smits, A.M.; Van Laake, L.W.; den Ouden, K.; Schreurs, C.; Szuhai, K.; van Echteld, C.J.; Mummery, C.L.; Doevendans, P.A.; Goumans, M.-J. Human cardiomyocyte progenitor cell transplantation preserves long-term function of the infarcted mouse myocardium. *Cardiovasc. Res.* **2009**, *83*, 527–535. [CrossRef] [PubMed]

122. Torán, J.L.; Aguilar, S.; Lopez, J.A.; Torroja, C.; Quintana, J.A.; Santiago, C.; Abad, J.L.; Gomes-Alves, P.; Gonzalez, A.; Bernal, J.; et al. CXCL6 is an important paracrine factor in the pro-angiogenic human cardiac progenitor-like cell secretome. *Sci. Rep.* **2017**, *7*, 12490. [CrossRef] [PubMed]

123. Sebastião, M.J.; Serra, M.; Pereira, R.; Palacios, I.; Gomes-Alves, P.; Alves, P.M. Human cardiac progenitor cell activation and regeneration mechanisms: Exploring a novel myocardial ischemia/reperfusion in vitro model. *Stem Cell Res. Ther.* **2019**, *10*, 77. [CrossRef] [PubMed]

124. Tang, Y.; Zhu, W.; Cheng, M.; Chen, L.; Zhang, J.; Sun, T.; Kishore, R.; Phillips, M.I.; Losordo, D.; Qin, G. Hypoxic Preconditioning Enhances the Benefit of Cardiac Progenitor Cell Therapy for Treatment of Myocardial Infarction by Inducing CXCR4 Expression. *Circ. Res.* **2009**, *104*, 1209–1216. [CrossRef]

125. Huang, M.; Nguyen, P.; Jia, F.; Hu, S.; Gong, Y.; de Almeida, P.E.; Wang, L.; Nag, D.; Kay, M.A.; Giaccia, A.J.; et al. Double Knockdown of Prolyl Hydroxylase and Factor-Inhibiting Hypoxia-Inducible Factor with Nonviral Minicircle Gene Therapy Enhances Stem Cell Mobilization and Angiogenesis After Myocardial Infarction. *Circulation* **2011**, *124*, S46–S54. [CrossRef]

126. André, M.E.; De Pauw, A.; Verdoy, M.R.; Brusa, D.; Bouzin, C.; Timmermans, A.; Bertrand, L.; Balligand, J.-L. Changes of Metabolic Phenotype of Cardiac Progenitor Cells during Differentiation: Neutral Effect of Stimulation of AMP-Activated Protein Kinase. *Stem Cells Dev.* **2019**, *28*, 1498–1513. [CrossRef]

127. Salabei, J.K.; Lorkiewicz, P.K.; Holden, C.R.; Li, Q.; Hong, K.U.; Bolli, R.; Bhatnagar, A.; Hill, B.G. Glutamine Regulates Cardiac Progenitor Cell Metabolism and Proliferation. *Stem Cells* **2015**, *33*, 2613–2627. [CrossRef]

128. Talkhabi, M.; Pahlavan, S.; Aghdami, N.; Baharvand, H. Ascorbic acid promotes the direct conversion of mouse fibroblasts into beating cardiomyocytes. *Biochem. Biophys. Res. Commun.* **2015**, *463*, 699–705. [CrossRef]

129. Lewandowski, J.; Kolanowski, T.J.; Kurpisz, M. Techniques for the induction of human pluripotent stem cell differentiation towards cardiomyocytes. *J. Tissue Eng. Regen. Med.* **2017**, *11*, 1658–1674. [CrossRef]

130. Mummery, C.; Zhang, J.; Ng, E.S.; Elliott, D.; Elefanty, A.; Kamp, T. Differentiation of Human Embryonic Stem Cells and Induced Pluripotent Stem Cells to Cardiomyocytes. *Circ. Res.* **2012**, *111*, 344–358. [CrossRef]

131. Kehat, I.; Kenyagin-Karsenti, D.; Snir, M.; Segev, H.; Amit, M.; Gepstein, A.; Livne, E.; Binah, O.; Itskovitz-Eldor, J.; Gepstein, L. Human embryonic stem cells can differentiate into myocytes with structural and functional properties of cardiomyocytes. *J. Clin. Investig.* **2001**, *108*, 407–414. [CrossRef] [PubMed]

132. Mummery, C.; Ward, D.; Brink, C.E.V.D.; Bird, S.D.; Doevendans, P.A.; Opthof, T.; De La Riviere, A.B.; Tertoolen, L.; van der Heyden, M.; Pera, M. Cardiomyocyte differentiation of mouse and human embryonic stem cells. *J. Anat.* **2002**, *200*, 233–242. [CrossRef] [PubMed]

133. Xu, C.; Police, S.; Rao, N.; Carpenter, M.K. Characterization and Enrichment of Cardiomyocytes Derived from Human Embryonic Stem Cells. *Circ. Res.* **2002**, *91*, 501–508. [CrossRef] [PubMed]

134. He, J.-Q.; Ma, Y.; Lee, Y.; Thomson, J.A.; Kamp, T. Human Embryonic Stem Cells Develop Into Multiple Types of Cardiac Myocytes. *Circ. Res.* **2003**, *93*, 32–39. [CrossRef] [PubMed]

135. Laflamme, M.A.; Chen, K.Y.; Naumova, A.V.; Muskheli, V.; Fugate, J.A.; Dupras, S.K.; Reinecke, H.; Xu, C.; Hassanipour, M.; Police, S.; et al. Cardiomyocytes derived from human embryonic stem cells in pro-survival factors enhance function of infarcted rat hearts. *Nat. Biotechnol.* **2007**, *25*, 1015–1024. [CrossRef]

136. Zhang, J.; Klos, M.; Wilson, G.F.; Herman, A.M.; Lian, X.; Raval, K.K.; Barron, M.R.; Hou, L.; Soerens, A.G.; Yu, J.; et al. Extracellular Matrix Promotes Highly Efficient Cardiac Differentiation of Human Pluripotent Stem Cells: The Matrix Sandwich Method. *Circ. Res.* **2012**, *111*, 1125–1136. [CrossRef]
137. Mummery, C.; Oostwaard, D.W.-V.; Doevendans, P.; Spijker, R.; Brink, S.V.D.; Hassink, R.; van der Heyden, M.; Opthof, T.; Pera, M.; de la Riviere, A.B.; et al. Differentiation of Human Embryonic Stem Cells to Cardiomyocytes: Role of coculture with visceral endoderm-like cells. *Circulation* **2003**, *107*, 2733–2740. [CrossRef]
138. Passier, R.; Oostwaard, D.W.; Snapper, J.; Kloots, J.; Hassink, R.J.; Kuijk, E.; Roelen, B.; de la Riviere, A.B.; Mummery, C. Increased Cardiomyocyte Differentiation from Human Embryonic Stem Cells in Serum—Free Cultures. *Stem Cells* **2005**, *23*, 772–780. [CrossRef]
139. Takahashi, K.; Yamanaka, S. Induction of Pluripotent Stem Cells from Mouse Embryonic and Adult Fibroblast Cultures by Defined Factors. *Cell* **2006**, *126*, 663–676. [CrossRef]
140. Takahashi, K.; Tanabe, K.; Ohnuki, M.; Narita, M.; Ichisaka, T.; Tomoda, K.; Yamanaka, S. Induction of Pluripotent Stem Cells from Adult Human Fibroblasts by Defined Factors. *Cell* **2007**, *131*, 861–872. [CrossRef]
141. Pushp, P.; Nogueira, D.E.S.; Rodrigues, C.A.V.; Ferreira, F.C.; Cabral, J.M.S.; Gupta, M.K. A Concise Review on Induced Pluripotent Stem Cell-Derived Cardiomyocytes for Personalized Regenerative Medicine. *Stem Cell Rev. Rep.* **2020**, *17*, 748–776. [CrossRef] [PubMed]
142. Kattman, S.J.; Witty, A.D.; Gagliardi, M.; Dubois, N.C.; Niapour, M.; Hotta, A.; Ellis, J.; Keller, G. Stage-Specific Optimization of Activin/Nodal and BMP Signaling Promotes Cardiac Differentiation of Mouse and Human Pluripotent Stem Cell Lines. *Cell Stem Cell* **2011**, *8*, 228–240. [CrossRef] [PubMed]
143. Chen, Y.; Zeng, D.; Ding, L.; Li, X.-L.; Liu, X.-T.; Li, W.; Wei, T.; Yan, S.; Xie, J.-H.; Wei, L.; et al. Three-dimensional poly-(ε-caprolactone) nanofibrous scaffolds directly promote the cardiomyocyte differentiation of murine-induced pluripotent stem cells through Wnt/β-catenin signaling. *BMC Cell Biol.* **2015**, *16*, 22. [CrossRef] [PubMed]
144. Burridge, P.W.; Matsa, E.; Shukla, P.; Lin, Z.C.; Churko, J.M.; Ebert, A.D.; Lan, F.; Diecke, S.; Huber, B.; Mordwinkin, N.M.; et al. Chemically Defined and Small Molecule-Based Generation of Human Cardiomyocytes. *Nat. Methods.* **2014**, *11*, 855–860. [CrossRef] [PubMed]
145. Chung, S.; Dzeja, P.P.; Faustino, R.S.; Perez-Terzic, C.; Behfar, A.; Terzic, A. Mitochondrial oxidative metabolism is required for the cardiac differentiation of stem cells. *Nat. Clin. Pract. Cardiovasc. Med.* **2007**, *4*, S60–S67. [CrossRef]
146. Yang, P.; Chen, X.; Kaushal, S.; Reece, E.A.; Yang, P. High glucose suppresses embryonic stem cell differentiation into cardiomyocytes. *Stem Cell Res. Ther.* **2016**, *7*, 187. [CrossRef]
147. Correia, C.; Koshkin, A.; Duarte, P.; Hu, D.; Teixeira, A.; Domian, I.; Serra, M.; Alves, P.M. Distinct carbon sources affect structural and functional maturation of cardiomyocytes derived from human pluripotent stem cells. *Sci. Rep.* **2017**, *7*, 8590. [CrossRef]
148. Robertson, C.; Tran, D.D.; George, S.C. Concise Review: Maturation Phases of Human Pluripotent Stem Cell-Derived Cardiomyocytes. *Stem Cells* **2013**, *31*, 829–837. [CrossRef]
149. Musunuru, K.; Sheikh, F.; Gupta, R.M.; Houser, S.R.; Maher, K.O.; Milan, D.J.; Terzic, A.; Wu, J.C. Induced Pluripotent Stem Cells for Cardiovascular Disease Modeling and Precision Medicine: A Scientific Statement from the American Heart Association. *Circ. Genom. Precis. Med.* **2018**, *11*, e000043. [CrossRef]
150. Zhang, H.; Badur, M.G.; Spiering, S.; Divakaruni, A.; Meurs, N.E.; Yu, M.S.; Colas, A.R.; Murphy, A.N.; Mercola, M.; Metallo, C.M. Lipid Availability Influences the Metabolic Maturation of Human Pluripotent Stem Cell-Derived Cardiomyocytes. *bioRxiv* **2020**. [CrossRef]
151. Feyen, D.A.; McKeithan, W.L.; Bruyneel, A.A.; Spiering, S.; Hörmann, L.; Ulmer, B.; Zhang, H.; Briganti, F.; Schweizer, M.; Hegyi, B.; et al. Metabolic Maturation Media Improve Physiological Function of Human iPSC-Derived Cardiomyocytes. *Cell Rep.* **2020**, *32*, 107925. [CrossRef] [PubMed]
152. Mills, R.J.; Titmarsh, D.M.; Koenig, X.; Parker, B.L.; Ryall, J.G.; Quaife-Ryan, G.A.; Voges, H.K.; Hodson, M.P.; Ferguson, C.; Drowley, L.; et al. Functional screening in human cardiac organoids reveals a metabolic mechanism for cardiomyocyte cell cycle arrest. *Proc. Natl. Acad. Sci. USA* **2017**, *114*, E8372–E8381. [CrossRef] [PubMed]
153. Dai, D.-F.; Danoviz, M.E.; Wiczer, B.; Laflamme, M.A.; Tian, R. Mitochondrial Maturation in Human Pluripotent Stem Cell Derived Cardiomyocytes. *Stem Cells Int.* **2017**, *2017*, 5153625. [CrossRef] [PubMed]
154. Rana, P.; Anson, B.; Engle, S.; Will, Y. Characterization of Human-Induced Pluripotent Stem Cell–Derived Cardiomyocytes: Bioenergetics and Utilization in Safety Screening. *Toxicol. Sci.* **2012**, *130*, 117–131. [CrossRef] [PubMed]
155. Hu, J.; Nie, Y.; Chen, S.; Xie, C.; Fan, Q.; Wang, Z.; Long, B.; Yan, G.; Zhong, Q.; Yan, X. Leucine reduces reactive oxygen species levels via an energy metabolism switch by activation of the mTOR-HIF-1α pathway in porcine intestinal epithelial cells. *Int. J. Biochem. Cell Biol.* **2017**, *89*, 42–56. [CrossRef]
156. Garbern, J.C.; Helman, A.; Sereda, R.; Sarikhani, M.; Ahmed, A.; Escalante, G.; Ogurlu, R.; Kim, S.L.; Zimmerman, J.F.; Cho, A.; et al. Inhibition of mTOR Signaling Enhances Maturation of Cardiomyocytes Derived from Human-Induced Pluripotent Stem Cells via p53-Induced Quiescence. *Circulation* **2020**, *141*, 285–300. [CrossRef]
157. Ye, L.; Zhang, X.; Zhou, Q.; Tan, B.; Xu, H.; Yi, Q.; Yan, L.; Xie, M.; Zhang, Y.; Tian, J.; et al. Activation of AMPK Promotes Maturation of Cardiomyocytes Derived from Human Induced Pluripotent Stem Cells. *Front. Cell Dev. Biol.* **2021**, *9*, 644667. [CrossRef]

158. Ieda, M.; Tsuchihashi, T.; Ivey, K.N.; Ross, R.S.; Hong, T.-T.; Shaw, R.M.; Srivastava, D. Cardiac Fibroblasts Regulate Myocardial Proliferation through β1 Integrin Signaling. *Dev. Cell* **2009**, *16*, 233–244. [CrossRef]

159. Ieda, M.; Fu, J.-D.; Delgado-Olguin, P.; Vedantham, V.; Hayashi, Y.; Bruneau, B.G.; Srivastava, D. Direct Reprogramming of Fibroblasts into Functional Cardiomyocytes by Defined Factors. *Cell* **2010**, *142*, 375–386. [CrossRef]

160. Jopling, C.; Boue, S.; Belmonte, J.C.I. Dedifferentiation, transdifferentiation and reprogramming: Three routes to regeneration. *Nat. Rev. Mol. Cell Biol.* **2011**, *12*, 79–89. [CrossRef]

161. Qian, L.; Huang, Y.; Spencer, C.I.; Foley, A.; Vedantham, V.; Liu, L.; Conway, S.J.; Fu, J.; Srivastava, D. In vivo reprogramming of murine cardiac fibroblasts into induced cardiomyocytes. *Nature* **2012**, *485*, 593–598. [CrossRef] [PubMed]

162. Song, K.; Nam, Y.-J.; Luo, X.; Qi, X.; Tan, W.; Huang, G.N.; Acharya, A.; Smith, C.L.; Tallquist, M.D.; Neilson, E.G.; et al. Heart repair by reprogramming non-myocytes with cardiac transcription factors. *Nature* **2012**, *485*, 599–604. [CrossRef] [PubMed]

163. Wada, R.; Muraoka, N.; Inagawa, K.; Yamakawa, H.; Miyamoto, K.; Sadahiro, T.; Umei, T.; Kaneda, R.; Suzuki, T.; Kamiya, K.; et al. Induction of human cardiomyocyte-like cells from fibroblasts by defined factors. *Proc. Natl. Acad. Sci. USA* **2013**, *110*, 12667–12672. [CrossRef] [PubMed]

164. Christoforou, N.; Chellappan, M.; Adler, A.F.; Kirkton, R.D.; Wu, T.; Addis, R.C.; Bursac, N.; Leong, K.W. Transcription Factors MYOCD, SRF, Mesp1 and SMARCD3 Enhance the Cardio-Inducing Effect of GATA4, TBX5, and MEF2C during Direct Cellular Reprogramming. *PLoS ONE* **2013**, *8*, e63577. [CrossRef] [PubMed]

165. Zhou, J.; Sun, J. A Revolution in Reprogramming: Small Molecules. *Curr. Mol. Med.* **2019**, *19*, 77–90. [CrossRef] [PubMed]

166. Nam, Y.J.; Song, K.; Luo, X.; Daniel, E.; Lambeth, K.; West, K.; Hill, J.A.; di Maio, J.M.; Baker, L.A.; Bassel-Duby, R.; et al. Reprogramming of human fibroblasts toward a cardiac fate. *Proc. Natl. Acad. Sci. USA* **2013**, *110*, 5588–5593. [CrossRef]

167. Fu, J.; Stone, N.R.; Liu, L.; Spencer, C.I.; Qian, L.; Hayashi, Y.; Olguín, P.D.; Ding, S.; Bruneau, B.G.; Srivastava, D. Direct Reprogramming of Human Fibroblasts toward a Cardiomyocyte-like State. *Stem Cell Rep.* **2013**, *1*, 235–247. [CrossRef]

168. Tani, H.; Sadahiro, T.; Ieda, M. Direct Cardiac Reprogramming: A Novel Approach for Heart Regeneration. *Int. J. Mol. Sci.* **2018**, *19*, 2629. [CrossRef]

169. Miyamoto, K.; Akiyama, M.; Tamura, F.; Isomi, M.; Yamakawa, H.; Sadahiro, T.; Muraoka, N.; Kojima, H.; Haginiwa, S.; Kurotsu, S.; et al. Direct In Vivo Reprogramming with Sendai Virus Vectors Improves Cardiac Function after Myocardial Infarction. *Cell Stem Cell* **2017**, *22*, 91–103.e5. [CrossRef]

170. Hashimoto, H.; Wang, Z.; Garry, G.A.; Malladi, V.; Botten, G.A.; Ye, W.; Zhou, H.; Osterwalder, M.; Dickel, D.; Visel, A.; et al. Cardiac Reprogramming Factors Synergistically Activate Genome-wide Cardiogenic Stage-Specific Enhancers. *Cell Stem Cell* **2019**, *25*, 69–86.e5. [CrossRef]

171. Wang, L.; Liu, Z.; Yin, C.; Asfour, H.; Chen, O.; Olivia, C.; Bursac, N.; Liu, J.; Qian, L. Stoichiometry of Gata4, Mef2c, and Tbx5 Influences the Efficiency and Quality of Induced Cardiac Myocyte Reprogramming. *Circ. Res.* **2015**, *116*, 237–244. [CrossRef] [PubMed]

172. Takeuchi, J.K.; Bruneau, B.G. Directed transdifferentiation of mouse mesoderm to heart tissue by defined factors. *Nature* **2009**, *459*, 708–711. [CrossRef] [PubMed]

173. Vaseghi, H.; Liu, J.; Qian, L. Molecular barriers to direct cardiac reprogramming. *Protein Cell* **2017**, *8*, 724–734. [CrossRef] [PubMed]

174. Liu, Z.; Wang, L.; Welch, J.D.; Ma, H.; Zhou, Y.; Vaseghi, H.R.; Yu, S.; Wall, J.B.; Alimohamadi, S.; Zheng, M.; et al. Single-cell transcriptomics reconstructs fate conversion from fibroblast to cardiomyocyte. *Nat.* **2017**, *551*, 100–104. [CrossRef] [PubMed]

175. Nóbrega-Pereira, S.; De Jesus, B.B. *Cellular Reprogramming and Aging*; Springer: Berlin/Heidelberg, Germany, 2020; pp. 73–91. [CrossRef]

176. Zhou, H.; Morales, M.G.; Hashimoto, H.; Dickson, M.E.; Song, K.; Ye, W.; Kim, M.S.; Niederstrasser, H.; Wang, Z.; Chen, B.; et al. ZNF281 enhances cardiac reprogramming by modulating cardiac and inflammatory gene expression. *Genes Dev.* **2017**, *31*, 1770–1783. [CrossRef] [PubMed]

177. Stone, N.R.; Gifford, C.A.; Thomas, R.; Pratt, K.J.; Samse-Knapp, K.; Mohamed, T.M.; Radzinsky, E.M.; Schricker, A.; Ye, L.; Yu, P.; et al. Context-Specific Transcription Factor Functions Regulate Epigenomic and Transcriptional Dynamics during Cardiac Reprogramming. *Cell Stem Cell* **2019**, *25*, 87–102.e9. [CrossRef]

178. Ishida, T.; Ueyama, T.; Baba, A.; Hasegawa, K.; Kawamura, T. The Role of Isocitrate Dehydrogenases in Direct Reprogramming to Cardiomyocytes. *Eur. Cardiol. Rev.* **2021**, *16*, e64. [CrossRef] [PubMed]

179. Wang, X.; Hodgkinson, C.P.; Lu, K.; Payne, A.J.; Pratt, R.E.; Dzau, V.J. Selenium Augments microRNA Directed Reprogramming of Fibroblasts to Cardiomyocytes via Nanog. *Sci. Rep.* **2016**, *6*, 23017. [CrossRef]

180. Suzuki, Y.J.; Shults, N.V. Antioxidant Regulation of Cell Reprogramming. *Antioxidants* **2019**, *8*, 323. [CrossRef]

181. Meng, S.; Chanda, P.; Thandavarayan, R.A.; Cooke, J.P. Transflammation: How Innate Immune Activation and Free Radicals Drive Nuclear Reprogramming. *Antioxid. Redox Signal.* **2018**, *29*, 205–218. [CrossRef]

182. Chen, J.X.; Krane, M.; Deutsch, M.-A.; Wang, L.; Rav-Acha, M.; Gregoire, S.; Engels, M.C.; Rajarajan, K.; Karra, R.; Abel, E.D.; et al. Inefficient Reprogramming of Fibroblasts into Cardiomyocytes Using Gata4, Mef2c, and Tbx5. *Circ. Res.* **2012**, *111*, 50–55. [CrossRef] [PubMed]

183. Yamakawa, H.; Muraoka, N.; Miyamoto, K.; Sadahiro, T.; Isomi, M.; Haginiwa, S.; Kojima, H.; Umei, T.; Akiyama, M.; Kuishi, Y.; et al. Fibroblast Growth Factors and Vascular Endothelial Growth Factor Promote Cardiac Reprogramming under Defined Conditions. *Stem Cell Rep.* **2015**, *5*, 1128–1142. [CrossRef] [PubMed]

184. Cheng, C.-W.; Yilmaz, H. 100 Years of Exploiting Diet and Nutrition for Tissue Regeneration. *Cell Stem Cell* **2021**, *28*, 370–373. [CrossRef] [PubMed]

185. Dhalla, N.S.; Elmoselhi, A.B.; Hata, T.; Makino, N. Status of myocardial antioxidants in ischemia–reperfusion injury. *Cardiovasc. Res.* **2000**, *47*, 446–456. [CrossRef]

186. Tangney, C.C.; Hankins, J.S.; Murtaugh, M.A.; Piccione, W. Plasma vitamins E and C concentrations of adult patients during cardiopulmonary bypass. *J. Am. Coll. Nutr.* **1998**, *17*, 162–170. [CrossRef]

187. Saisho, Y. Metformin and Inflammation: Its Potential Beyond Glucose-lowering Effect. *Endocr. Metab. Immune Disord. Drug Targets* **2015**, *15*, 196–205. [CrossRef]

188. Ramachandran, R.; Saraswathi, M. Postconditioning with metformin attenuates apoptotic events in cardiomyoblasts associated with ischemic reperfusion injury. *Cardiovasc. Ther.* **2017**, *35*, e12279. [CrossRef]

189. Zhang, L.; Chen, J.; Yan, L.; He, Q.; Xie, H.; Chen, M. Resveratrol Ameliorates Cardiac Remodeling in a Murine Model of Heart Failure with Preserved Ejection Fraction. *Front. Pharmacol.* **2021**, *12*, 646240. [CrossRef]

190. Li, Y.-G.; Zhu, W.; Tao, J.-P.; Xin, P.; Liu, M.-Y.; Li, J.-B.; Wei, M. Resveratrol protects cardiomyocytes from oxidative stress through SIRT1 and mitochondrial biogenesis signaling pathways. *Biochem. Biophys. Res. Commun.* **2013**, *438*, 270–276. [CrossRef]

191. Sahin, E.; Colla, S.; Liesa, M.; Moslehi, J.; Muller, F.; Guo, M.; Cooper, M.; Kotton, D.; Fabian, A.J.; Walkey, C.; et al. Telomere dysfunction induces metabolic and mitochondrial compromise. *Nature* **2011**, *470*, 359–365. [CrossRef]

192. de Jesus, B.B.; Vera, E.; Schneeberger, K.; Tejera, A.M.; Ayuso, E.; Bosch, F.; Blasco, M.A. Telomerase gene therapy in adult and old mice delays aging and increases longevity without increasing cancer. *EMBO Mol. Med.* **2012**, *4*, 691–704. [CrossRef] [PubMed]

193. Bär, C.; de Jesus, B.B.; Serrano, R.M.; Tejera, A.M.; Ayuso, E.; Jimenez, V.; Formentini, I.; Bobadilla, M.; Mizrahi, J.; De Martino, A.; et al. Telomerase expression confers cardioprotection in the adult mouse heart after acute myocardial infarction. *Nat. Commun.* **2014**, *5*, 5863. [CrossRef] [PubMed]

194. Hsu, C.-P.; Zhai, P.; Yamamoto, T.; Maejima, Y.; Matsushima, S.; Hariharan, N.; Shao, D.; Takagi, H.; Oka, S.; Sadoshima, J. Silent Information Regulator 1 Protects the Heart from Ischemia/Reperfusion. *Circulation* **2010**, *122*, 2170–2182. [CrossRef] [PubMed]

195. Brunet, A.; Sweeney, L.B.; Sturgill, J.F.; Chua, K.F.; Greer, P.L.; Lin, Y.; Tran, H.; Ross, S.E.; Mostoslavsky, R.; Cohen, H.Y.; et al. Stress-Dependent Regulation of FOXO Transcription Factors by the SIRT1 Deacetylase. *Science* **2004**, *303*, 2011–2015. [CrossRef] [PubMed]

196. Alcendor, R.R.; Gao, S.; Zhai, P.; Zablocki, D.; Holle, E.; Yu, X.; Tian, B.; Wagner, T.; Vatner, S.F.; Sadoshima, J. Sirt1 Regulates Aging and Resistance to Oxidative Stress in the Heart. *Circ. Res.* **2007**, *100*, 1512–1521. [CrossRef]

197. Planavila, A.; Iglesias, R.; Giralt, M.; Villarroya, F. Sirt1 acts in association with PPARα to protect the heart from hypertrophy, metabolic dysregulation, and inflammation. *Cardiovasc. Res.* **2010**, *90*, 276–284. [CrossRef]

198. Gao, J.; Feng, Z.; Wang, X.; Zeng, M.; Liu, J.; Han, S.; Xu, J.; Chen, L.; Cao, K.; Long, J.; et al. SIRT3/SOD2 maintains osteoblast differentiation and bone formation by regulating mitochondrial stress. *Cell Death Differ.* **2017**, *25*, 229–240. [CrossRef]

199. Zhang, Q.; Li, D.; Dong, X.; Zhang, X.; Liu, J.; Peng, L.; Meng, B.; Hua, Q.; Pei, X.; Zhao, L.; et al. LncDACH1 promotes mitochondrial oxidative stress of cardiomyocytes by interacting with sirtuin3 and aggravates diabetic cardiomyopathy. *Sci. China Life Sci.* **2021**. [CrossRef]

200. Gorski, P.A.; Jang, S.P.; Jeong, D.; Lee, A.; Lee, P.; Oh, J.G.; Chepurko, V.; Yang, D.K.; Kwak, T.H.; Eom, S.H.; et al. Role of SIRT1 in Modulating Acetylation of the Sarco-Endoplasmic Reticulum Ca $^{2+}$ -ATPase in Heart Failure. *Circ. Res.* **2019**, *124*, e63–e80. [CrossRef]

201. Chen, Y.; Li, S.; Zhang, Y.; Wang, M.; Li, X.; Liu, S.; Xu, D.; Bao, Y.; Jia, P.; Wu, N.; et al. The lncRNA Malat1 regulates microvascular function after myocardial infarction in mice via miR-26b-5p/Mfn1 axis-mediated mitochondrial dynamics. *Redox Biol.* **2021**, *41*, 101910. [CrossRef]

202. Yu, H.; Zhang, F.; Yan, P.; Zhang, S.; Lou, Y.; Geng, Z.; Li, Z.; Zhang, Y.; Xu, Y.; Lu, Y.; et al. LARP7 Protects against Heart Failure by Enhancing Mitochondrial Biogenesis. *Circulation* **2021**, *143*, 2007–2022. [CrossRef] [PubMed]

203. Cui, M.; Atmanli, A.; Morales, M.G.; Tan, W.; Chen, K.; Xiao, X.; Xu, L.; Liu, N.; Bassel-Duby, R.; Olson, E.N. Nrf1 promotes heart regeneration and repair by regulating proteostasis and redox balance. *Nat. Commun.* **2021**, *12*, 5270. [CrossRef] [PubMed]